



HAL
open science

2023 roadmap for potassium-ion batteries

Yang Xu, Magda Titirici, Jingwei Chen, Furio Cora, Patrick Cullen,
Jacqueline Sophie Edge, Kun Fan, Ling Fan, Jingyu Feng, Tomooki Hosaka,
et al.

► **To cite this version:**

Yang Xu, Magda Titirici, Jingwei Chen, Furio Cora, Patrick Cullen, et al.. 2023 roadmap for potassium-ion batteries. *JPhys Energy*, 2023, 5 (2), pp.021502. 10.1088/2515-7655/acbf76 . hal-04066036

HAL Id: hal-04066036

<https://cnrs.hal.science/hal-04066036>

Submitted on 12 Apr 2023

HAL is a multi-disciplinary open access archive for the deposit and dissemination of scientific research documents, whether they are published or not. The documents may come from teaching and research institutions in France or abroad, or from public or private research centers.

L'archive ouverte pluridisciplinaire **HAL**, est destinée au dépôt et à la diffusion de documents scientifiques de niveau recherche, publiés ou non, émanant des établissements d'enseignement et de recherche français ou étrangers, des laboratoires publics ou privés.

ROADMAP • OPEN ACCESS

2023 roadmap for potassium-ion batteries

To cite this article: Yang Xu *et al* 2023 *J. Phys. Energy* **5** 021502

View the [article online](#) for updates and enhancements.

You may also like

- [Progress of graphdiyne-based materials for anodes of alkali metal ion batteries](#)
Manman Liu, Yue Ma, Xiaofeng Fan *et al.*
- [Unveiling the Sodium/Potassium Storage Mechanisms of Nanoporous Indium-Bismuth Anode Using Operando X-ray Diffraction](#)
Zhiyuan Guo, Jingyu Qin, Bin Yu *et al.*
- [Porous hard carbon spheres derived from biomass for high-performance sodium/potassium-ion batteries](#)
Shuijiao Chen, Kejian Tang, Fei Song *et al.*



ROADMAP

2023 roadmap for potassium-ion batteries

OPEN ACCESS

RECEIVED

30 September 2022

REVISED

18 January 2023

ACCEPTED FOR PUBLICATION

27 February 2023

PUBLISHED

6 April 2023

Original content from this work may be used under the terms of the [Creative Commons Attribution 4.0 licence](https://creativecommons.org/licenses/by/4.0/).

Any further distribution of this work must maintain attribution to the author(s) and the title of the work, journal citation and DOI.



Yang Xu^{1,2,3,*}, Magda Titirici^{2,23}, Jingwei Chen³, Furio Cora^{1,4}, Patrick L Cullen⁵, Jacqueline Sophie Edge², Kun Fan⁶, Ling Fan⁷, Jingyu Feng⁵, Tomooki Hosaka⁸, Junyang Hu⁹, Weiwei Huang¹⁰, Timothy I Hyde¹¹, Sumair Imtiaz^{12,13,14}, Feiyu Kang⁹, Tadhg Kennedy^{12,13}, Eun Jeong Kim⁸, Shinichi Komaba⁸, Laura Lander², Phuong Nam Le Pham^{15,16}, Pengcheng Liu¹⁷, Bingan Lu⁷, Fanlu Meng³, David Mitlin¹⁷, Laure Monconduit^{15,16,18}, Robert G Palgrave¹, Lei Qin¹⁹, Kevin M Ryan^{12,13,14}, Gopinathan Sankar¹, David O Scanlon^{1,4,20}, Tianyi Shi¹, Lorenzo Stievano^{15,16,18}, Henry R Tinker¹, Chengliang Wang⁶, Hang Wang²¹, Huanlei Wang³, Yiying Wu¹⁹, Dengyun Zhai⁹, Qichun Zhang²², Min Zhou²¹ and Jincheng Zou⁶

¹ Department of Chemistry, University College London, 20 Gordon Street, London WC1H 0AJ, United Kingdom

² Imperial College London, London, United Kingdom

³ Ocean University of China, Qingdao, People's Republic of China

⁴ Thomas Young Centre, University College London, Gower St, London, United Kingdom

⁵ School of Engineering and Materials Science, Queen Mary University of London, London, United Kingdom

⁶ School of Optical and Electronic Information, Wuhan National Laboratory for Optoelectronics (WNLO), Huazhong University of Science and Technology, Wuhan, People's Republic of China

⁷ School of Physics and Electronics, Hunan University, Changsha, People's Republic of China

⁸ Department of Applied Chemistry, Tokyo University of Science, 1-3 Kagurazaka, Shinjuku, Tokyo 162-8601, Japan

⁹ Shenzhen Geim Graphene Center, Institute of Materials Research, Tsinghua University, Shenzhen, People's Republic of China

¹⁰ School of Environmental and Chemical Engineering, Yanshan University, Qinhuangdao, People's Republic of China

¹¹ Johnson Matthey Technology Centre, Sonning Common, Reading, United Kingdom

¹² Bernal Institute, University of Limerick, Limerick, Ireland

¹³ Department of Chemical Sciences, University of Limerick, Limerick, Ireland

¹⁴ The SFI Research Centre for Energy, Climate and Marine (MaREI), University of Limerick, Limerick, Ireland

¹⁵ ICGM, University Montpellier, CNRS, Montpellier, France

¹⁶ Alistore-ERI, CNRS, Amiens, France

¹⁷ Materials Science and Engineering Program & Texas Materials Institute (TMI), The University of Texas at Austin, Austin, TX, United States of America

¹⁸ RS2E, CNRS, Amiens, France

¹⁹ Department of Chemistry and Biochemistry, The Ohio State University, Columbus, OH, United States of America

²⁰ The Faraday Institution, Quad One, Becquerel Avenue, Harwell Campus, Didcot, United Kingdom

²¹ Hefei National Laboratory for Physical Sciences at the Microscale, School of Chemistry and Materials Science, University of Science and Technology of China, Hefei, People's Republic of China

²² Department of Materials Science and Engineering, City University of Hong Kong, Hong Kong SAR, People's Republic of China

²³ Guest Editor of the Roadmap.

* Author to whom any correspondence should be addressed.

E-mail: y.xu.1@ucl.ac.uk

Keywords: potassium-ion batteries, energy storage, electrolytes, solid-electrolyte interphase, sustainability, techno-economic assessment, next generation battery

Abstract

The heavy reliance of lithium-ion batteries (LIBs) has caused rising concerns on the sustainability of lithium and transition metal and the ethic issue around mining practice. Developing alternative energy storage technologies beyond lithium has become a prominent slice of global energy research portfolio. The alternative technologies play a vital role in shaping the future landscape of energy storage, from electrified mobility to the efficient utilization of renewable energies and further to large-scale stationary energy storage. Potassium-ion batteries (PIBs) are a promising alternative given its chemical and economic benefits, making a strong competitor to LIBs and sodium-ion batteries for different applications. However, many are unknown regarding potassium storage processes in materials and how it differs from lithium and sodium and understanding of solid-liquid interfacial chemistry is massively insufficient in PIBs. Therefore, there remain outstanding issues to advance the commercial prospects of the PIB technology. This Roadmap

highlights the up-to-date scientific and technological advances and the insights into solving challenging issues to accelerate the development of PIBs. We hope this Roadmap aids the wider PIB research community and provides a cross-referencing to other beyond lithium energy storage technologies in the fast-pacing research landscape.

Contents

1. Introduction	4
2. Layered TMOs	6
3. Prussian blue and analogues	9
4. Polyanionic compounds	12
5. OEMs for PIBs	16
6. Graphite and hard carbon	18
7. Conversion materials	21
8. Alloys	24
9. MXenes	28
10. Organic compounds and MOFs	32
11. Computational discovery of materials	35
12. Organic electrolytes—salts	38
13. Organic electrolytes—solvents	41
14. IL electrolytes for potassium ion batteries	44
15. The SEI in potassium ion batteries	47
16. X-ray absorption spectroscopy (XAS)	51
17. X-ray pair distribution function (XPDF)	54
18. <i>In-situ</i> characterization	58
19. Cost-effectiveness and techno-economic analysis of PIBs	62
References	65

1. Introduction

Yang Xu

Department of Chemistry, University College London, 20 Gordon Street, London WC1H 0AJ, United Kingdom

Potassium-ion batteries (PIBs) have captured rapidly growing attention due to chemical and economic benefits. Chemically, the potential of K^+/K was proven to be low (-2.88 V vs. standard hydrogen electrode) in carbonate ester electrolytes [1], which implies a high energy density using K-ion as the charge carrier and a low risk of K plating. K-ion has a high ion conductivity and thus a fast diffusion rate in carbonate ester electrolytes such as propylene carbonate [2]. Economically, K resource is practically inexhaustible and globally distributed [3], being reflected on the low price of potassium carbonate (\$1000 per tonne, compared with \$6500 for lithium carbonate) [4]. Also, the best performing PIB electrode materials so far do not contain Co and other high-price transition metals (TMs). Moreover, PIBs can employ Al to replace costly Cu as the anode current collector, because K does not thermodynamically form intermetallic compounds with Al, further reducing manufacture cost. In addition, PIBs can be manufactured using the existing plants in the lithium-ion battery (LIB) industry, ensuring a swift transition to commercial production.

Potassium battery chemistry is diverse. This is seen from a range of materials showing some of the best performance. Cathodes can be made from Prussian blue analogues (PBA), layered transition metal oxides (TMOs), and polyanionic compounds, all of which show competitiveness in one or more aspects of performance (voltage, capacity, rate capability, and cycle life). Unlike sodium battery chemistry, graphite is a star material for potassium battery anodes, in combination with various graphitic and non-graphitic carbons. Other anode materials (alloys, metal chalcogenides, etc) also show promises in high capacity and/or high power. The diversification of electrode materials will allow for the diversification of manufacturers' profiles and target markets.

The tremendous potential of PIBs has led to a recent announcement from an Austin-based battery start-up Group1 that they plan to commercialize a Prussian White cathode material for PIBs to benchmark the $LiFePO_4$ cathode used in LIBs, and they aim for a large-scale launch of the product by 2027 [5]. Besides the encouraging announcement from the private sector, significant research effort from academia has been devoted to developing PIBs in the last five years. A substantial number of publications have been seen from eastern Asia, US, Australia, and Singapore, and research projects on potassium batteries have been prioritized in some of the countries. In the UK, some recent investments from UK Research and Innovation have recognized the research prospects of potassium batteries [6, 7], aiming to diversify the UK's energy research portfolio of beyond-lithium batteries.

This 2023 PIB roadmap contains contributions from academics in the field of PIBs across the globe, highlighting the progress of PIB development. The contributions are divided into six research themes: (a) cathode materials; (b) anode materials; (c) computational discovery of materials; (d) electrolytes and solid-electrolyte interphase (SEI); (e) advanced characterization techniques; (f) economic analysis. They range from fundamental understanding of materials and computational science as well as solid-liquid interfacial processes, to methodological advances to develop understanding, and further to techno-economic metrics to guide the road towards future commercialization.

Sections 2 and 3 present an overview of the most up to date cathode and anode materials, respectively. Focus is given to electrode materials that are scalable and industry relevant (e.g. PBA and graphite), but sight is not lost on emerging materials (e.g. Mxene and metal-organic frameworks (MOFs)) that have the potential to become a game changer. Both inorganic and organic electrode materials (OEMs) are discussed, as they complement each other for diversified applications. In addition, computational insights into materials discovery for PIBs are presented in section 4, with an emphasis on computational screening of materials candidates and understanding of electrode intermediates, as well as the promise of machine learning and artificial intelligence.

Electrolytes and SEI of PIBs are presented in section 5. Anions and solvents are equally important components of PIB electrolytes, but the interactions between K-ion and anions/solvents are ambiguous and as a result, one of the most intriguing aspects of PIBs. This section covers electrolyte salts and solvents as well as emerging ionic liquid (IL) electrolytes, with the focus on molecular designs and cation solvation structure. Moreover, electrolyte plays a crucial role in dictating interfacial chemistry. At present, there are many unknown underlying mechanisms and massive uncertainties associated with SEI layer; therefore, we included a subsection on SEI layer, given its extremely challenging but fascinating nature.

Furthermore, understanding of the complexity of the electrode/electrolyte interface and the charge storage processes in electrode materials during PIB operation, particularly in a short-range and at an atomic scale, is of paramount importance in drawing correlations between materials/structural design and PIB

performance. Section 6 describes advanced characterization techniques that are placed at a strong position to aid the acquisition of the understanding. In addition, PIB is a complicated system where all components perform a concerted action, and thus we include a subsection covering *in-situ* characterizations as a powerful means to capture intermediate states of the components and decipher the action. Finally, we present in section 7 a techno-economic analysis of PIBs in comparison with LIBs to reveal economic benefits and drawbacks, directing develop strategies to improve the economic viability of PIBs.

This collective roadmap is not an exhaustive list and intensive discussions of electrode materials and cell components of PIBs. For this purpose, readers are recommended to consult previously published review articles focusing on a comprehensive summary of PIBs [8, 9] and specific cell components such as cathode [10, 11], anode [12, 13], and electrolyte [14]. Instead, the roadmap is to provide insights into scientific and technological advances based on the challenges faced by the PIB field, thus signposting potential future research directions. Furthermore, the roadmap serves as a referencing platform for researchers at different career stages and working on different energy materials and technologies. We hope the roadmap is an introductory reading of PIBs for the public and provides key information of PIBs to private sectors and government organizations. While the PIB technology is at its infancy, the maturity of the technology will be fast increased in the next decade, making it a competitor technology in certain applications.

2. Layered TMOs

Eun Jeong Kim, Tomooki Hosaka and Shinichi Komaba

Department of Applied Chemistry, Tokyo University of Science, 1-3 Kagurazaka, Shinjuku, Tokyo 162-8601, Japan

Email: eunjeong.kim@rs.tus.ac.jp, hosaka@rs.tus.ac.jp and komaba@rs.tus.ac.jp

Status

Given the success of layered lithium TMOs in commercialization, and their superiority over other chemistries for LIBs and sodium-ion batteries (SIBs), scientific interest in layered potassium TMOs ($K_x\text{MeO}_2$) as cathode materials in PIBs has spontaneously generated, expecting analogous performance to that of Li and Na counterparts. In fact, early studies on $K_x\text{MeO}_2$ were limited on synthesis, structural characterization, and electrochemical interaction in aqueous K-ion capacitors. Since Vaalma *et al* [15] reported reversible K^+ (de)intercalation in $K_{0.3}\text{MnO}_2$ in aprotic K cells, extensive studies on $K_x\text{MeO}_2$ in PIBs have been performed.

Most of $K_x\text{MeO}_2$ that have been explored in PIBs exhibit K-deficient phases, adopting P(')2- or P(')3-type structures because larger ionic radius of K^+ than Na^+ renders O(')3 structure unstable. The symbols of P2, P3 and O3 follow the notification proposed by Delmas *et al* [16], P and O indicates the coordination of trigonal prismatic and octahedral K^+ sites, respectively, and the number corresponds to the number of MeO_2 slabs in a hexagonal unit cell. When the hexagonal lattice is distorted, prime symbol (') is added between the alphabet and the number while the number of MeO_2 is counted in a pseudohexagonal unit cell.

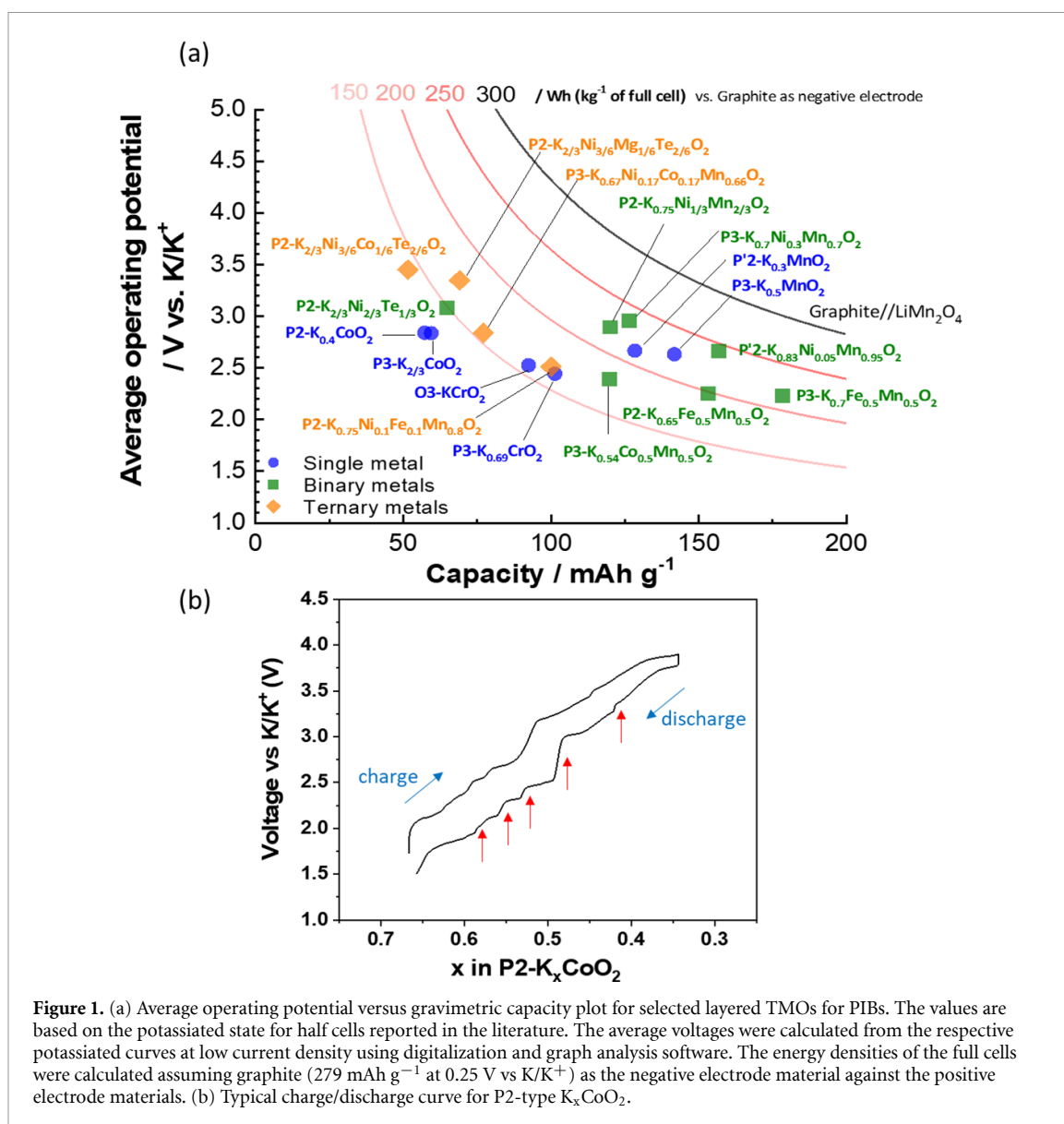
According to Kim *et al* [17], strong K^+ - K^+ electrostatic repulsion in $K_x\text{MeO}_2$ is responsible for unstable O3 phase at high K concentration except KCrO_2 and KScO_2 . The peculiar case of stoichiometric KCrO_2 originates from the strongly preferred CrO_6 coordination with the electronic configuration of Cr^{3+} (half-filled t_{2g}). In the case of KScO_2 , the large enough ionic radius of Sc^{3+} is the reason as the penalty from the K^+ - K^+ repulsion is compensated. In this respect, design of high K concentration compounds would be feasible using large Me (III, IV) ions. Albeit the disadvantage due to the strong K^+ - K^+ repulsion, it can play a positive role in suppressing phase transformation. In contrast to Li and Na systems, interslab distance for $K_x\text{MeO}_2$ progressively expands or remains constant upon depotassiation regardless of phase changes such as P3 to O3 [18], resulting in less favorable Me migration into the interslab through the intermediate tetrahedral site. Besides, the preference for crystallizing in P-type structure is expected to offer lower K^+ diffusion barrier with open path for K^+ compared to that in O-type structure. Easy crystallization at relatively lower temperature for $K_x\text{MeO}_2$ in comparison with Na_xMeO_2 can also be a benefit, providing environmentally and cost friendly synthetic conditions [19].

Current and future challenges

Current and future challenges associated with $K_x\text{MeO}_2$ are linked to the enhancement of their energy density since the inferiority of average operating potential and capacity for $K_x\text{MeO}_2$ offer lower energy density than the LIB based on graphite and LiMn_2O_4 (figure 1(a)).

The limited capacity, that is a narrow intercalation range, is the consequence of significantly inclined voltage slope and multiple plateaus in voltage curves. These features are essentially related to the large ionic radius of K^+ that increases the interslab spacing, rendering the oxygen–oxygen distances between MeO_2 slabs much apart. Thereby the oxide anions of MeO_2 slabs weakly screen the K^+ - K^+ repulsion and yields several intermediate phases stabilized upon (de)intercalation which are often emerged due to K^+ -vacancy ordering [20, 21]. Most of $K_x\text{MeO}_2$ consisting of a single Me characterizes the stepwise voltage curves where the voltage jumps are related to the formation of highly stable phases in a narrow K^+ concentration range [22]. For example, five voltage jumps (red arrows) are observed for P2- $K_x\text{CoO}_2$ between 1.5 and 3.9 V (figure 1(b)) [19]. Although detailed studies are required to understand the complex voltage curve, a significant jump at $x \approx 0.5$ is most likely related to the peculiar K^+ -vacancy ordering. As K^+ cations prefer to remain locked in their sites, such ordered structure generally induces additional activation energy barrier for K^+ diffusion, reducing K^+ mobility [23].

The multiple plateaus are related to the two-phase reactions during which the newly emerged phases either retain an original framework or adopt different crystal structures due to distortion and/or gliding of MeO_2 slabs. To ensure reversible phase transition, optimization of voltage window is required as shown in the $K_{0.3}\text{MnO}_2$ [15]. Despite of its relatively high capacity delivered in 1.5–4.0 V, capacity fade is notable over cycling. Lowering the upper cut-off voltage to 3.5 V permits stable cyclability [15]. The reasons for the capacity fade can be attributed to structural degradation as reported in P3- $K_{0.5}\text{MnO}_2$ where stacking faults at the deep charge state are repeatedly formed and the defects are only partially recovered. Another example is



O3-KCrO_2 that becomes amorphous-like phase after charge to 4.5 V without recovery to the original phase even after subsequent discharge to 1.5 V [17].

In addition to the aforementioned issues, chemical instability of K_xMeO_2 in air and highly preferred K-deficient compounds at a pristine state are major challenges to be solved for practical application, considering that stoichiometric K_xMeO_2 tends to be less stable in air.

Advances in science and technology to meet challenges

Scientific efforts for development of K_xMeO_2 should be centered around optimal material design to overcome the limited energy density. As previously mentioned, large Me atoms favor to stabilize fully occupied KMeO_2 , adopting O3 phase (figure 2). From this point of view, a judicious selection of the large Me can accommodate a reasonable $\text{K}^+ - \text{K}^+$ distance, increasing concentration of K^+ at a pristine state. In addition, the use of large Me can render voltage slopes less inclined, providing wider K^+ intercalation range in a set voltage window. This can be explained by the influence of $\text{K}^+ - \text{K}^+$ repulsion on Me–O bond length [8]. For example, the $\text{K}^+ - \text{K}^+$ repulsion change upon deintercalation of K^+ in K_xRhO_2 is expected to be less significant than that in K_xCoO_2 because Rh offers reasonably enlarged $\text{K}^+ - \text{K}^+$ distance, resulting in less pronounced evolution in Rh–O bond length as a function of K^+ concentration. In the case of K_xCoO_2 , the impact of $\text{K}^+ - \text{K}^+$ repulsion on Co–O bond length becomes more significant by varying K^+ concentration. One may concern the decrease in potential at a given K^+ concentration induced by more covalent character of Me–O with larger Me. Therefore, pros and cons for the large Me strategy should be balanced by cation permutation.

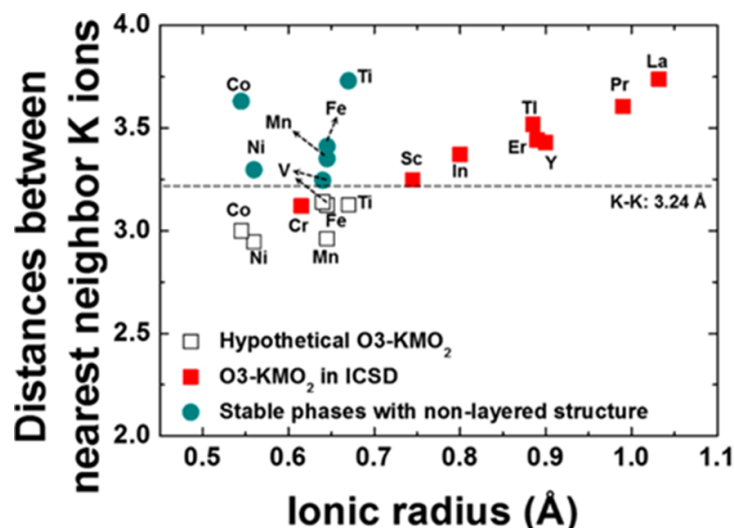


Figure 2. Plots of distance between nearest-neighbor K^+ versus ionic radius of metals in KMO_2 . The open and filled squares are unstable (hypothetic) and stable (reported in the ICSD) compounds with layered structures, respectively. The filled circles are the stable compounds with nonlayered structures. Reprinted with permission from [17]. Copyright (2018) American Chemical Society.

Multiple Me systems are ones that improve electrochemical properties by cooperative effects of Me such as smoothing voltage curves, increasing average operating potential, maintaining structural integrity, etc. Regarding cost-effective approaches, the use of earth abundant Mn and Fe is attractive and P2- and P3-type $K_xFe_{0.5}Mn_{0.5}O_2$ deliver large capacities, originating from their rational morphological designs, e.g. hierarchical morphology consisting of primary nanoparticles (≈ 100 nm) and nanowire [24, 25]. Despite of practical difficulties of manipulating nanoparticles, integrating unique morphological designs can provide synergistical effects based on their individual characteristics. In the same vein, heterostructure compounds would be beneficial to improve electrochemical performance as O3/P2 mixed phase is applied in commercial SIBs [26].

Among various Me, Ni is also preferred as the Ni-based compounds can offer high average operating potential and specific capacity. While the beneficial effects of Ni substituted $KMeO_2$ have been widely studied, the presence of honeycomb ordering between Te and Ni/M in $K_{2/3}Ni_{2/3-x}M_{1/3-x}Te_{1/3}O_2$ ($x = Mg, Co$) [27] shows interesting electrochemical properties such as the highest average operating potential among $KMeO_2$ and activation of oxygen redox. Cumulative cation and anion redox processes can offer a means of enhancing capacity, however lattice oxygen loss and large voltage hysteresis should be suppressed.

Concluding remarks

The potential rewards for $KMeO_2$ in terms of green economy and cost-effectivity make it as an important family for future development of PIBs. However, achieving both high capacity and high average operating potential is a major challenge with regard to the successful exploitation. Recent efforts to smooth the voltage curves, retain the structural stability as well as reversibility, trigger the anion redox through the application of multiple Me are intriguing. Regarding the anion redox, two mechanisms could be considered: (i) the formation of non-bonded O $2p$ states pinned just below the Fermi level and (ii) ligand-to-metal charge transfer, called as reductive coupling mechanism. Since the formal scenario often occurs with structural changes, a careful selection of Me to mitigate the phenomena is critical. Based on the dynamic ligand-to-metal charge transfer mechanism [28], recently proposed to rationalize the latter, high-covalent Me–O systems can accelerate oxygen redox, which would be the case for K_xMeO_2 with $4d$ or $5d$ Me. Further examination of the influence of large Me in combination with the effect of substituted elements will assist the enhancement in the electrochemical performance. In addition to that, fundamental understanding on the influence of mixed morphological designs, crystal phases may provide synergistical enhancement.

Acknowledgments

The authors thank the JSPS KAKENHI (Grant Nos. JP18K14327, JP20J13077, JP20H02849, and JP21K20561) for financial support.

3. Prussian blue and analogues

Yang Xu and Henry R Tinker

Department of Chemistry, University College London, 20 Gordon Street, London WC1H 0AJ, United Kingdom

Email: y.xu.1@ucl.ac.uk

Status

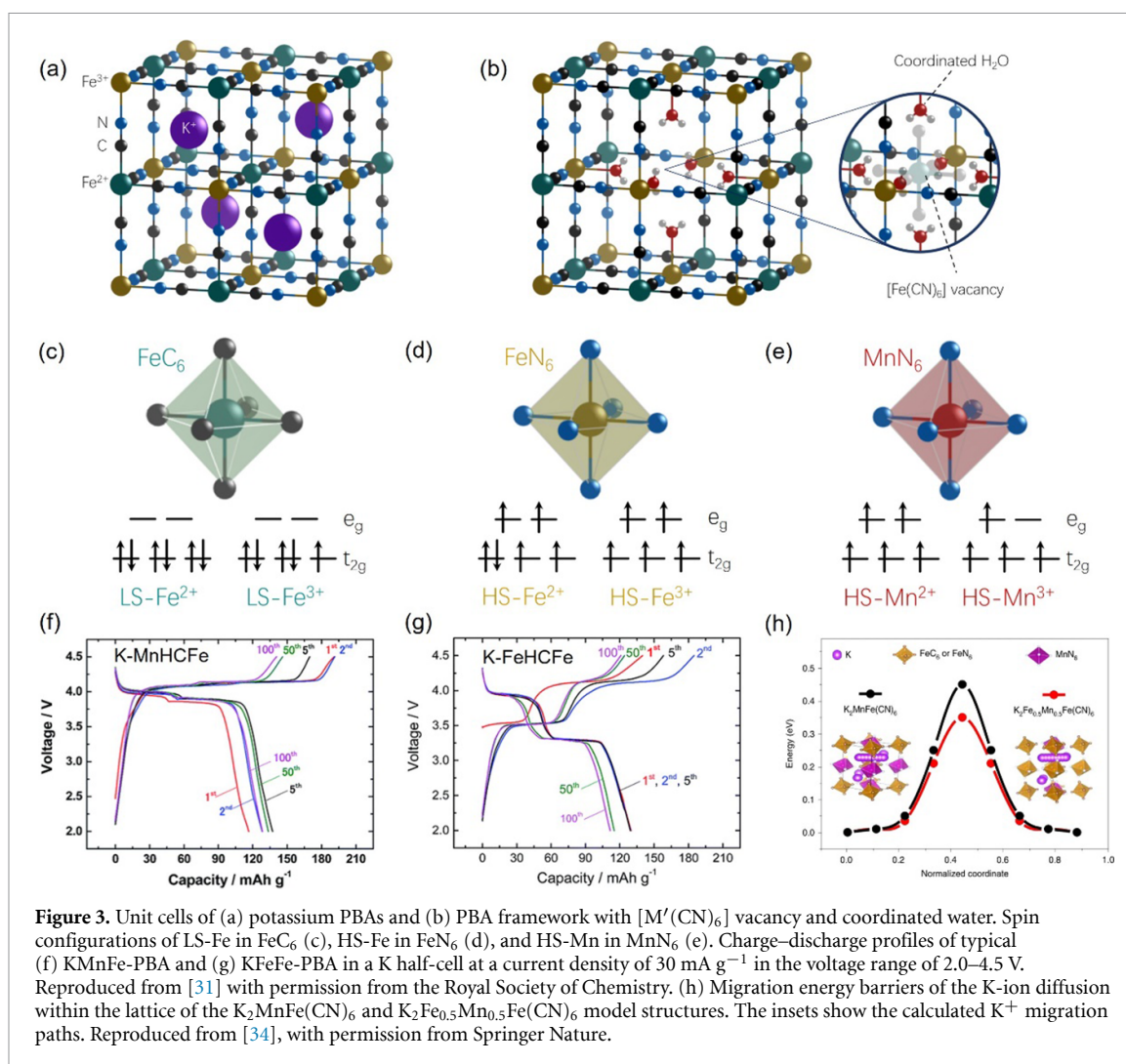
PBAs are widely studied cathode materials for PIBs with the general formula $K_xM[M'(CN)_6]_{1-y} \cdot zH_2O$ (figures 3(a) and (b)), where M and M' are TMs, most commonly Fe, Mn, or Ni, y is the number of $[M'(CN)_6]^{n-}$ vacancy, and z is the number of H_2O molecules, either occupying K sites (interstitial water) or coordinating to M metal at vacancy sites (coordinated water). MN_6 and $M'C_6$ octahedra are alternatively connected by $-CN-$ linkers forming a cubic framework structure that has open diffusion channels along the $\langle 100 \rangle$ directions to allow for K diffusion. PBAs can be synthesized using low-cost aqueous reactions from abundant precursors and hence, PBAs capitalize on the key advantage of PIBs, a cost-effectiveness and environmentally sustainable alternative to LIBs. Recognized as a K host in 2004 [29], PBAs did not receive extensive interest as PIB cathodes until the work by Zhang *et al* [30]. In the past five years, there has been a significantly improvement in the electrochemical performance of PBAs, making them one of the most promising PIB cathode materials.

Currently, KMnFe-PBA and KFeFe-PBA are the best performing PBA cathodes. KMnFe-PBA enjoys a high average discharge voltage, owing to the high Mn^{3+}/Mn^{2+} redox potential. $K_{1.75}Mn[Fe(CN)_6]_{0.93} \cdot 0.16H_2O$ [31] and $K_{1.89}Mn[Fe(CN)_6]_{0.92} \cdot 0.75H_2O$ [32] delivered an average voltage of 3.8–3.9 V (*vs.* K^+/K , figure 3(c)) and a high capacity of >140 mAh g^{-1} , resulting in a high energy density comparable to that of $LiCoO_2$, but the Jahn–Teller (JT) active high-spin (HS) Mn^{3+} (figure 3(e)) can cause structural distortion by the repeated phase transition from cubic (Mn^{2+}) to tetragonal (Mn^{3+}) [31, 33]. Comparing to KMnFe-PBA, KFeFe-PBA has less JT distortion of low-spin (LS) Fe^{3+} (figure 3(c)) and HS- Fe^{2+} (figure 3(d)), which benefits cycling stability. However, the lower Fe^{3+}/Fe^{2+} redox potential compromises the average discharge voltage (~ 3.6 V, figure 3(d)). A variety of strategies were used to control crystallinity, particle size, morphology, surface coating, and doping, aiming to improve the redox activity of TMs, structural stability, and K diffusivity, but not for all. Despite the reported capacity of PBAs approaching their theoretical values, reasonable rate capability is limited to ~ 3 C (≤ 500 mA g^{-1}) without the presence of carbons. High rate capability and cycling life exceeding thousands of cycles are only seen in aqueous K electrolytes, because the interfacial charge transfer kinetics are far more favorable than in organic electrolytes [34, 35]. This highlights the vital need for a good understanding of PBAs' structural complexities to rationalize the crystal structure—electrochemical performance relationship.

Current and future challenges

Extensive research has been carried out to address two issues: $[Fe(CN)_6]^{4-}$ vacancy and water. $[Fe(CN)_6]^{4-}$ vacancies are believed to worsen the structural stability and maximum capacity of PBAs, because it reduces usable redox-active Fe^{2+} and K uptake (charge compensation). A common synthetic approach to suppress vacancy formation is chelate-assistance precipitation. Chelating agents such as citrate and ethylenediaminetetraacetic acid (EDTA) enabled 6% vacancy in KFeFe-PBA [36] and 0.6% vacancy in KMnFe-PBA [37], respectively. Another approach uses a single Fe-precursor in an acidic solution to realize slow Fe^{2+} release from the $[Fe(CN)_6]^{4-}$ precursor and thus slows precipitation, suppressing the vacancy to, e.g. 3% in KFeFe-PBA [38]. In all cases, high capacities of >135 mAh g^{-1} were obtained. Interstitial water occupies K sites, competing with K intercalation, while coordinated water links to the exposed M metal sites, strongly correlating with $[Fe(CN)_6]^{4-}$ vacancy, as it exposes M metal. The influence of water content on the performance of PBAs is complicated. Water is responsible for side reactions, as it can react with electrolytes once released from the structure or oxidize inside the structure at a high voltage (>4 V), worsening coulombic efficiency (CE). However, one can argue that unlike the removal of interstitial water improving the SIB performance of PBAs [39], no such observation has been reported for PIBs. Whether water content does not influence the phase transition of PBAs in PIBs to the same extent as in SIBs, or water may reduce volume change of PBAs, potentially enhancing structural stability [40]; these remain open questions for PIBs and require in-depth investigation.

Unlike M' metal, M metal enjoys a diverse substitution and hence it is challenging to understand how exactly M metal substitution affects performance. Substituting JT-active Mn with JT-inactive Fe [34] effectively inhibited the tetragonal phase transition during the charging process and reduce K-ion migration energy barrier (figure 3(e)), enabling a lifespan over 10 000 cycles at a 100 C rate. A 5% substitution of HS-Fe

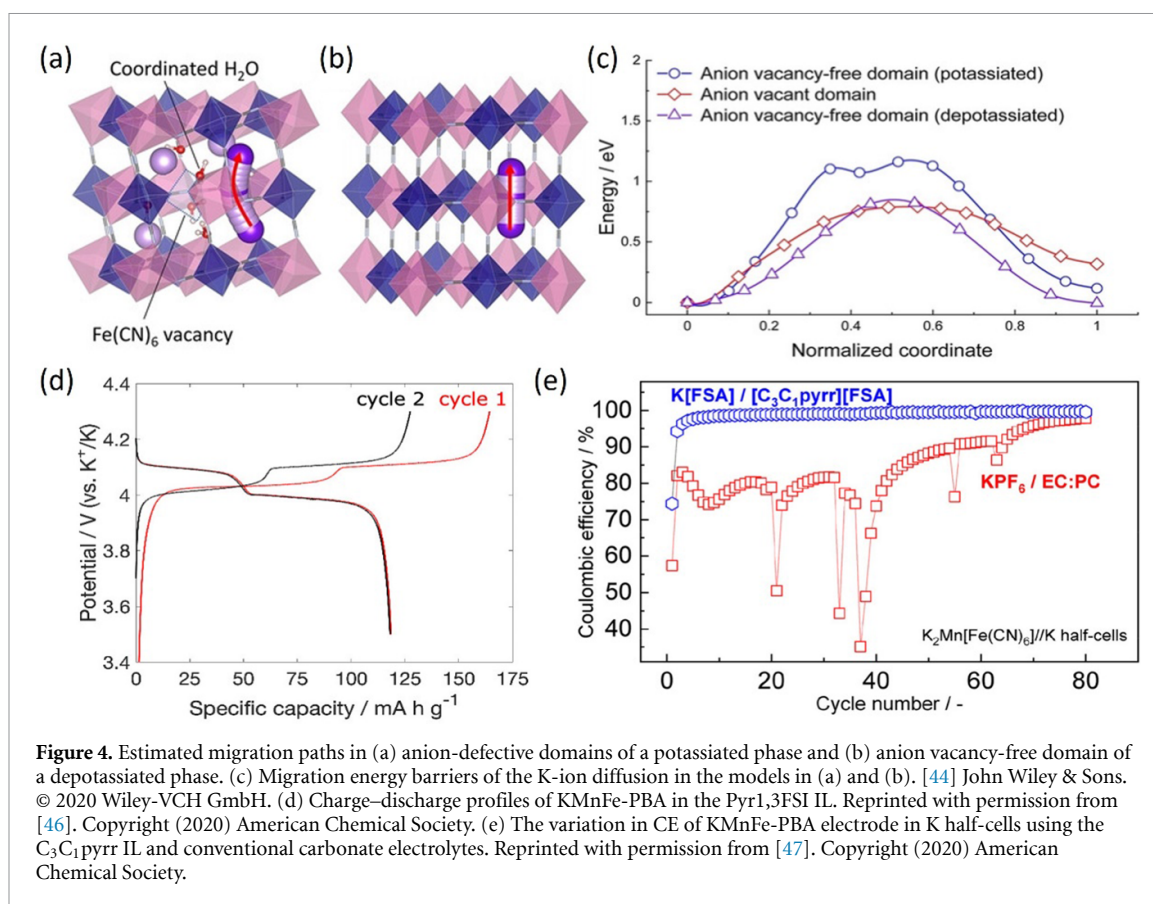


by Ni ($K_2Ni_{0.05}Fe_{0.95}Fe(CN)_6$) [41] can enhance the redox activity of the LS-Fe (difficult to be fully activated) in the structure, because the substitution weakens the crystal field splitting of the LS-Fe and eases the electron transfer from e_g to t_{2g} orbitals. Therefore, synthesizing PBAs with multiple M metals, be it electrochemically active or not, may present an exciting research direction to fine tune the capacity, rate capability, or cycling life of PBAs.

Advances in science and technology to meet challenges

Minimum $[Fe(CN)_6]^{4-}$ vacancy is being highly pursued for PBA cathodes. An interesting contrast is that the best performing PBA cathodes have both low vacancies ($<10\%$) and a small size of primary crystals, typically $<400\text{ nm}$, whereas those with similarly low vacancies but with sizes in the micrometer size range demonstrated inferior performances, which was simply ascribed to the size effect, i.e. a kinetic limitation in K diffusion distance. One would question if minimum $[Fe(CN)_6]^{4-}$ vacancy is absolutely crucial? Computational simulations carried out by Ishizaki *et al.*, suggested anion vacancies in $Fe[Fe(CN)_6]_y$ can enhance K diffusion [42]. This means that K diffusion could take a detour along vacancies other than the $<100>$ channels [43], being distinct from smaller sized Na and Li. Komaba's group showed that despite a large size of several micrometers, $Na_{0.10}K_{1.58}Mn[Fe(CN)_6]_{0.85}$ delivered a large capacity ($\sim 140\text{ mAh g}^{-1}$ at 0.1 C) and great rate capability ($\sim 100\text{ mAh g}^{-1}$ at 10 C), and the enhancement of K diffusion was enabled by a 15% vacancy (figures 4(a)–(c)) [44]. Furthermore, $[Fe(CN)_6]^{4-}$ vacancy may accommodate the JT-driven axial distortions of the MN_6 octahedra by aligning the longer M–N bonds with the vacancy, which avoids long-range distortions and stabilizing crystal structure [45]. It would be exciting to see if such a benefit can be experimentally proven for K intercalation.

Conventional KPF₆/carbonate ester based electrolytes are unstable at high potentials, resulting in a low CE ($<95\%$), which is critical for high-voltage $KMnFe$ -PBA. Electrolyte formation is an emerging research direction for PBA cathodes, particularly in regard to IL, due to its high-temperature stability, wide



electrochemical stability window, and high ionic conductivity at room temperature. Foire *et al* used 1 mol kg⁻¹ potassium bis(fluorosulfonyl)imide (KFSI) in the IL N-butyl-N-methylpyrrolidinium bis(fluorosulfonyl)imide (Pyr1,3FSI) as the electrolyte for KMnFe-PBA (figure 4(d)), achieving a stable CE of 99.3% and capacity retention of 87.4% over 100 cycles [46]. A similar electrolyte using the IL N-methyl-N-propylpyrrolidinium (C₃C₁pyrr) showed no corrosion of the Al current collector above 4 V and outperformed conventional electrolytes (figure 4(e)) [47]. These results are encouraging in terms of safely and efficiently operating PBA cathodes, but more electrolyte formulations need to be explored, and K solvation and transport properties should be investigated, particularly regarding solid–liquid interfacial kinetics. Researchers should also be mindful of the high cost and tedious preparation/purification of ILs. The use of ILs could be counterproductive to the purpose of developing cost-effective and sustainable PIB technology.

Concluding remarks

The structural complexity of PBAs makes them a challenging class of compounds to investigate for PIBs and opens much space to produce knowledge, even unknown, of the crystal structure—electrochemical performance relationship. Improvements have been made through the fine tuning the PBAs synthesis and untangling the web between vacancy, water content and crystal size. The latter should be a focus going forward, in combination with phase transition during K (de)intercalation. Further improvement will be enabled through investigating morphologies, coating, composites, and suitable dopants. The potential of PBAs as cathode materials in K system is unambiguous, in terms of both cost and performance. A good understanding of PBAs' structural complexity and their interactions with K and electrolytes at a fundamental level, particularly in a full-cell configuration, will foster future advancement of PIB technology.

Acknowledgments

The authors gratefully acknowledge the support of the Engineering and Physical Sciences Research Council (EP/V000152/1, EP/X000087/1), the Leverhulme Trust (RPG-2021-138), and the Royal Society (RGS\R2\212324, SIF\R2\212002). For the purpose of open access, the author has applied a Creative Commons Attribution (CC BY) licence to any Author Accepted Manuscript version arising.

4. Polyanionic compounds

Tomooki Hosaka and Shinichi Komaba

Department of Applied Chemistry, Tokyo University of Science, 1-3 Kagurazaka, Shinjuku, Tokyo 162–8601, Japan

Status

The well-known polyanionic compound, olivine-type LiFePO_4 , has been utilized in commercial LIBs, even for electric vehicles, due to cost-effectiveness, excellent thermal stability, and long-term cycle performance [48]. Following the great success of olivine-type LiFePO_4 in LIBs [49], K-ion insertion into polyanionic compounds has been intensively studied [49, 50]. Polyanionic frameworks consist of MO_x ($M = \text{TMs}$) and $(\text{XO}_4)^{n-}$ ($X = \text{P, S, As, Si, Mo, or W}$) polyhedra, which can offer an open framework structure allowing fast ionic diffusion of the alkali metal ions. Moreover, polyanionic compounds generally show higher operating potential than layered TMOs due to the inductive effect [51]. The increase in redox potential is caused by the decrease in the covalency of the $M\text{--O}$ bonds, which is reduced by the highly covalent $X\text{--O}$ bond [52].

Figure 5(a) shows the discharge capacity and discharge voltage of reported polyanionic compounds for PIBs. At the early stage, K-ion insertion into amorphous FePO_4 [53] and heterosite- FePO_4 [50], which is delithiated phase of olivine-type LiFePO_4 , were investigated in K cell. Amorphous FePO_4 showed reversible K-ion insertion with a capacity of $>150 \text{ mAh g}^{-1}$, whereas the average discharge potential was as low as $\sim 2 \text{ V}$ [53]. Similarly, heterosite- FePO_4 delivered low discharge potential and significant crystallinity lowering after K-ion insertion [50]. This result indicates that the tetrahedral sites in heterosite- FePO_4 are not suitable for the insertion of large K^+ ions. Moreover, thermodynamically stable KFePO_4 (space group: $P2_1/n$) is electrochemically inactive, except for nanoparticles, because of the lack of an ionic diffusion path [50, 54]. Therefore, polyanionic compounds that can reversibly accommodate K^+ ions have been explored. NASICON-type $\text{K}_3\text{V}_2(\text{PO}_4)_3$ are electrochemically active as both cathode and anode materials [55]. In addition, a series of KTiOPO_4 (KTP)-type materials such as KVPO_4F [56, 57], KVOPO_4 , [58] KFeSO_4F [50], and KTiPO_4F [58] have been attracted attention as promising cathode materials. Figures 5(b) and (c) show the structures, the K diffusion paths, and activation energies estimated by bond valence energy landscape (BVEL) calculations [59] for NASICON-type $\text{KTi}_2(\text{PO}_4)_3$ and KTP. In the NASICON-type structure, although K^+ ions have a three-dimensional (3D) diffusion path, their activation energy is as high as 3.46 eV. In contrast, K^+ ions can diffuse easily along the b -axis in KTP structure as the activation energy is 0.52 eV (figure 5(c)). Moreover, KTP-type KVOPO_4 showed small lattice volume changes of -3.3% during K-ion extraction [57].

Because of the structural and compositional diversity, there is significant room for material exploration in polyanionic compounds to demonstrate high-rate and long-life PIBs. In addition, optimization of structure and composition could maximize the energy density.

Current and future challenges

The major challenges of polyanionic compounds are to achieve high energy density and high electronic/ionic conductivity. The reported materials delivered a reversible capacity of $<130 \text{ mAh g}^{-1}$ or working voltages of $<4 \text{ V}$ (figure 5(a)), leading to a lower energy density of PIBs than that of LIBs. The theoretical capacity of the polyanionic compounds is $100\text{--}135 \text{ mAh g}^{-1}$ based on a one-electron redox of M . Since the multi-electron reaction of $\text{V}^{3+/4+/5+}$ could be active in an appropriate voltage range, $\text{K}_n\text{V}(\text{III})_m(\text{XO}_4)$ ($n/m > 1$) are the potential high-energy cathode materials.

Even when the reversible capacity is restricted to $\sim 130 \text{ mAh g}^{-1}$, a practical energy density can be achieved by demonstrating a 4 V-class operation. Previous studies highlighted the significant impact of the primary inductive effect (figure 6(a)), coordination arrangement (figure 6(b)), and secondary inductive effect from the alkali metal ion (figure 6(c)) on the redox potential [51, 52, 60]. To analyze the influence of these factors, we performed a multiple regression analysis. The experimental average discharge potentials were fitted using the following descriptors: representative redox potential of $M^{n/(n+1)}$ redox couples (E_M) that are redox potentials of NASICON-type materials in Li cells [49], a number of anion groups (N_{PO_4} , $N_{\text{P}_2\text{O}_7}$, N_{SO_4} , N_{F}) coordinated to M (figure 6(a)), edge-sharing (N_{edge} , figure 6(b)), and commonly shared oxygen (N_{O} , figure 5(c)) [22, 60] per M . Figure 6(d) shows experimental vs. predicted average discharge voltage plots from the multiple linear regression. The results well fitted experimental values with R^2 value of 0.917 and the following regression equation:

$$V_{\text{ave}} = 1.2 \times E_M + 0.63 \times N_{\text{F}} + 0.52 \times N_{\text{edge}} + 0.48 \times N_{\text{SO}_4} + 0.38 \times N_{\text{P}_2\text{O}_7} + 0.29 \times N_{\text{PO}_4} + 0.08 \times N_{\text{O}} - 3.0.$$

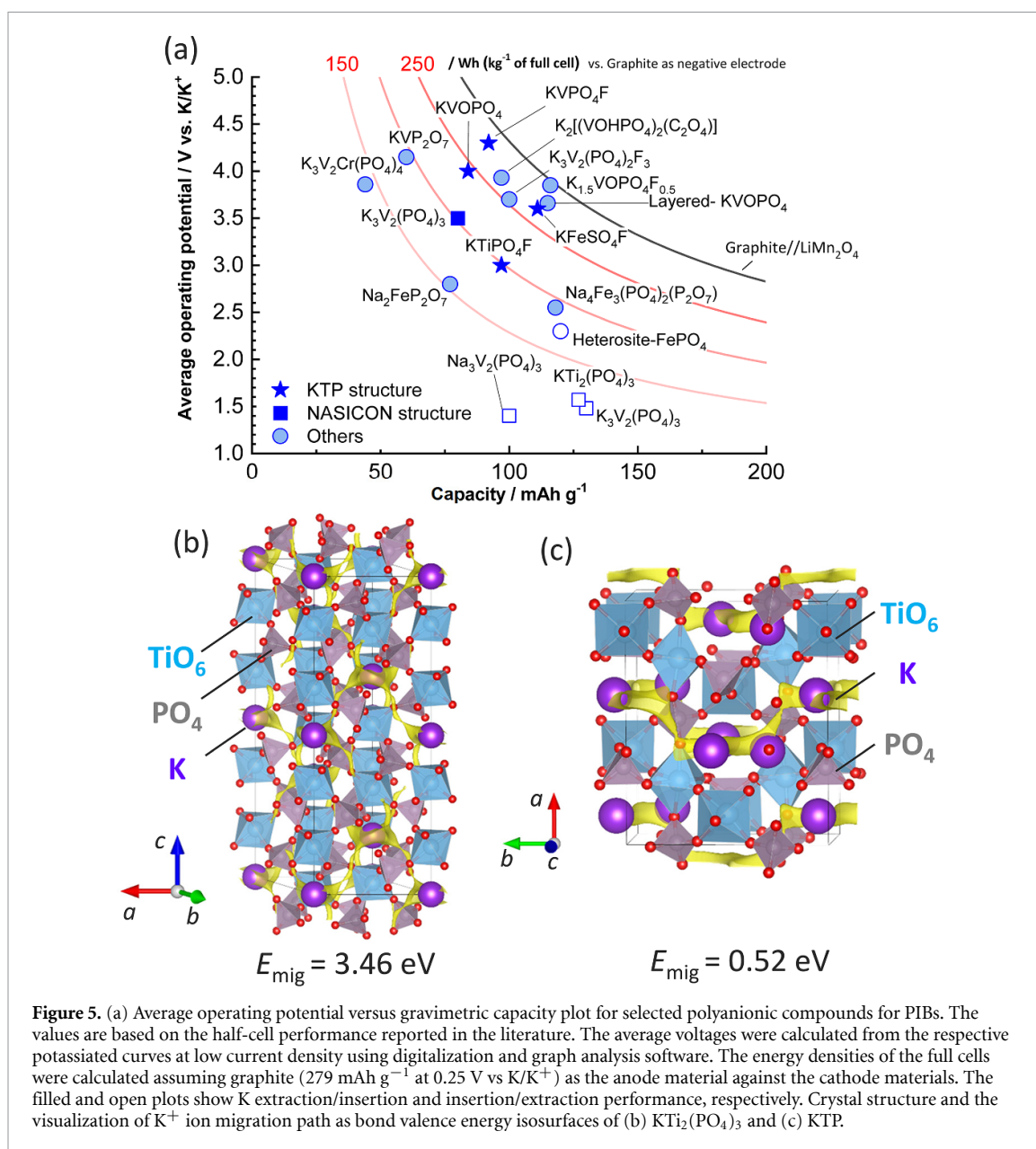


Figure 5. (a) Average operating potential versus gravimetric capacity plot for selected polyanionic compounds for PIBs. The values are based on the half-cell performance reported in the literature. The average voltages were calculated from the respective potassiated curves at low current density using digitalization and graph analysis software. The energy densities of the full cells were calculated assuming graphite (279 mAh g^{-1} at 0.25 V vs K/K^+) as the anode material against the cathode materials. The filled and open plots show K extraction/insertion and insertion/extraction performance, respectively. Crystal structure and the visualization of K^+ ion migration path as bond valence energy isosurfaces of (b) $KTi_2(PO_4)_3$ and (c) KTP.

Figure 6(e) shows the partial regression coefficients and their p -values, which are the probabilities that the true coefficients are 0. Obviously, the E_M was an important factor, with large regression coefficients and a low p -value (<0.05). All other descriptors showed positive regression coefficients, and the p -values for N_F , N_{SO_4} , and $N_{P_2O_7}$ were less than 0.05, statistically significant. Note that the p -value for N_{edge} was >0.05 , probably because only $FePO_4$, $Na_4Fe_3(PO_4)_2(P_2O_7)$, and $Na_2FeP_2O_7$ have edge-sharing. Regarding the primary inductive effect, the order of the regression coefficients, i.e. the impact on the potential increase, was $(PO_4^{3-}) \leq P_2O_7^{4-} \leq SO_4^{2-} \leq F^-$, which is consistent with the trend in Li-ion insertion and the order of covalency of the polyanion group [49, 52]. Furthermore, this analysis suggests that up to ~ 3.4 and $\sim 3.7 \text{ V}$ operations can be demonstrated in $Fe-P_2O_7-F$ and $Fe-SO_4-F$ systems. These results demonstrate the significant importance of structural and compositional optimization to increase redox potentials and energy density.

Advances in science and technology to meet challenges

In this section, the technologies and strategies for developing materials with superior electrochemical properties will be discussed. In recent years, computational screening has been available thanks to the development of databases and calculation methods. For example, BVEL calculations can estimate ion diffusivity with low calculation costs [59]. Moreover, density functional theory (DFT) calculation is widely used to estimate ionic diffusion barriers and open-circuit potentials [61]. Combining these methods with

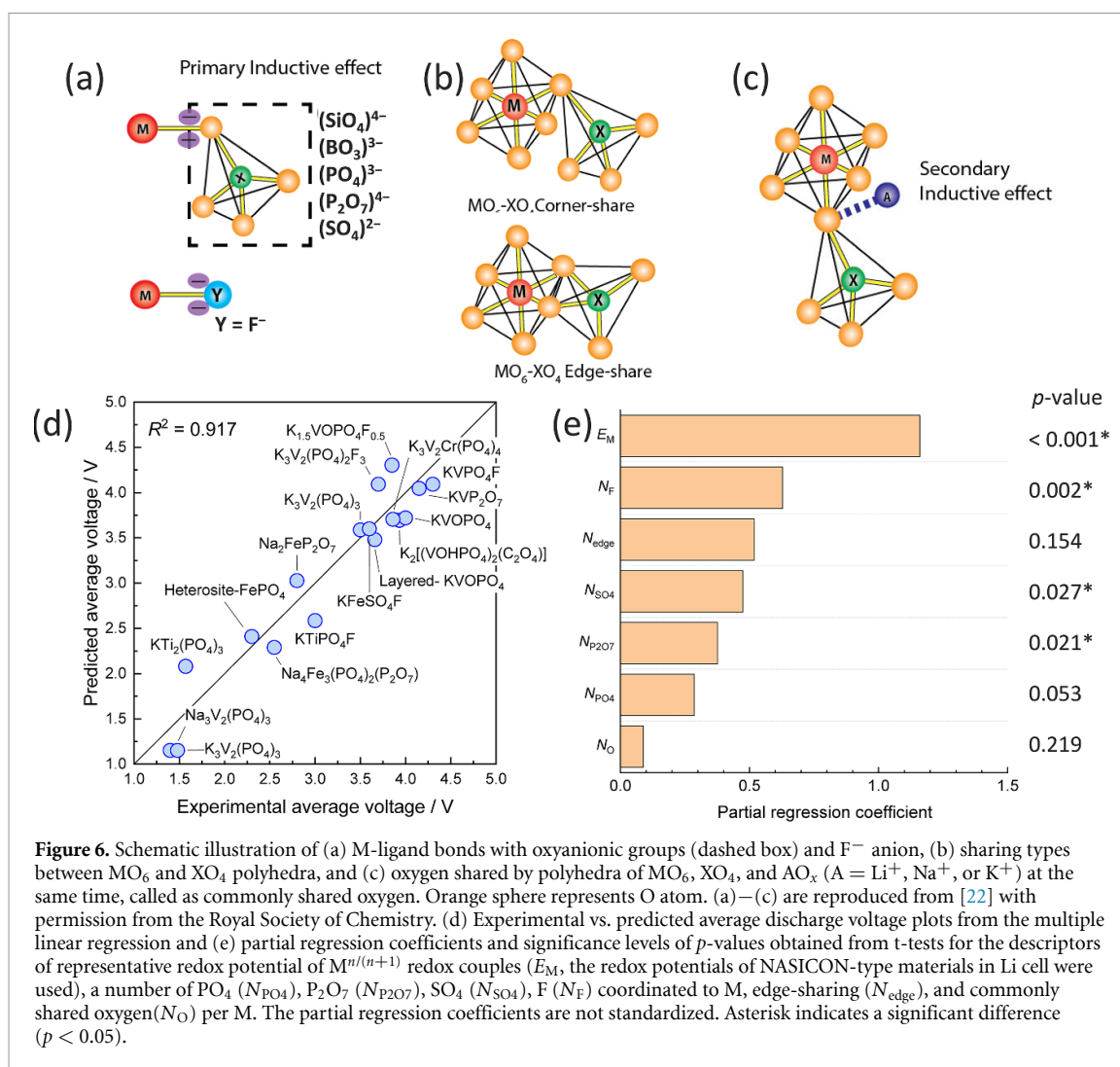


Figure 6. Schematic illustration of (a) M-ligand bonds with oxyanionic groups (dashed box) and F^- anion, (b) sharing types between MO_6 and XO_4 polyhedra, and (c) oxygen shared by polyhedra of MO_6 , XO_4 , and AO_x ($A = \text{Li}^+$, Na^+ , or K^+) at the same time, called as commonly shared oxygen. Orange sphere represents O atom. (a)–(c) are reproduced from [22] with permission from the Royal Society of Chemistry. (d) Experimental vs. predicted average discharge voltage plots from the multiple linear regression and (e) partial regression coefficients and significance levels of p -values obtained from t-tests for the descriptors of representative redox potential of $\text{M}^{n/(n+1)}$ redox couples (E_M , the redox potentials of NASICON-type materials in Li cell were used), a number of PO_4 (N_{PO_4}), P_2O_7 ($N_{\text{P}_2\text{O}_7}$), SO_4 (N_{SO_4}), F (N_F) coordinated to M, edge-sharing (N_{edge}), and commonly shared oxygen (N_O) per M. The partial regression coefficients are not standardized. Asterisk indicates a significant difference ($p < 0.05$).

experimental search, we can find candidate materials with a minimum number of experiments. Indeed, Wang *et al* screened polyanionic compounds from inorganic crystal structure database (ICSD) with K content, TM valence, theoretical capacity, and working potential estimated by DFT calculations [62]. As a result, they found $\text{K}_2\text{Mn}_2\text{P}_2\text{O}_7\text{F}_2$, $\text{K}_2\text{Fe}_2\text{P}_2\text{O}_7\text{F}_2$, $\text{K}_2\text{MnP}_2\text{O}_7$, $\text{K}_6\text{V}_2(\text{PO}_4)_4$, and $\text{K}_3\text{Cr}_3(\text{PO}_4)_4$ as potential positive electrode materials and synthesized them. Furthermore, $\text{K}_3\text{V}_2\text{Cr}(\text{PO}_4)_4$ was also synthesized by substituting V^{3+} for Cr^{3+} in $\text{K}_3\text{Cr}_3(\text{PO}_4)_4$. The $\text{K}_3\text{V}_2\text{Cr}(\text{PO}_4)_4$ demonstrated a reversible capacity of 40 mAh g^{-1} and a discharge voltage of around 4.0 V at room temperature. We also conducted an exhaustive search based on theoretical capacity and ionic diffusion path estimated by BVEL calculation from ICSD and demonstrated reversible 4 V-class operation of $\text{K}_6(\text{VO})_2(\text{V}_2\text{O}_3)_2(\text{PO}_4)_4(\text{P}_2\text{O}_7)$ [63].

Such an approach of finding promising materials or structures from databases and improving their electrochemical properties by optimizing their composition is reasonable and efficient. The promising frameworks in which potassium ions can diffuse easily mostly consist of a corner-sharing framework, which can offer wide diffusion channels [64]. Indeed, most of the reported K polyanionic compound materials for PIBs have corner-sharing frameworks. In contrast, corner-sharing frameworks generally have low electronic conductivity. The improvement of the intrinsic low electronic conductivity of the polyanionic compounds is challenging. However, partial substitution of XO_4 group, e.g. PO_4 by MoO_4 , could improve the electronic conduction because previous DFT calculation indicated that the Mo 4d orbitals are located at the bottom of the conduction band unlike P 2p orbitals, resulting in electron transport in the M-O-Mo-O-M pathway [65]. In addition, carbon coating and a decrease in particle size can improve electronic conductivity and resultant electrochemical performances, as reported in many studies. Demonstrating high ionic conductivity, electronic conductivity, and operating potential is essential for achieving practical specific/volumetric energy densities. In particular, the development of high potential Fe-based polyanionic compounds through structural and compositional design is one of the promising strategies for cost-effective PIBs.

Concluding remarks

Polyanionic compounds are important candidates as positive electrode materials for PIBs due to their excellent thermal stability and open framework structure that allows highly reversible K-ion insertion. However, achieving large specific/volumetric energy densities and high electronic/ionic conductivities are the main challenges. Previous intensive studies have found several structures suitable for K-ion insertion/migration and revealed the dominant factors of the redox potential. Therefore, we expect to improve energy density by optimizing the structures and compositions governing the inductive effect. In addition, the exploration of new frameworks suitable for K-ion insertion will enable diverse and attractive material designs.

Acknowledgments

The authors thank the JSPS KAKENHI (Grant Nos. JP18K14327, JP20J13077, JP20H02849, and JP21K20561) for financial support. Schematic illustrations of the crystal structures were drawn using the program VESTA [66], and BVOL analysis was conducted with the Bond_Str program.

5. OEMs for PIBs

Weiwei Huang¹ and Qichun Zhang²

¹ School of Environmental and Chemical Engineering, Yanshan University, Qinhuangdao, People's Republic of China

² Department of Materials Science and Engineering, City University of Hong Kong, Hong Kong SAR, People's Republic of China

Status

There is no doubt that the energy storage has become one of the hottest topics in the world today. The chemical energy storage is the most cost-effective technology, and the research of electrochemical energy storage has long been blooming in enterprises and scientific research institutions [67, 68]. The most representative LIBs have increased exponentially in the past few decades, but during the expansion of the energy storage market, the limited lithium resources as well as its uneven distribution have strongly hindered the application of LIBs [69, 70]. On the other hand, Potassium, which is the same family member as lithium, has become one of the effective alternatives. In particular, in the last 5 years, the study on PIBs has been conducted rapidly [71]. Of course, the progress in PIBs is inseparable from the research basis of LIBs. However, since the K^+ radius is nearly twice the Li^+ , most materials are unsatisfactory in the PIBs [72]. This urgently needs to vigorously develop new electrode materials suitable for PIBs.

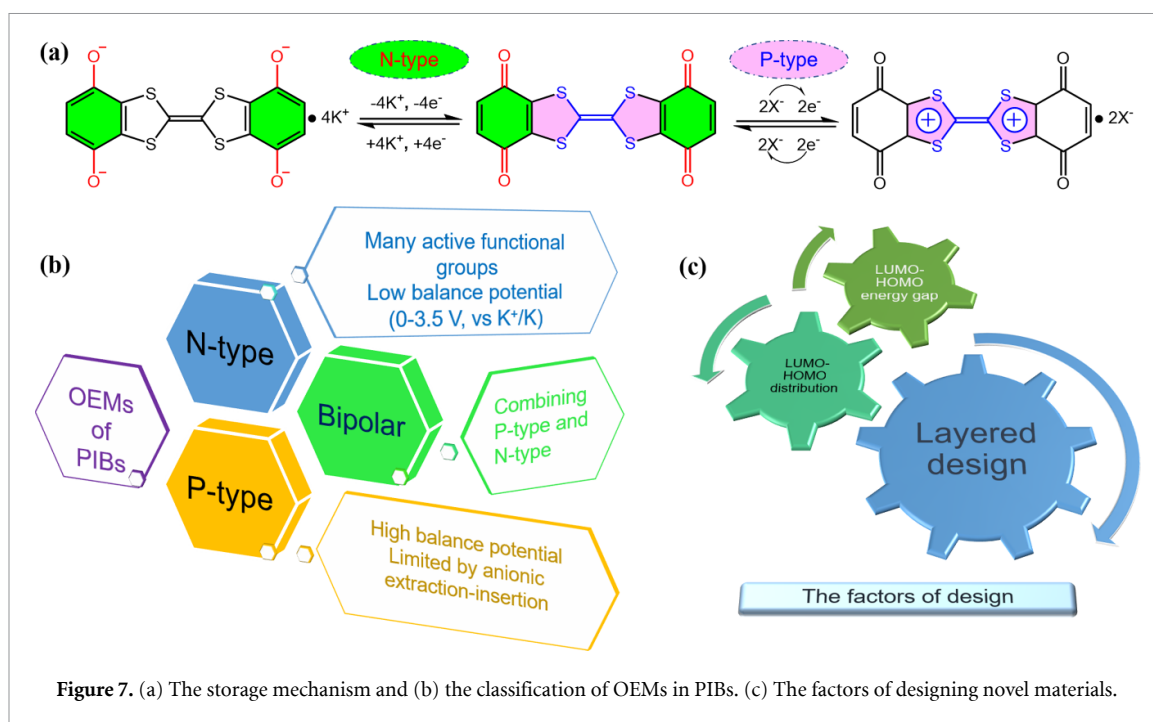
OEMs are undoubtedly up-and-coming, because their main components are light-weight elements such as C, H, O, N, and S, which is beneficial for the cost and environmental protection [73, 74]. Simultaneously, the design flexibility and application infinity have become the favorite peculiarity of scientific researchers. Although K^+ ions are slightly biased by the size, OEMs do exhibit new vitality due to their flexibility and weak interaction with metals (or ions) [75]. Therefore, in the post-lithium era, organic potassium ion batteries (OPIBs) have great potential applications. Currently, OEMs can be divided into N-type, P-type and bipolar. As shown in figures 7(a) and (b), the N-type materials are the one, whose redox reaction occurs between neutral molecules and corresponding negative charge state ions. Generally, their balance potential is low, distributed at 0–3.5 V (vs. K^+/K). By utilizing the different potentials, OEMs can be selected to support positive and negative charges [76, 77]. The P-type materials are the one, whose redox reaction occurs between neutral molecules and the corresponding positive charge state ions. Normally, their balance potential is high, so they are good choices for designing high voltage electrodes [78]. Bipolar electrode materials, combined with both N-type and P-type characteristics, have a wide voltage range and high theoretical specific capacity, which is extremely attractive [79]. It is indisputable that few organic materials are reported to be used in PIBs. To achieve the wide application of PIBs, it is extremely necessary to further design novel OEMs.

Current and future challenges

The disadvantages exposed by OEMs are non-negligible. On one hand, small molecules are easily dissolved during the electrochemical process, resulting in significant reduction in the capacity with the increase of the cycles. Learning the research experience from LIBs, the issue of high solubility can be avoided by several techniques such as surface coating, polymerization, the usage of salt, and electrolyte curing [74]. Among them, polymerization has become the most standardized choice for the design of OEMs. Especially, the lately hotspot materials of MOFs and covalent organic frameworks (COFs), which could contain large pores in organic batteries, have been consecutively reported to show new breakthroughs [71, 80]. Some challenges in this direction are the synthesis methods and the yield of products, etc [81]. On the other hand, the conductivity of the OEMs is relatively poor, which is one big disadvantage in their electrochemical properties. Mixing the organic materials with the conductive carbon can increase certain electrical conductivity. However, this is not optimal for organic materials, whose volume energy density itself is not high. One good choice is to introduce heteroatoms in OEMs with high electron density to enhance electron delocalization and conductivity, however, the relative mechanism is still ambiguous. In addition, extending the conjugate system to enhance the conductivity of the as-prepared OEMs is a recognized effective way. This includes both the π - π conjugate large plane molecular design, as well as the π -d conjugate metal coordination design [82]. It is worth noting that the metal-containing OEMs have a significant effect on electrochemical properties due to their variable electrostatic repulsive force and van der Waals force.

Advances in science and technology to meet challenges

The theoretical calculation has an important guiding significance to the study of OEMs (figure 7(c)). According to the frontier molecular orbital theory, lower lowest unoccupied molecular orbital (LUMO) energy means a greater electron affinity and higher oxidation capacity, thereby exhibiting a higher reduction potential [83]. Furthermore, the energy gap (E_g) of highest occupied molecular orbital (HOMO)-LUMO



can also be used to assess the electron transfer properties of the materials. Zhou *et al* [84], calculated the HOMO and LUMO of the polymers constructed from three different connecting fragments. The LUMO of polydiaminoanthraquinones (PQs) PQ-CN is -3.53 eV (PQ-1, 4 is 2.39 eV, and PQ-1, 5 is 2.39 eV), and E_g only is 2.29 eV. These results indicate that the redox voltage and the magnification performance of PQ-CN are higher than that of the other two. The design of organic conjugated molecules with a hierarchical structure can effectively enhance the storage and transfer of K⁺. Yu *et al* [85], revealed that the lattice stripe of layered methylene blue (MB) molecule MB·5H₂O is 0.05 Å different from the calculated value, and the molecules with such lattice enable a specific capacity of 75 mAh g⁻¹ over 4500 cycles at a high current density of 2.0 A g⁻¹. Combining organic molecules with carbon nanotubes, carbon fibers, graphene, etc materials can establish a stable conductive framework to obtain better conductivity and multiplier performance. The few-layered COFs integrated with carboxylated carbon nanotubes (DAAQ-COF@CNT) synthesized by Duan *et al* [86], have a rich active site and appropriate nanopore surface area, which can accelerate K⁺ diffusion and achieve high conductivity.

Concluding remarks

The research on OPIBs have driven the big progress in the energy storage system. Further development of novel OEMs is necessary and highly desirable. From the design to specific performance, from theoretical calculations to experimental data, and how to better apply computational predictions to molecular design are extremely challenging. Therefore, there are still many doubts about OEMs in PIBs that need to be explored, however, these materials have been demonstrates to show great potential in PIBs. Beyond this, for the specific application of OPIBs, the synthetic route and the yield of OEMs should be further be considered.

Acknowledgments

W H acknowledges the financial support of the National Natural Science Foundation of China (No. 21875206). Q Z thanks the support from starting funds from City University of Hong Kong.

6. Graphite and hard carbon

Phuong Nam Le Pham^{1,2}, Laure Monconduit^{1,2,3} and Lorenzo Stievano^{1,2,3}

¹ ICGM, University Montpellier, CNRS, Montpellier, France

² Alistore-ERI, CNRS, Amiens, France

³ RS2E, CNRS, Amiens, France

Status

Offering such advantages as high abundance, low operating voltage and low cost, carbon-based materials have been widely investigated as anodes for PIBs [87]. Graphite and hard carbon are considered as the most promising carbonaceous negative materials for PIBs. Even though they both offer a discharge capacity of *ca.* 250–300 mAh g⁻¹, hard carbon remains less favorable in terms of CE, especially concerning the first potassiation/depotassiation cycle. High surface area as well as the large amount of structural defects formed by the connection of randomly oriented graphitic domains lead to higher irreversible capacity (>20%) than graphite. Observing a decrease in the interplanar space after one potassiation/depotassiation cycle, Wang *et al*, proposed an explanation for the high capacity loss, whereby the K⁺ intercalation irreversibly graphitizes the carbon layers in short-range [88]. Therefore, during depotassiation, K⁺ cannot be extracted completely from the graphitic stacking. In contrast, Katorova and co-workers believed that the closed cages formed by curled graphitic layers trap K⁺ ions, leading to high capacity loss in the first cycle [89].

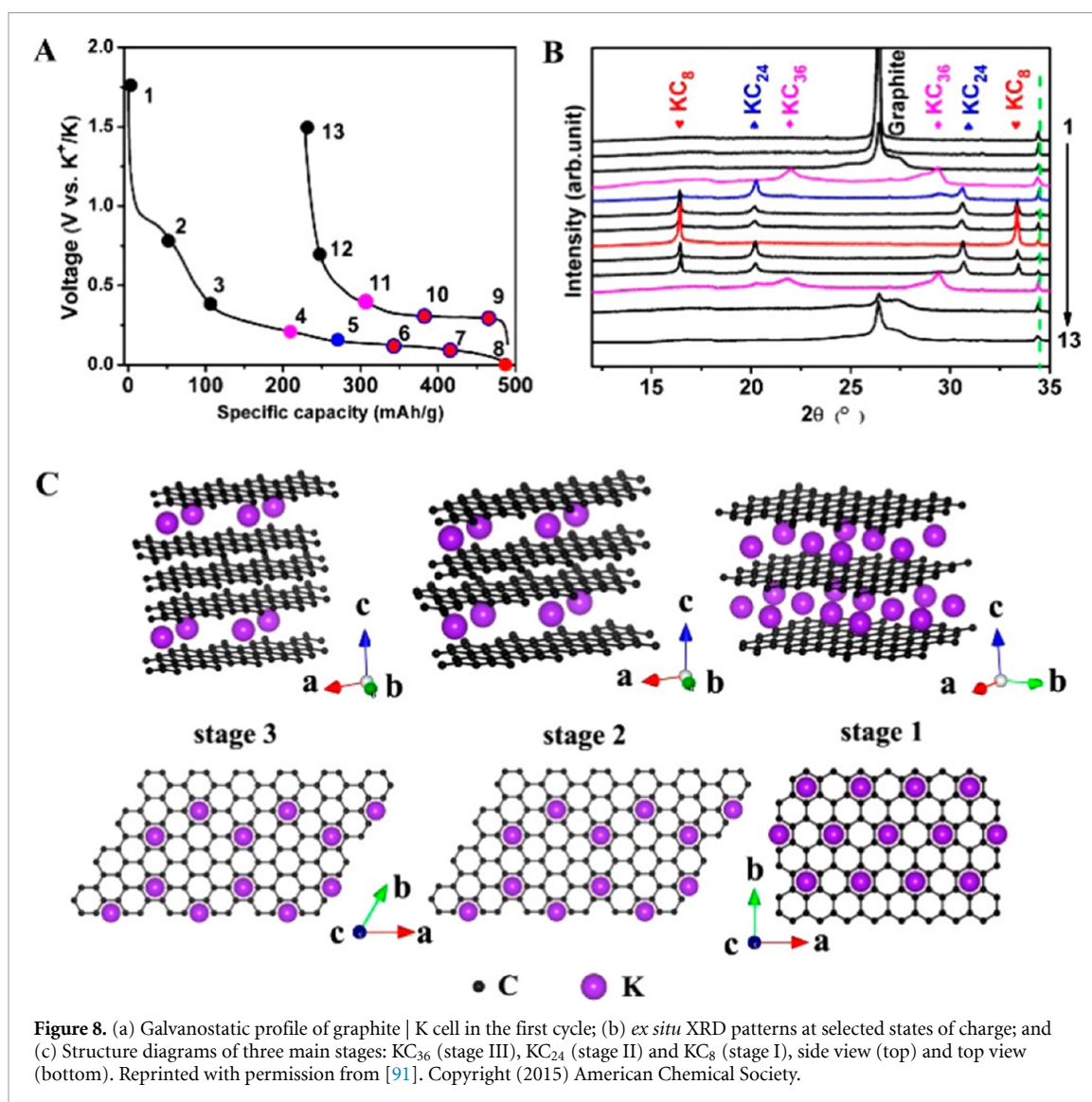
With the ability to sustainably and reversibly (de-)intercalate K⁺ ions, graphite has become the center of attention among the studied carbonaceous negative electrodes. In PIBs using conventional carbonate electrolytes, graphite exhibits a fairly high capacity of *ca.* 279 mAh g⁻¹, but the cycling retention strongly depends on the electrolyte [90].

Graphite consists of graphene layers that are stacked in ABAB (hexagon) or ABCABC (rhombohedral) sequences. An insertion of a guest cation M⁺ (M = Li, K) leads to the re-ordering of the slabs from either of the aforementioned stacks to AMA-type structure. This characteristic transformation—known as staging process—can be easily followed by x-ray diffraction (XRD), yet the structural evolution sequence is still a matter of debate. *Ex situ* XRD described the electrochemical potassiation of graphite in three consecutive stages (figure 8): KC₃₆ → KC₂₄ → KC₈ [91]. By *operando* XRD, however, Fan and co-workers suggested a four-stages mechanism: KC₄₈ → KC₃₆ → KC₂₄ → KC₈ [90]. On the other hand, Luo *et al* [92], compared computed potential profiles of several staging routes with the experimental electrochemistry, and proposed that KC₂₄, KC₁₆ and KC₈ correspond to stage III to stage I, respectively.

An interesting phenomenon of graphite is the co-intercalation of K⁺ and solvent molecules when using low-concentration glyme-based electrolytes, e.g. 1.0 M KFSI in 1,2-dimethoxyethane (DME). The co-intercalation occurs at higher potential (*ca.* 1.0 V vs. K⁺/K) than the pure intercalation (*ca.* 0.2 V vs. K⁺/K) and undergoes a larger volume expansion due to the size of the intercalated species. Herein, graphite also undergoes a staging process [93], yet the intrinsic nature of each stage is still a mystery. Despite this volumetric hindrance, the electrochemical performance of graphite in 1 M KPF₆/diglyme was stable up to 1000 cycles with the initial capacity of 100 mAh g⁻¹ at 2 A g⁻¹ [94]. More interesting, highly increasing salt concentration alters the mechanism from co-intercalation to K⁺ intercalation [93, 95]. For years, this alternation was associated with the stability of the SEI and its ability to block the solvent molecules. More recently, however, by combining statistically DFT calculation with Raman spectroscopy, it was shown that potassium solvation represents the main driving force directing the potassiation mechanism: low salt concentration corresponds to high solvation number and leads to co-intercalation, and vice-versa [93].

Current and future challenges

The major quest for graphite is to improve the cycle life and reduce the irreversible capacity caused by continuous electrolyte decomposition leading to SEI formation and lower CE, and at the same time provide high capacity. Each component of the battery, such as electrolyte (salt and solvents), counter electrode, binder, carbon additives, even the nature of graphite itself, can affect the electrochemical performance of graphite electrodes. Comparing the two storage mechanisms of graphite, bare intercalation is indeed superior in terms of capacity and energy density. Therefore, electrolytes that can boost K⁺ intercalation are preferred. Either conventional carbonate-based or high-concentration glyme-based electrolytes promote this condition. However, carbonate electrolytes were found to be incompatible with graphite, resulting in poor cyclability and rapid capacity fading [96]. Therefore, highly concentrated electrolytes using a glyme as the solvent are the better choice as they can tackle the long-term performance issue of the carbonate-based ones [97]. The choice of the potassium salt is also essential for the stability of the SEI, which is one of the key factors influencing the cycling performance. KPF₆ and KFSI are the most common salts used for half cells; while KPF₆ is safe for the current collectors but has low solubility in all solvents and leads to an unstable SEI,



and thus short cycle life, KFSI can form an inorganic rich SEI and provides excellent electrochemistry, but strongly corrodes Al current collectors. For these reasons, appropriate salt or of salt mixtures should be considered to meet the cell life requirements.

The nature and the morphology of graphite is also challenging for battery scientists. The simple intercalation of K^+ ions to form KC_8 engenders an interlayer breathing of 60% (from 3.36 Å to 5.35 Å). This drastic volume expansion/shrinkage can break the SEI layer formed in the first discharge, leading to continuous electrolyte decomposition to recompose the SEI in the following cycles—a possible reason for battery failure. Besides, crystallinity, shape and size of graphite particles deserve more consideration. Tuning one of these properties may improve the performance of graphite in both half cells and full cells. Despite their importance, up to now, there is no statistical study on their impact on graphite in PIBs.

In the case of hard carbon, obtaining anode materials with high initial CE and high rate capability is still one of the most critical challenges to reach practical application. Enhancing the porosity as well as doping strategies are often among the chosen methods to improve ionic diffusion and thus enhance rate capability [98, 99]. As mentioned above, however, obtaining better initial coulombic efficiencies (ICE) is still an important challenge for the practical application of hard carbons.

Given its high chemical reactivity, K metal is not a good counter/reference electrode to couple with carbon-based electrodes in half-cell experiments. Most electrolytes do react with K metal, inducing the formation of shuttling species that can migrate to the working electrode and further react at its surface, modifying its electrochemical behavior [100]. In addition, the potential of K metal is unstable, which makes the precise measurement of the electrode potential difficult. It is thus preferable to evaluate graphite's performance in full cells, or three-electrode systems with suitable references.

Binders also play an important role in electrochemical performance of carbon-based materials, strongly influencing both physicochemical and mechanical properties of the electrodes. According to Wu *et al*, carboxymethylcellulose sodium (CMCNa) and polyacrylate sodium (PANa) are more efficient than poly(vinylidene fluoride) (PVdF) [101]. Graphite | K cells using CMCNa or PANa as the binder show higher initial ICE than when using PVdF. Additionally, PANa acts as an artificial SEI which prevents cracks on electrode surface, and hence, allows a long and stable cycle life.

Advances in science and technology to meet challenges

Several strategies have been worked out recently to improve both ICE and cyclability of graphite and hard carbon. One major approach is altering electrolyte components without any severe modification on the electrode. As mentioned, carbonate-based electrolytes always promote K-intercalation. Binary-salt KPF₆/KFSI in EC-DEC at the appropriate molar ratios (10 or 25% of KFSI) enhanced the ICE and cycling retention of graphite comparing with those when using single salt electrolytes [102]. On the other hand, replacing carbonate ester with ether solvents was an effective practice to extend graphite's cycle life. Highly concentrated KFSI in DME provided K⁺ intercalation with a specific capacity close to the theoretical value up to 50 cycles [95].

The large volume expansion of graphite is another issue needed to be tackled. Expanded graphite with larger interlayer distance (3.87 Å) exhibits superior cyclability and stable capacity over 200 mAh g⁻¹ at 50 mA g⁻¹ up to 200 cycles [103]. Etching graphite with KOH at high temperature can slightly enlarge the space between graphene layers, which increases the initial discharge capacity of graphite up to 350 mAh g⁻¹ at the current rate of 50 mA g⁻¹ [104]. This mechanical expansion increases K⁺ diffusion up to seven times, which indeed improves the electrochemistry of graphite.

As discussed above, a stable SEI is essential for long-lifetime batteries. However, electrochemical SEI is not uniform due to the continuous decomposition/reformation when the battery is working. A thin homogeneous layer of artificial SEI formed by the deposition of the products of the chemical reaction between KFSI/DME and K metal reduces the irreversible capacity and enhances the lifetime of graphite | K cells up to 1000 cycles with the ICE of 93% and capacity retention approaching 100% [105]. This artificial SEI, mainly consisting of inorganic compounds, sufficiently prevents the electrolyte from further decomposition, hence, excellent cyclability could be obtained.

Concluding remarks

Many studies have confirmed that graphite is a promising anode material for PIBs. With an appropriate electrolyte, graphite can provide high capacity via K⁺ intercalation mechanism. Despite the big efforts made, the cyclability of graphite in PIBs is still far from being comparable with that in Li-ion systems. Nonetheless, the current attempts to improve the electrochemical performance have provided interesting hints, thus encourage new studies to further optimize electrolyte and electrode formulation. Moreover, computational chemistry, modeling and machine learning will be good companions for hands-on practices on the way bringing graphite-PIB to industry.

Acknowledgments

This work was supported by a public grant overseen by the French National Research Agency (ANR) as part of the 'Investissements d'Avenir' programme (Project ANR-10-LABX-76-01, Labex STOREX). The Alistore-European Research Institute (ALISTORE-ERI) network is warmly thanked for funding the PhD Grant of P N Le Pham.

7. Conversion materials

Ling Fan and Bingan Lu

School of Physics and Electronics, Hunan University, Changsha, People's Republic of China

Status

Conversion materials including metal oxides, sulphides, selenides, and phosphides are extensively investigated as anode for PIBs due to their advantages of abundant resources and multielectron conversion reactions. Among them, metal sulphides [106] and selenides [107] are more promising due to their superior electron conductivities and higher reversible capacity (figure 9), further conducive to developing high energy and high power PIBs. Moreover, the finally conversion products of metal sulphides and selenides with K ions is highly stable against air and water, making them higher security when assembled to full batteries.

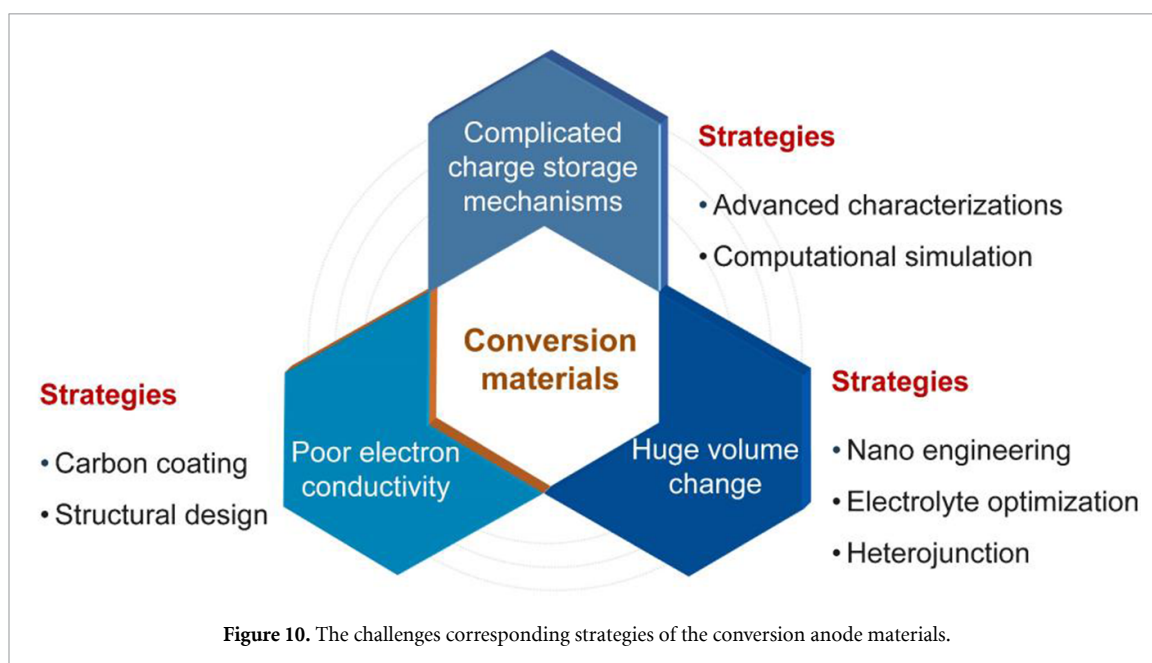
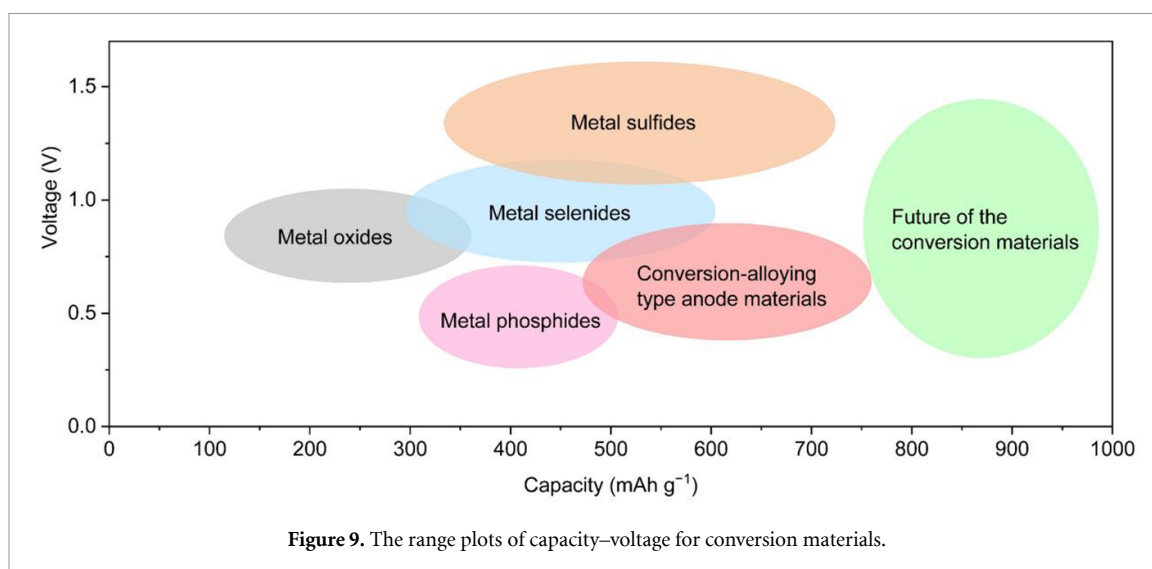
At present, the reversible capacity of some conversion materials has been broken through 600 mAh g⁻¹, which is far exceed from the capacity of graphite (279 mAh g⁻¹) and other carbonaceous anode materials [108]. Besides, the cycle stability of many conversion materials could reach up to thousands of cycles. More importantly, some of the conversion materials could exhibit ultrafast rate capability. For instance, Wang *et al* [109], reported a (Bi,Sb)₂S₃ anode with a high reversible capacity of 611 mAh g⁻¹ benefiting from the conversion-alloying reactions. Yao *et al* [110], reported a Yolk-shell NiS_x@C nanosheets, which exhibited long cycle performance of 8000 cycles due to its unique structure. Zhao *et al* [111], reported a graphene matrix supported yolk-shell FeS₂@C composite, which delivered a high-rate capability of 166 mAh g⁻¹ even at a high current density of 15 A g⁻¹ benefiting from the capacitive behavior. The excellent electrochemical performance of conversion materials has accelerated their applications in potassium ion full batteries and potassium ion capacitors or potassium dual ion batteries [112].

Actually, the electrochemical performance of conversion materials could be further improved in the future. For example, the currently reversible capacity of conversion materials still far behind the theoretical capacity (the theoretical capacity of FeS₂ and Sb₂S₃ could reach up to 893 and 945 mAh g⁻¹, respectively). Besides, the improvement on cycle stability and initial CE of conversion materials could be also realized by electrolyte and structural engineering. Overall, there is a foreseeable future for conversion materials as anode for high-energy and high-power potassium-based devices.

Current and future challenges

It should be pointed that the research on conversion anode materials for PIBs are still in the early stages, and there are several major challenges should be addressed before its practical applications. Firstly, the charge storage mechanisms of conversion materials are quite complicated according to the discrepancy on structure, operating voltage, and metal elements. Besides, the intrinsic drawback of conversion anode materials for PIBs is the huge volume change during charge-discharge processes, originating from their conversion reactions with large-sized K⁺. And the large volume change can result in severely structural failure (such as aggregation and pulverization), which will further cause more surface contact between the electrode materials and electrolyte, leading to degradation of SEI and continuous decomposition of electrolyte. Consequently, the conversion electrode materials usually exhibit poor CE and fast capacity decay. Moreover, the electron conductivity of the conversion products is inferior, leading to the large polarization voltage of conversion anode materials during charge-discharge processes and finally poor energy efficiency [113]. Addressing these issues are necessary before they could be used as anode materials for long-cycle and high-energy potassium ion full batteries.

At present, researchers have developed the structural engineering and electrolyte optimization strategies to address the huge volume change and poor electron conductivity of conversion anode materials. It is reported that the hierarchical nanostructures and carbon-coating could effectively mitigate the volume change and improve the electron conductivity. For example, Li *et al* [114], developed a confined SnS₂ with N, S-co-doped carbon nanofibers, which delivers a cycling stability of 1000 cycles at 2.0 A g⁻¹. Xie *et al* [115], developed a bimetallic-sulphide (NiCo_{2.5}S₄ microrods) wrapped by reduced graphene oxide (RGO) electrode, which shows a long cycle life over 314 d at 200 mA g⁻¹, and such a cycle-life is comparable to the long-term stability of graphite anode (over 17 months) [90]. Furthermore, the designing of heterojunction structure is also an effectively approach to improve the cycle performance. Generally, the heterogeneous surfaces are conduced to generating a built-in electric field, which will lower down the energy barrier for K atom diffusion and facilitate the charge transfer on the heterogeneous surfaces. Shan *et al* [116], reported an ultrafine CoSe₂-FeSe₂ heterojunctions as anode for PIBs, which exhibits enhanced cycle stability and rate properties. These results have demonstrated that the drawbacks of conversion anode materials could be overcome by reasonable development of structural engineering.



Advances in science and technology to meet challenges

Much efforts have been dedicated to addressing the above challenges during the past several years, and significant achievements on mechanism and electrochemical performance of conversion materials have been made. Particularly, the combination of advanced *in-situ* characterization technique with computer simulation technology to unveil the charge storage mechanisms and the volume change of conversion anode materials. For certain of conversion anode materials, their charge storage mechanisms could be further regard as intercalation–conversion reactions and conversion–alloying reactions, which could be confirmed by the *in-situ* XRD, synchrotron neutron powder diffraction, x-ray powder diffraction (XRPD) and other advanced characterization techniques [117–120]. For example, combining the DFT calculations with the *in-situ* experimental characterizations, Wu *et al* [121], revealed that the α -NiS with hexagonal structure possesses higher pseudo-capacitive behavior and better mechanical capability, leading to an enhanced cycle stability and rate capability. In addition, it is demonstrated that the electrolyte chemistry and the electrode–electrolyte interface have significant impact on the electrochemical performance of conversion anode materials. Ge *et al* [122], reported a MoSe₂/N-doped carbon composite with different electrolytes, the cycle stability of this electrode with 1M KFSI in ethyl methyl carbonate (EMC) as electrolyte is superior to that with other electrolytes.

Overall (figure 10), the complicated charge storage mechanisms of the conversion materials could be revealed by the advanced characterizations and computational simulations. While nano engineering, electrolyte optimization and heterojunction structure design are promising strategies to address the

challenge of huge volume change of conversion materials during the charge–discharge processes. Meanwhile, the carbon-coating and structural design strategies could be effectively methods to enhance the electron conductivity of conversion materials.

Concluding remarks

The conversion anode materials have high theoretical capacity, yet formidable volume change and the consequent challenges are the major obstacles before their practical applications in potassium ion full batteries. Advanced characterization techniques along with the computer simulation technologies could lead the way of structural design and electrolyte optimization for high performance conversion materials. And the specific capacity, cycle stability, and rate capability of conversion anode materials need to be further strengthened by reasonable innovation.

Acknowledgments

This work was financially supported by National Natural Science Foundation of China (Nos. 22005093, U20A20247, and 51922038) and the Fundamental Research Funds for the Central Universities (No. 531119200156).

8. Alloys

Sumair Imtiaz^{1,2,3}, Tadhg Kennedy^{1,2} and Kevin M Ryan^{1,2,3}

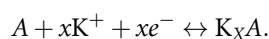
¹ Bernal Institute, University of Limerick, Limerick, Ireland

² Department of Chemical Sciences, University of Limerick, Limerick, Ireland

³ The SFI Research Centre for Energy, Climate and Marine (MaREI), University of Limerick, Limerick, Ireland

Status

Considering the great success of graphite as an intercalation anode in LIBs, the extension of its use to other alkali ion intercalation has also been studied with recent emphasis in-particular on PIBs. The theoretical capacity of graphite as an anode in PIBs is 279 mAh g⁻¹, which is ~25% less than its capacity in LIBs [123]. However, a greater issue is that the output voltage of graphite is close to the deposition potential of K, leading to safety problems involving K metal plating [91]. Alloying anode materials (AAMs) are an interesting alternative because they offer higher theoretical capacities, a low working potential, and a high attainable cell energy density [13]. The AAMs operate through alloying/de-alloying reactions, and are generally able to combine with more K⁺ ions (for instance, one mole of Sb can react with three moles of K⁺ ions and electrons, contributing to a theoretical capacity of 660 mAh g⁻¹) than carbon-based anode materials [124]. Generally, the AAMs follow the following redox reaction mechanism:



Although, AAMs have potential for high capacities, a number of challenges need to be overcome before their application as a PIB anode material can be fully realized. For example, the ionic radius of K⁺ (0.138 nm) is relatively large compared to the Li⁺ (0.068 nm) and Na⁺ (0.097 nm) [125, 126], and this causes sluggish redox kinetics in the anodes [127]. In addition, the large volume variation (table 1) of AAMs upon potassiation/depotassiation processes exerts a huge mechanical strain, resulting in the severe pulverization, degradation and delamination from the current collector [128], leading to rapid capacity fade. The most viable AAMs for K alloying are from Group 14 & 15 with high theoretical reversible capacities and moderately low operating voltage for PIBs. Table 1 provides the stoichiometry of final alloying product, volume change (%), theoretical gravimetric (Q_g) and volumetric capacities (Q_v) of various AAMs in PIBs, where Q_v is calculated as Q_g × ρ (ρ = density of potassiated alloy obtained from Materials Project, materialsproject.org).

Interestingly Si, the most promising candidate in LIBs, has not shown any experimental evidence of alloying in PIB systems [128]. Regardless of the high cost of Ge, it is a common candidate in LIBs, but experimental studies on the application of Ge in PIBs are also limited. Sn is also a popular choice of anode in LIBs and SIBs because of high theoretical capacities of 990 (Li₂₂Sn₅) and 847 mAh g⁻¹ (Na₁₅Sn₄), respectively. However, studies reveal that Sn can alloy with K in a one-to-one ratio to form KSn, with a mediocre theoretical capacity of 226 mAh g⁻¹.

Moving to Group 15, P for instance is extremely attractive material, as it can react via a three-electron reaction mechanism leading to ultrahigh theoretical specific capacity of 2596 mAh g⁻¹, assuming the formation of K₃P, with the volume expands up to 593% [124, 133]. However, the formation of K₃P is highly speculative, and the formation of KP and K₄P₃ are considered as the most stable phases of the K-alloying process, providing the theoretical capacities of 865 and 1154 mAh g⁻¹, respectively [124, 133]. However, even with the formation of the KP and K₄P₃ phases, the volume expands to 232% and 293%, respectively [133]. Another main disadvantage of P is its low electronic conductivity that restricts the electrochemical redox reactions. Sb is considered as the most promising candidate in PIBs owing to its high gravimetric capacity (more than twice that of graphite), and low charge/discharge plateaus, high electrical conductivity (2.56 × 10⁶ S m⁻¹), yet its volume also expands to beyond 400% upon alloying with K [132]. Metallic Bi is also a popular choice of AAMs in PIBs due to its large crystal lattice along the c-axis (0.395 nm), low average potential, and relatively flat plateaus. But again, the large volume expansion of ~400% is projected on the formation of K₃Bi upon potassiation, which leads to the growth of an unstable SEI layer, cracking of the anode material, and concomitant electrolyte consumption resulting in significant capacity fade [134].

Current and future challenges

Given the large volume expansion during the potassiation/depotassiation processes and the relatively low electrical conductivities demands that AAMs are designed with a robust architecture that can sustain structural changes during potassiation/depotassiation with enhanced conductivity.

Besides AAMs themselves, studies showed that the choice of compatible binder, electrolyte salt and solvent is also challenging because of higher reactivity of K, large volumetric change (~400%) and/or the

Table 1. Theoretical gravimetric and volumetric capacities for the potassiation of group 14 and 15 elements, Stoichiometry of the final alloying product and their estimated percent volume expansion upon potassiation.

Material	Stoichiometry of final Alloying Product	Density of potassiated alloy ($\text{g}\cdot\text{cm}^{-3}$)	Theoretical gravimetric capacity (Q_g) ($\text{mAh}\cdot\text{g}^{-1}$)	Theoretical volumetric capacity (Q_v) ($\text{mAh}\cdot\text{cm}^{-3}$)	Volume change (%)	References
Si	KSi	1.43	954	1364	334	[129]
	K1.1Si	—	1049	—	Not reported	[130]
Ge	KGe	2.34	369	863	Not reported	[124]
Sn	KSn	3.34	226	755	~180	[131]
Sb	K3Sb	2.24	660	1478	407	[124]
Bi	K3Bi	3.26	385	1255	>400	[132]
P	K3P	1.7	≤ 2596	4413	593	[129, 133]
	K4P3	1.92	1154	2216	293	[133]
	KP	1.53	865	1323	232	[133]

fragile SEI, all these factors severely influences stability and capacity of AAMs in PIBs [13, 123, 135, 136]. Appropriate binders and electrolyte formulations enforce structural integrity, maintain a stable SEI layer and promote the cycle life of AAM anodes. In addition, the reaction mechanism of alloying anode in PIBs system is different from that of LIBs and SIBs. Understanding the exact alloying reaction mechanism of AAMs in PIBs is highly challenging as they form multiple phases during cycling that are voltage dependent, with most of the phases formed being either amorphous, low crystalline, or metastable. Therefore, advanced operando characterizations are required to provide an in-depth understanding and to reliably observe the electrochemical alloying and de-alloying processes.

Advances in science and technology to meet challenges

Nano-structuring is a common tactic to alleviate the structural strains in AAMs and facilitate charge transfer and ionic diffusion. Other than that, the advanced structural engineering by manipulation and integration of AAMs with one-dimensional (1D), two-dimensional (2D) and 3D carbonaceous materials have shown considerable advantages to tolerate the volume variation issues [133, 137, 138]. For instance, ultrafine Sb nanocrystals within carbon nanofibers composed of an array of nano-channels provided significant mitigation of the volume expansion and fast K^+ transportation, maintaining a gravimetric capacity of 225 mAh g^{-1} after 2000 cycles at 1 A g^{-1} (figures 11(a) and (b)) [137]. Similarly, to improve the electronic conductivity and cycling stability of P, Yu and co-workers [127] encapsulated red P nanoparticles within freestanding electrospun nitrogen doped porous hollow carbon nanofibers (red P@NPHCNFs), which demonstrated unprecedented long cycle life with a reversible capacity of 465 mAh g^{-1} after 800 cycles at 2 A g^{-1} (figures 11(c) and (d)). The strategy of incorporation of carbonaceous materials into AAMs has a number of advantages; accommodate of volume expansion, improvement of the K^+ kinetics and enhancement of conductivity. However, it may substantially mitigate the advantage of high specific capacity and volumetric energy density of pure AAMs, because of the typically lower capacity of carbonaceous materials. Thus, a reasonable compromise between cycle life and energy density is required for these composite structures. Alternately, generating AAMs in (zero-dimensional) 0D and 1D morphology could be a possible solution. The 0D morphology can boost ionic adsorption and alleviate stress variation due to surface effect and small size effect [139]. Whereas the high length-to-diameter ratio of 1D structure can provide high mechanical robustness and enhance the electronic and ionic transfer [139, 140]. The benefits of 0D, 1D and/or hybrid 0D–1D anodes have been extensively demonstrated for LIB applications [141–143], therefore, there is a depth of knowledge already available which could expedite the development of AAM anodes for PIBs.

Apart from the anode structural design, the selection of electrolyte solvent, salt, and their concentration play a critical role on the electrochemical performance of AAMs. Previous studies have found that KFSI salt is more suitable for AAMs than KPF_6 , providing good C.E. and capacity retention. More specifically, the studies have shown that AAMs perform better with high concentration of KFSI (especially 5.0 M KFSI) than diluted electrolyte (1.0 M KFSI) (figure 11(e)), due to the elevated reduction resistance that reduces the irreversible electrochemical reactions [136, 144]. Nonetheless, KFSI salt is not suitable for high voltage cathodes due to the corrosive effect of FSI^- on Al foil during anodic polarization ($>4.0 \text{ V vs. K}^+/\text{K}$) [145]. To fully realize the potential of AAMs for practical batteries, further research efforts need to be devoted to electrolyte optimization. ILs electrolytes could be a potential choice rather than the organic solvents, as they offer higher ionic conductivity, higher operational safety, effective SEI, and wider electrochemical stability windows. The cycling of a graphite anode and potassium manganese hexacyanoferrate cathode in a KFSI in

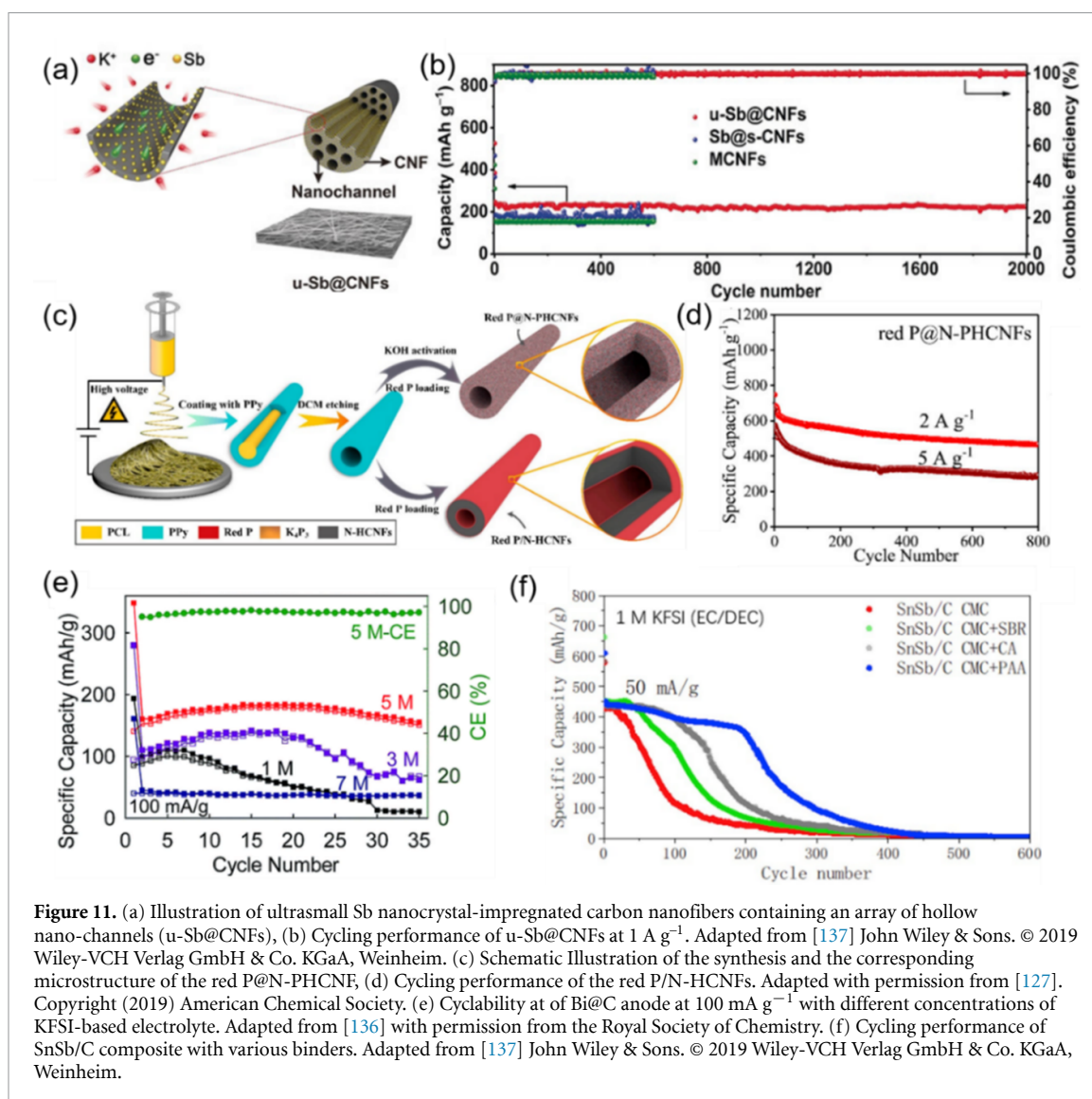


Figure 11. (a) Illustration of ultrasmall Sb nanocrystal-impregnated carbon nanofibers containing an array of hollow nano-channels (u-Sb@CNFs), (b) Cycling performance of u-Sb@CNFs at 1 A g^{-1} . Adapted from [137] John Wiley & Sons. © 2019 Wiley-VCH Verlag GmbH & Co. KGaA, Weinheim. (c) Schematic Illustration of the synthesis and the corresponding microstructure of the red P@N-PHCNF, (d) Cycling performance of the red P@N-PHCNFs. Adapted with permission from [127]. Copyright (2019) American Chemical Society. (e) Cyclability of Bi@C anode at 100 mA g^{-1} with different concentrations of KFSI-based electrolyte. Adapted from [136] with permission from the Royal Society of Chemistry. (f) Cycling performance of SnSb/C composite with various binders. Adapted from [137] John Wiley & Sons. © 2019 Wiley-VCH Verlag GmbH & Co. KGaA, Weinheim.

Pyr_{1,3}FSI ILs electrolyte up to 4.3 V (versus K⁺/K) showed minimal corrosion effects on the Al current collector as well as high CE [46].

The choice of binders for preparing electrode slurries also plays a key role in mechanical robustness and electrochemical performance of AAMs. Wu *et al* [146], presented an improvement in the initial C.E. and cycling performance of P/C composite anodes with carboxymethyl cellulose (CMC) compared to PVDF due to the preformed SEI effect of CMC and avoidance of defluorination. Guo's group [135] compared various binders and found that the combination of CMC + polyacrylic acid (PAA) provide better performance for SnSb/C composite (figure 11(f)). Despite the huge impact of binders on the electrochemical performance of AAMs, this area of research is still in its infancy. This demands enormous consideration on the binder optimization to meet challenges of AAMs for PIBs. It seems that due to the huge volume expansion of AAMs, linear polymer binders (such as CMC, PAA) with single function might not meet the requirements of high adhesive strength, electrochemical and mechanical stability, and high initial CE. Therefore, other than these linear polymer binders, branched, cross-linked conductive polymer binders and combination of different structures must be explored.

Beside the anode and electrolyte optimization, good progress has been achieved on using *operando* characterization techniques (XRD, Raman, transmission electron microscopy (TEM)) to probe the K-storage mechanisms of various AAMs, yet this area still demands much advanced characterization tools to record the multi-phase electrochemical alloying processes. Particularly, the alloying mechanism of some of the key AAMs such as Si, Ge, and P are still not fully established and under debate, and the future technological development of these materials in PIBs demands more advanced nanoscale *operando* tools such as *operando* nuclear magnetic resonance (NMR) spectroscopy, *in-situ* scattering (neutron diffractions (NDs), pair distribution function (PDF)) for in-depth analysis.

Concluding remarks

To sum up, AAMs represent an exciting class of anode materials for PIBs, due to their abundance, cost, and high gravimetric and volumetric capacities. While progress has been made in past few years from a relatively small number of groups to overcome the severe volume expansion issues, persistent and continued efforts are required to design suitable and robust anode structures without sacrificing the key advantage of high energy density. Several other aspects of these AAMs, such as their compatibility issues with electrolyte chemistries, anode/electrolyte interfaces, alloying reaction mechanisms and full cell studies with operando tools require more in-depth research to challenge benchmark materials. Even though the road to successful implementation of AAMs in practical PIBs is challenging, there is no doubt that these materials show outstanding promise for sustainable battery storage and a confluence of advances focused on addressing the challenges outlined can deliver on this promise.

Acknowledgments

K M R acknowledges Science Foundation Ireland (SFI) under the Principal Investigator Program under Contract No. 16/IA/4629 and under Grant No. SFI 16/M-ERA/3419 and European Union's Horizon 2020 Research and Innovation Program under Grant Agreement No. 814464 (Si-DRIVE project). K M R further acknowledges IRCLA/2017/285 and SFI Research Centers MaREI, AMBER and CONFIRM 12/RC/2278_P2, 12/RC/2302_P2, and 16/RC/3918.

9. MXenes

Hang Wang and Min Zhou

Hefei National Laboratory for Physical Sciences at the Microscale, School of Chemistry and Materials Science, University of Science and Technology of China, Hefei, People's Republic of China

Status

In the wake of the revelation of graphene, the emerging 2D materials serve as the pioneer zone of innovation-driven development of energy storage. In 2011, the first report of MXene by Barsoum, Gogotsi and co-workers introduce a new family of 2D materials to the attention of the community [147]. MXene is usually considered as a class of 2D layered TM carbides/nitrides/carbon nitrides, with the stoichiometry of $M_{n+1}X_nT_x$, where M is early TM such as Ti, V, Mo, W, Nb, Ta, etc, X is C and/or N, and T is surface terminations, such as F, Cl, Br, O, S, Se, Te, OH, NH_2 , etc [148]. As shown in figure 12, the configuration of each layer consists of 3, 5, 7, 9 sub-layers with alternate M and X atoms represented as M_2C , M_3C_2 , M_4C_3 , and M_5C_4 ($n = 1, 2, 3, 4$) with surface terminations [149]. The M sub-layers with hexagonal symmetry were sandwiched by the double neighbored X sub-layers. About surface terminations, previous studies evidence a random distribution [150]. These layers stack to form a periodic structure with weak coupling between layers. The first MXene is $Ti_3C_2T_x$, fabricated from layered ternary MAX phase by a top-down etching process. Most MXenes can be achieved using corresponding precursors by wet chemical routes, molten salt routes, electrochemical routes. Alternatively, bottom-up methods, like chemical vapor deposition, plasma-enhanced pulsed laser deposition, chemical vapor deposition, and template methods, etc, have also been developed to realize ultrathin MXenes with large size, such as Mo_2C .

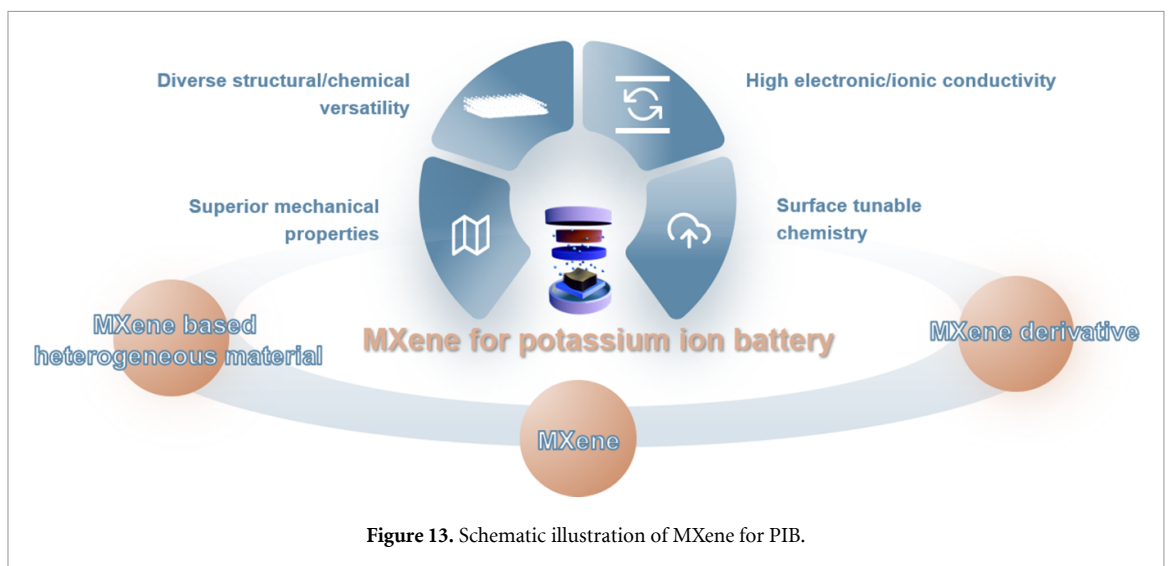
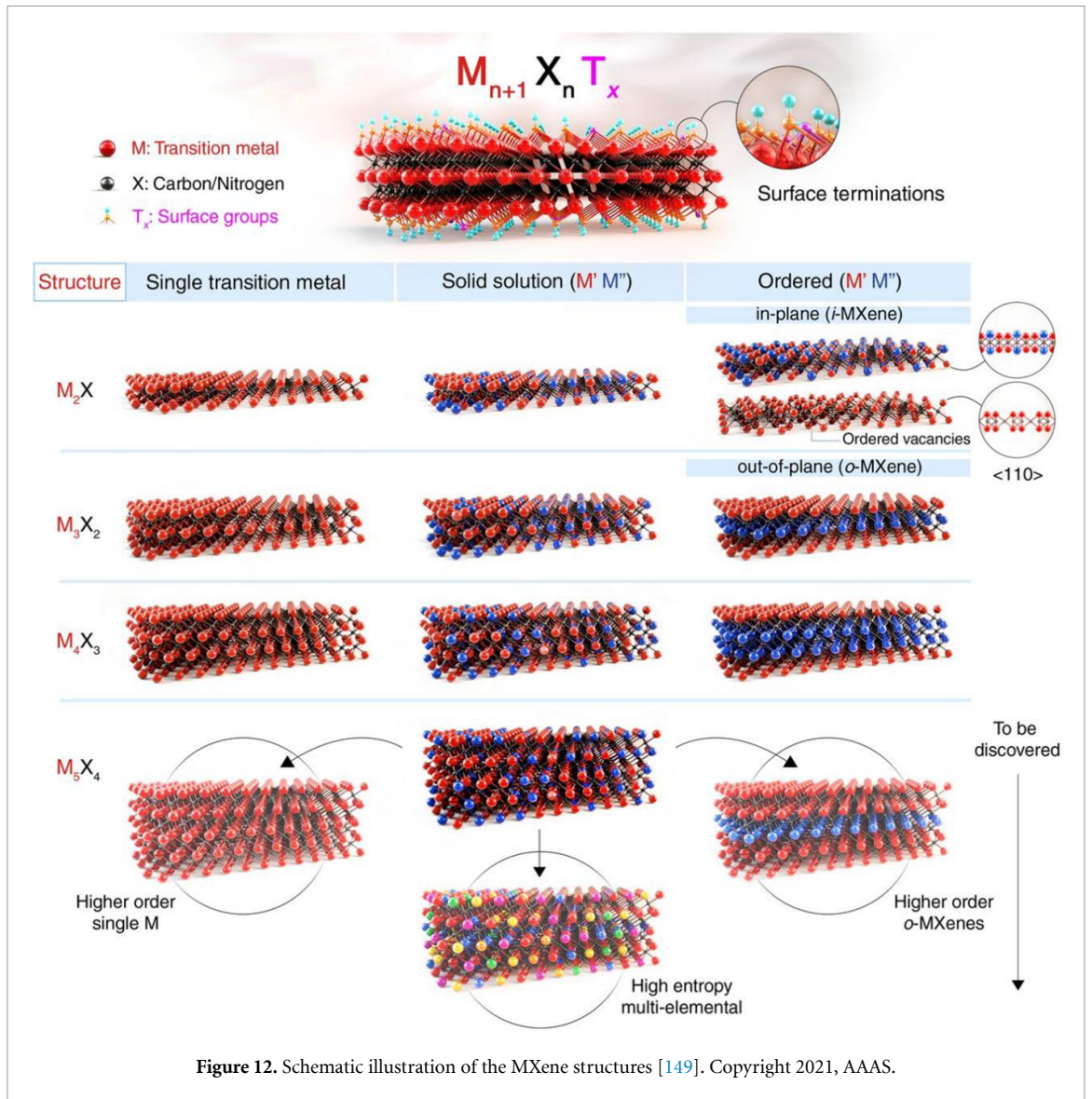
As shown in figure 13, compared with most 2D materials, MXenes are commonly excellent ionic and electronic conductors rather than semiconductors or insulators. Their combined superiorities of 2D features, diverse structural/chemical versatility and distinct physico-chemical properties further solidified MXenes with all the potentials for PIB [151]. MXenes with high electronic conductivity and superior mechanical properties also allow their applications as highly conductive and stable skeletons. Besides, the diversity of structural configurations and rich surface chemistry modifications of MXenes offer the possibilities for them to be precursors or templates to realize various functional materials for potassium storage. In view of these, MXenes have attracted intensive attentions for PIB during the recent decades.

Current and future challenges

To date, there have been over 30 stoichiometric varieties of MXenes with single and multiple solid solution/high-entropy configurations [152]. Hundreds more have been predicted to be thermodynamically stable [153]. Computational studies have explored MXenes with single, mixed, and noninherent surface terminations. The diverse and tunable surface as well as bulk chemistry of MXenes affords unprecedented tunability of electrochemical properties. Intensive progress has evidenced the potential of MXenes for PIB into pure MXenes, MXene based heterogeneous materials, and MXene derivatives, where MXenes serve as active materials, conductive skeletons, and precursors/templates, respectively, as shown in figure 13.

MXene active materials

MXenes have been extensively employed in other ion batteries with typical intercalation mechanism [154]. Given the merits of rich surface chemistry and adjustable interlayer with high electronic/ionic conductivity, MXenes are expected as promising electrodes [155]. According to the energy analysis, K^+ prefers to intercalate into the spacing between layers and be absorbed on surface/interface rather than entering the inner interstitial sites [156]. Taking Ti_3C_2 as an example, the theoretical capacity of monolayer is inversely proportionally to the effective radius of metal ions. The value is only 191.8 mAh g^{-1} using the center of the carbon hexagon sites as the main active sites [155, 156]. Further studies verify the theoretical capacity in V_3C_2 monolayer is $269.86 \text{ mAh g}^{-1}$, which is approaching that of graphite. Other MXenes, like Ti_2CO_2 , V_2CO_2 , Nb_2CO_2 , etc all exhibit the potential for potassium storage. However, related studies are still in theoretical stage, and the achievable potassium storage of MXenes are far from satisfactory. To exploit the potential of MXenes, further promotion approaches can be classified into three categories. (i) Composition optimization. Different M and X contribute to adjustable electronic structures, leading to optimized potassium absorption and intercalation. For example, Ti_3CN show better capacities and stability than those of Ti_3C_2 [157]. (ii) Interlayer space adjustment. Considering large size of K ions, the ion accommodation become more difficult. Enlarged interlayer space via pillared ions or molecules is helpful for ion intercalation and diffusion. K pre-intercalated V_2C shows greatly enhanced potassium storage ability with a high capacity of 152 mAh g^{-1} at 100 mA g^{-1} [158]. Similar trends can be found in C pre-intercalated Nb_2C [159]. (iii) Morphology control. It is common that the storage ability of the few-layer and monolayer MXenes are better



than that of multi-layer MXenes, in particular in capacity decay. Suitable morphology control can accelerate ion diffusion and shorten ion/electron migration paths. The constructions of porous nanosheet and 3D porous skeleton composed of alkalized nanoribbon are two typical examples to inhibit agglomeration and restacking, realizing better potassium storage performance.

MXene based heterogeneous materials

Most active materials for potassium storage are semiconductive with poor electronic conductivity. Metallic MXenes with a high electronic conductivity similar to metals are expected to be a great conductive matrix/additive to construct conductive networks and accelerate the electron transfer. $\text{Ti}_3\text{C}_2\text{T}_x$ as a typical MXene has a higher electronic conductivity (6500 S cm^{-1}) than many 2D materials including graphene nanosheets (400 S cm^{-1}) [160, 161]. Their abundant surface terminals allow benign affinity and thus good dispersion with a range of materials, leading to stable heterogeneous structures. Particularly, various metal elements can be chosen to fabricate stable MXenes with diverse composition (single, double, and ternary), proportion, and arrangement [150]. MXene as a matrix can provide abundant active sites. Besides, Young's modulus of MXenes reaches 400–1000 GPa [162]. Especially, the elastic modulus of monolayer $\text{Ti}_3\text{C}_2\text{T}_x$ can be as high as 502 GPa, surpassing that of monolayer MoS_2 (270 GPa) [163, 164]. The excellent mechanical properties endow MXenes as stable buffer layers and skeletons to tolerate the volume change of active materials and ease the problems of chalking and shedding. Thirdly, heterostructures can keep MXene from restacking to some extent, thus benefit for the ion/electrolyte contact and active material utilization. Hence, the MXene based heterogeneous materials have gained attentions for potassium storage with the help of combined advantages. Up to date, many binary heterogeneous materials have successfully constructed. Ti_3C_2 is the most commonly used MXene. Several anode materials like Sb, Sn, Bi, MoS_2 , VSe_2 , SnS_2 , N-rich porous carbon nanochips have all exhibited improved stability during potassium storage. In addition, complex ternary heterogeneous materials have also been designed to achieve high capacity and extraordinary structural stability, such as $\text{MoSe}_2/\text{Ti}_3\text{C}_2/\text{C}$ [165], $\text{Fe}_{x-1}\text{Se}_x/\text{Ti}_3\text{C}_2/\text{Carbon}$ [166], $\text{ReSe}_2/\text{Ti}_3\text{C}_2/\text{N-doped graphene}$ [167], MSe_2 ($\text{M} = \text{Cu, Ni, Co}$) / $\text{Ti}_3\text{C}_2/\text{CNRib}$ [168]. Strong interactions at the interfaces promote the charge transfer, resulting in promoted rate performance.

MXene derivatives

Due to diverse structural/chemical versatility and surface tunable chemistry, MXenes can be employed as precursors or templates. Barsoum and co-workers first realized TiO_2/C derived from Ti_3C_2 by thermal oxidation, marking the beginning of MXene derivatives [169]. Then, many efforts have devoted to MXene derivatives, such as oxides, sulphides, nitrides, fluorides, chlorides, MOF, etc. In addition, MXene derivatives can inherit unique features of MXene, such as the 1D or 2D parent morphology [170]. $\text{TiO}_2/\text{graphene}$ [171], TiO_2/rGO [172], $\text{TiO}_x\text{N}_y/\text{C}$ [173], TiS_2/C [174], $\text{K}_2\text{Ti}_4\text{O}_9/\text{graphene}$ [175], etc have been used as examples in PIBs. Given the rational design of initial MXenes, these derivatives all showed extraordinary rate performance and stability.

Advances in science and technology to meet challenges

Despite intense interests and efforts in recent decades, MXenes have shown huge potentials in PIBs. But more advanced requirements to adapt the relatively large ion size often compromises electrochemical performances. To meet these challenges, a deeper understanding and exploration is necessary to realize their full potential.

First, although MXene family has expanded rapidly recently, most studies for potassium storage are still focused on the first MXene, Ti_3C_2 . Other MXenes, such as Ti_3CN , have shown the ability to optimize K^+ kinetics. It is expected that the diverse structural/chemical versatility and associated physico-chemical properties of MXenes would enable promoted potassium storage. Various solid solution MXenes are possible examples to extend active MXene family for PIBs. Green and precise synthesis methods would be helpful to realize new MXenes which have only been predicted before. Rational high-throughput screening of suitable MXenes is also significant for enhanced performance.

Second, surface chemistry plays a critical role on the electronic structure and thus the electrochemical activity. According to the simulation results, bare and O-terminated MXenes typically exhibit better potassium storage ability. But it is difficult to realize complete control of surface terminations of MXenes, bare MXenes even appear to be practically unattainable. Regulating the surface terminations in view of the type and composition but remains challenging. One possible direction is to carefully select etchants and delicately design etching processes. Post-treatment, such as plasma modification, heat, is also helpful to manipulate the surface terminations.

Third, it is still unclear to understand the K^+ kinetics and charge storage performance of MXenes. Deep studies on the storage mechanism require various state-of-the-art *in-situ* and *ex-situ* characterization tools to

provide valuable information toward the storage processes, such as electrochemical Raman spectroscopy, electrochemical scanning electronic microscopy, electrochemical quartz crystal microbalances, NMR, synchrotron x-ray, and ND analysis, etc.

Concluding remarks

As a widely concerned family of 2D metallic materials with diverse structural/chemical versatility, great developments of MXenes have been achieved in PIBs during the past years. But there are still several challenges not only in their synthesis, but also in the theoretical understandings of structural evolution during potassium storage, as a tip of an iceberg. Current success and challenges encourage more efforts on maximizing their merits and enable more breakthroughs PIB and other energy storage fields. It would be expected to transfer MXene-based materials 'from lab to fab' in the near future.

Acknowledgments

The authors acknowledge supports from National Key R&D Program of China (2021YFA1501502), National Natural Science Foundation of China (22075263, 52002366), USTC start-up funding (KY2060000165), the Fundamental Research Funds for the Central Universities (WK2060000039).

10. Organic compounds and MOFs

Kun Fan, Jincheng Zou and Chengliang Wang

School of Optical and Electronic Information, Wuhan National Laboratory for Optoelectronics (WNLO), Huazhong University of Science and Technology, Wuhan, People's Republic of China

Status

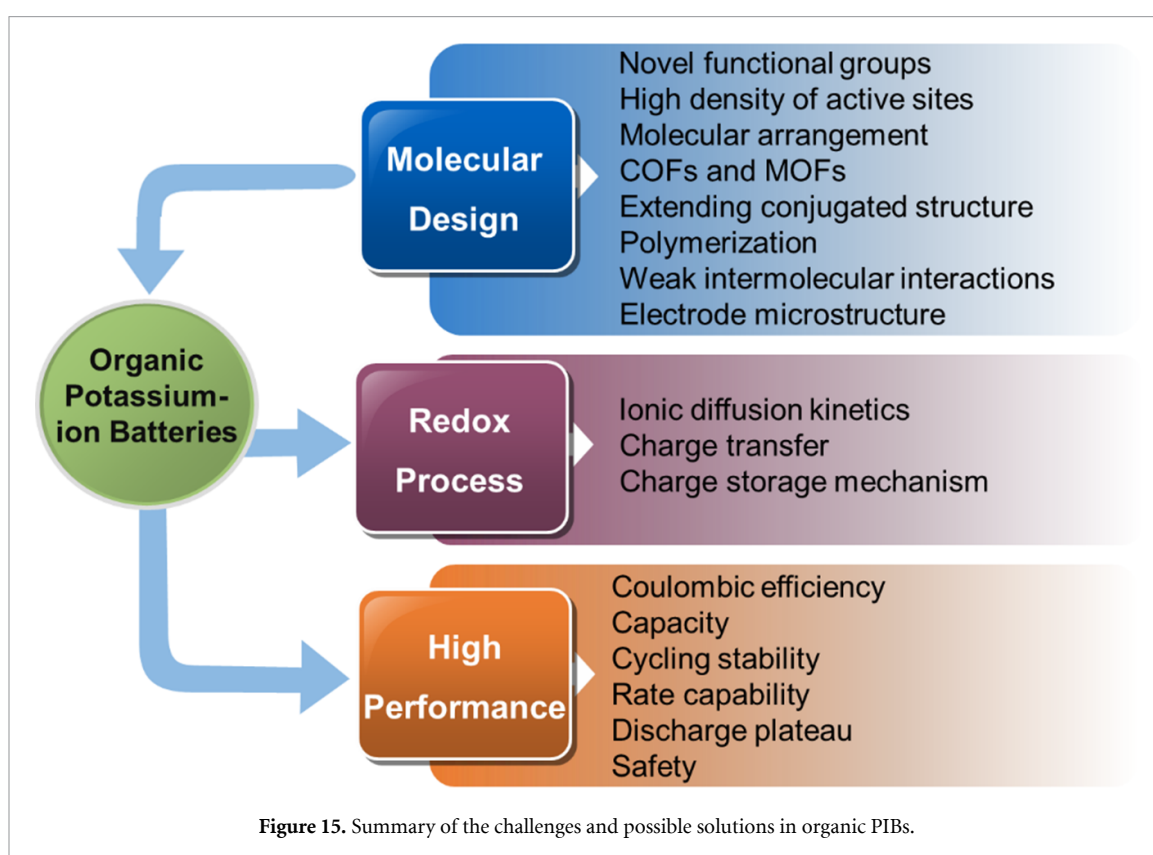
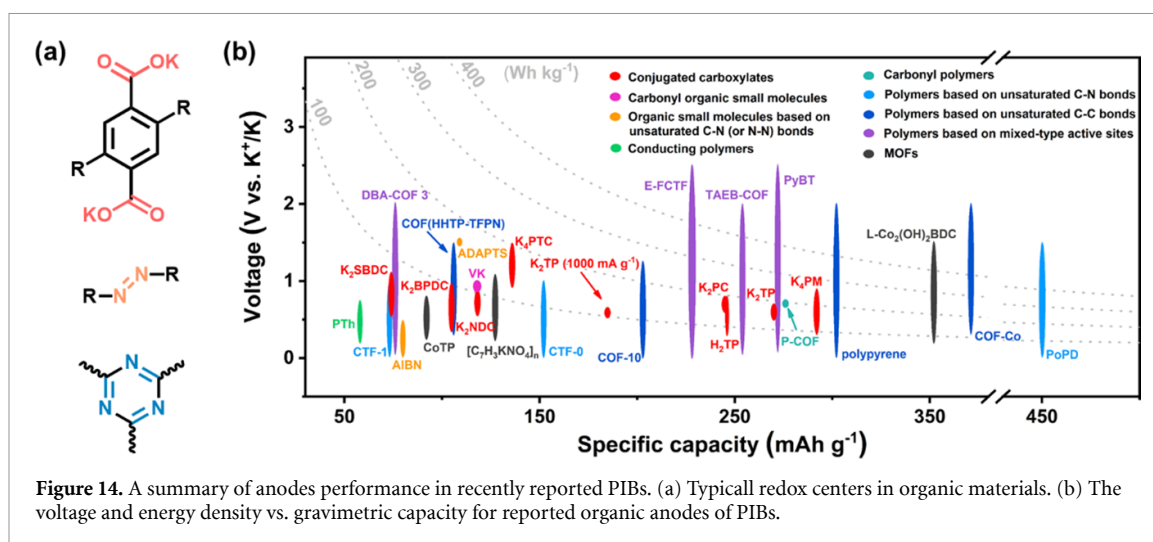
The practical applications of PIBs are strongly dependent on the development of anodes, because of the extremely high activity and the low melting point (63 °C) of K metal which make it unsuitable as an anode for PIBs. Although K^+ ions can be inserted into graphite to give an intercalation compound (KC_8), the development of graphite as anodes is hindered by the limited capacity ($\sim 279 \text{ mAh g}^{-1}$) and inferior cycling stability [176]. In addition, the carbon-based materials usually deliver a low voltage plateau ($< 0.2 \text{ V vs. K/K}^+$), which may result in safety concerns associated with the K metal plating. Besides, although tremendous efforts have been devoted to other inorganic electrodes, they are held back by resource shortage and the environmental hazards in production. More seriously, traditional inorganic materials as anodes are facing the prominent challenge of storing large sized K^+ ions for PIBs, resulting in large volume changes during the potassiation/depotassiation, sluggish reaction kinetics and poor cycling performance [72].

By contrast, organic materials have gained rising attention as promising alternatives of inorganic materials for batteries [82]. Organic compounds have the merits of eco-friendly, cost efficient, structure designability and good adaptability to electrolytes [73]. What is more, benefiting from the flexibility and relatively weak intermolecular interactions of organic materials [75], the large-sized K^+ ions can be inserted/extracted into/from OEMs without distinct volume expansion [177], which is the key challenge facing by inorganic materials for electrodes as mentioned above. In addition, judiciously choosing the functional groups via molecule design can endow organic materials with multi-electron electrochemical behaviors and tunable energy levels, which can ensure high-capacity and appropriate charge–discharge plateaus to prevent K metal deposition. Nevertheless, the studies of organic PIBs are still in the infancy stage. The anode electrochemical performance of organic PIBs, especially the specific capacity and cycling stability, are still not competitive with those of organic LIBs and SIBs even when using the same active molecule. In other words, the larger K^+ ion size results in poorer K^+ ion storage in PIBs than the Li^+ and Na^+ ion storage in LIBs and SIBs, respectively. In summary, the development of feasible organic anodes is imperative and urgent for PIBs.

Current and future challenges

There are several kinds of organic materials which have been reported as potential anodes for PIBs. Among them, small molecular carboxylic acid may have the possible redox reactions, which show relatively low redox voltages (around 0.5 V vs. K/K^+) and potentially high capacity (figure 14(a)) [178]. However, such small molecular carboxylic acids suffer from the fatal flaw of the high solubility in liquid organic electrolytes, leading to rapid decline in capacity. Moreover, the effect of $-OH$ groups in the acids on the electrochemical performance is controversial and needs further investigation. The salification of carboxylic acid results into conjugated carboxylates which are typical anodes for LIBs, SIBs and PIBs, although it often leads to low theoretical specific capacity [179]. For example, for the reported conjugated carboxylates so far, the highest theoretical capacity is only about 263 mAh g^{-1} based on tetrapotassium pyromellitic (K_4PM) with four active sites [76]. Other moieties, such as unsaturated N-containing bonds in $C=N$ and $N=N$ groups, could also be redox-active in principle [180, 181], which have yet been well studied. On the other hand, there are several reports on the materials which are involving the reduction of $C=C$ bonds and this charge storage mechanism is worthy of further investigation [182]. It should be assured whether the capacity is originated from the decomposition or the reversible redox reaction.

Moreover, although it is believed that organic materials are superior in storage of large sized ions, due to the weak intermolecular interactions and large intermolecular space, the bulk samples often displayed relatively sluggish reaction kinetics of K ion intercalation/deintercalation, leading to charge–discharge polarization and long activation process [183]. In addition, organic materials often suffer from the low CE, which also requires further investigations [184]. Another feature of organic electrodes is the poor electrical conductivity, which imposes a fundamental limitation for rate capability. Compositing with carbon/or conductive polymers can improve the electrical conductivity of electrodes, which, however, will definitely reduce the energy density [179]. Last but not the least, organic materials often possess low density, which is one of the demerits of OEMs, leading to low energy density. Hence, it is necessary to further enhance the performance of organic anode materials, so as to promote the practical applications of organic PIBs.



Advances in science and technology to meet challenges

To address the above-mentioned challenges, the first possible advance in science and technology should be the full utilization of the advantage of organic materials, i.e. the molecular design strategy (figure 15). Firstly, in order to achieve a high theoretical and actual capacity, the organic materials should possess a high density of active sites and appropriate working voltage, which requires delicate chemical structural design of organic materials, including the selection of functional groups, linkages, substituents and the molecular construction [82]. Secondly, suitable arrangement or packing is important for ion diffusion. For example, layer-by-layer packing that ensures the ion diffusion in the interlayer channels will result in the high rate capability [185]. On the other hand, porous materials, such as COFs with ordered nanopores should be conducive to the ionic diffusion, although exfoliation may be necessary to better expose the active centers [183]. Furthermore, extending the conjugated structure and polymerization are supposed to enhance the structural stability and electrical conductivity [186] as well as reduce the solubility [184]. Fourthly, it should be noted that various

weak intermolecular interactions, such as van der Waals forces, hydrogen bonds, π - π interactions, and electrostatic Coulomb forces, may also be adopted to reduce the solubility of the materials and lead to enhanced cyclability and rate performance of batteries [75]. In addition, optimizing the electrode microstructure, such as controlling the particle sizes, morphologies, and porosity, is another efficient strategy to improve the performances of the PIBs. For example, nanosizing of the bulk sample will shorten the ionic diffusion path and charge transfer length, favoring a high rate capability, while exfoliation of layered materials can increase the utilization of active materials for high practical capacity [183].

Apart from normal organic/polymeric materials, MOFs have highly tailorable pore size and structure, which have similarity with COFs can provide large space for the accommodation of large-sized K^+ , thus benefiting fast ionic transport [187]. Moreover, both the ligands and metal clusters can be served as redox-active sites to achieve high theoretical capacity, which hence could combine the merits of both organic materials and inorganic electrode materials [81]. The high capacity enables the high energy density. The porous structure and the presence of organic elements guarantee the accommodation of large-sized ions and the rapid ionic transport, which helps for the rate capability and cyclability. Nevertheless, some aspects should be carefully considered, such as the electrical conductivity, the bond stability after accepting electrons and the match of the redox potentials of both ligands and metal centers. From this point of view, the conjugated coordination polymers (CCPs) [188, 189], which usually have high electrical conductivity, are particularly promising. Moreover, although the MOFs normally showed high capacity, the charge storage mechanism is not well defined and so-called activation process is often observed showing low CE and increasing capacity.

Concluding remarks

Due to the flexibility and weak intermolecular interactions, organic materials seem particularly intriguing for batteries with de-/intercalation of large sized ions, including K^+ ions, and hence organic materials could be promising as electrode materials of PIBs. Although the organic electrodes face some critical issues as mentioned above, there are many strategies that could be adopted to meet the challenges. Through the delicate molecular design, it is possible to develop novel materials with functional groups of multi-electron transfer, thereby enabling the high capacity and high energy density. In addition, the combination of inorganic and organic units into MOFs, particularly the conductive MOFs (e.g. CCPs), are deserved to be further studied. The nano crystallization of bulk materials and the exfoliation of the layered structures could enhance the exposure of active centers, the ionic diffusion and the redox kinetics. Along with the exploration of high-performance electrode materials, more investigations and analysis should be conducted to reveal the charge storage mechanisms, particularly in the cases that the same material show quite different performance in LIBs, SIBs and PIBs, as well as quite different performance in different electrolytes. As such, the mass production, cost, recycling, and safety of organic materials are also essential aspects to be addressed, which are the inevitable route for practical applications of PIBs.

Acknowledgments

This work was supported by the National Natural Science Foundation of China (52173163), the National 1000-Talents Program, the innovation Fund of WNLO and China Postdoctoral Science Foundation (2021TQ0115, 2021M701302 and 2020M672323).

11. Computational discovery of materials

Furio Cora^{1,2} and David O Scanlon^{1,2,3}

¹ Department of Chemistry, University College London, 20 Gordon Street, London WC1H 0AJ, United Kingdom

² Thomas Young Centre, University College London, Gower St, London, United Kingdom

³ The Faraday Institution, Quad One, Becquerel Avenue, Harwell Campus, Didcot, United Kingdom

Status

Computational studies on materials for PIBs have taken inspiration from the more mature LIB and SIB fields [190, 191], and followed a similar developmental pathway. K⁺ intercalation has been studied into hosts known from Li and Na battery applications; initial work on cathode materials focused in particular on the layered TMOs that have been so well studied for both Li-ion and Na-ion chemistries, however it has now become clear that issues around the larger radius of the K⁺ ion have a negative effect on the achievable capacity and average voltage, regardless of the TM chemistry at play [124].

The large size of K⁺ compared to Li⁺ and Na⁺ makes identification of new intercalation hosts for PIBs particularly challenging. While binary oxides of TM ions in high oxidation state often provide intercalation sites accessible to Li⁺ with little structural distortions, so that a search in structural databases provides a multitude of targets, intercalation of K⁺ requires materials with lower packing density to provide not only larger intercalation sites but especially large enough channels for K⁺ transport. Such low-density structures are intrinsically unstable in the chemistry of ionic oxides and halides. Low density polymorphs are more common in compounds with some degree of directional bonding. One realization of structures with low density because of bonding constraints is represented by polyanionic compounds; these are increasingly screened computationally, primarily using DFT [192]. The large K⁺-K⁺ distances in polyanionic compounds have been shown to generate a less sloped voltage profile, and the inductive effect of the polyanion generally results in a higher voltage [192]. Ceder *et al* screened the ICSD database for K-containing polyanionic materials with the composition K-TM-XO-C, where TM represents one of more TMs (V, Cr, Mn, Fe, Ni) with multi electron redox capability, XO represents a polyanion group (PO₄³⁻, SO₄²⁻, SiO₄⁴⁻ or BO₄⁵⁻), and C represents a counter anion (F⁻ or O²⁻) [62]. The 74 candidates they found were further down selected to 21 by excluding compounds with a K/TM ratio less than 1, and by the requirement that the TM is in an octahedral coordination environment with an appropriate oxidation state. 19 of the 21 candidates had not been tested electrochemically before and using DFT based filtering of theoretical capacities and voltages, ten potential K polyanion cathodes with theoretical capacities greater than 100 mAh g⁻¹ were identified, with four experimentally realized and electrochemically tested. Nudged elastic band calculations, however, showed that despite having less sloped voltages than layered oxides, the very high K-ion migration barriers and high oxidation voltages pose significant challenges to the realization of high performance PIBs [62].

Another example of low-density compounds is the family of PBA materials, built on the hexacyanoferrate [Fe(CN)₆]⁴⁻ ion (HCF). PBAs can be imagined as a double perovskite A₂MM'X₆, where the monoatomic oxide or halide anions (X) are replaced by bridging cyanide ligands that expand the separation between adjacent metal sites. Experimental studies of PBAs as K intercalation hosts show promising activity but limited cycling stability [193, 194]; experimental progress however is not yet matched by modeling work.

For anodes, computational screening of candidates from the Materials Project database using DFT has been conducted, where grand potential diagrams as a function of the chemical potential of K were constructed to study the reaction potential and theoretical capacity of a range of possible candidates [195]. The authors screened 279 binary compounds (phosphides, oxides and sulphides), and 14 metal/metalloids that could potentially form alloying anodes. The authors predicted that P, As, Si, Sb, Bi and Ge will exhibit higher theoretical capacities than conventional graphite anodes and identified 18 binary compounds that should possess a low reaction potential and a high capacity (<0.7 V and >450 mAh g⁻¹). Detailed studies of intercalation/conversion have not, however been conducted.

Current and future challenges

As in other areas of materials science, also in the field of PIB computational chemistry methods can provide important information relating to atomic level mechanisms at play during the battery operation, and a more efficient identification of new intercalation materials. Both applications present challenges to overcome: the former to ensure adequate accuracy in the calculation of energies and the latter to extend beyond screening of known crystal structures databases.

The intercalation chemistry of oxide and halide compounds for K-ion batteries builds on the knowledge gained for LIBS and NIBS; other than the increased importance of steric effects, the change of alkali metal does not introduce new challenges for computational studies. Compounds with less conventional anions,

such as the PBA family, instead are less well characterized from a fundamental point of view, and a deeper understanding of their structural and defect chemistry through accurate quantum chemical techniques is still needed. PBAs often contain a large number of intrinsic defects such as HCF vacancies and have a range of distortion modes not accessible to oxide/halide perovskites [45]. The large interstices of the PBA lattice exceed even the dimensions of K^+ , and the lattice undergoes tilting distortions upon intercalation in a way consistent with small A-site ions in perovskites. The interplay between defect chemistry and distortion modes of the PBA lattice upon K intercalation is a topic suitable for computational analysis but not yet explored in detail. Calculations of PBA cells with different distribution of vacancies will require very large unit cells, often with multiple metals and with multiple oxidation states. In addition, crystal field effects in such coordination compounds are likely to be much more pronounced than in oxidic hosts, which provides a stress test even for the most accurate DFT functionals based on hybrid exchange.

Widening the number of potential electrodes that we can test for improved PIB performance is a key challenge for the field. While computational screening of known inorganic solids has been successful in finding new potential K-ion electrodes, the limitation of only studying known phases (or elemental substitutions of known phases) is quite restrictive. It is likely that there are many undiscovered K-ion containing systems that would warrant computational/experimental investigation. An alternative way to push the boundaries of our knowledge of K-ion containing solids is to use targeted crystal structure prediction. In this way we can computationally probe the phase diagrams of complex potassium containing compounds, including polyanionic and non-oxide based anions, with designer element choice, where factors such as earth abundance and techno-economic considerations can be taken into account. This approach has begun to be used in the Li-ion and Na-ion fields [196–198], and recently has been demonstrated for the ternary K-Sn-P composition space [199, 200].

Another challenge that the field faces is modeling the performance of K-ion electrodes at varying states of charge. It is no longer enough to study a fully intercalated and then deintercalated structure to simulate an average voltage. As a community, we need to understand what occurs to the defect chemistry of these systems during charge and discharge (e.g. TM ion migration, anion redox mechanisms, volume expansion, structural distortions etc) and ideally under standard operating temperature and bias. Computational toolkits are being developed for automating defect chemistry analysis [201–203], however, often these studies are only valuable at very computationally expensive levels of theory (typically hybrid DFT).

Ab initio molecular dynamics is a very valuable tool to probe ionic movement in solids, however it is often prohibitively expensive at one elemental composition, let alone at multiple compositions during charge and discharge. The usually high activation barriers associated with K^+ migration may in addition require methods for rare event sampling, such as metadynamics. Interatomic potentials, although much cheaper, typically cannot capture the correct physics/chemistry of bond breaking and formation, of charge transfer, or of mixed oxidation state systems. Therefore, a clear challenge for the field is to gain insights into long timescale calculations of materials at realistic operation conditions.

Advances in science and technology to meet challenges

A complex problem such as identifying computationally a new, likely as yet unknown, structure type and composition for optimal K intercalation chemistry cannot be achieved by brute force alone and with currently available methods only. On one hand, we will require fast but accurate computational methods to calculate energies, electronic structure and equilibrium geometries of large unit cells with multiple redox active ions. Machine learning/artificial intelligence has emerged as a key enabler for next generation calculation techniques. Recently, high dimensional neural network potentials (HDNNPs) have been developed for Li-ion systems that can capture the redox behavior, magnetic ordering and charge transfer properties of the $Li_xMn_2O_4$ system [204–206], paving the way for simulations of tens of thousands of atoms for nanosecond timescales. Indeed, these HDNNPs have been used to model the $Li_xMn_2O_4$ spinel/water interface, allowing a new understanding of Mn dissolution and hydrolysis [207]. Such advances in machine learned potentials will allow much more insight into PIB materials moving forward.

Machine learning potentials can also accelerate crystal structure prediction searches. Recently Picard has demonstrated a scheme for the rapid construction of disposable, or ephemeral, data derived potentials [208], which can then be used for crystal structure prediction in the AIRSS code [209] to massively speed up searches in complex phase space versus brute DFT searches. Again, this highlights the ability of machine learning to accelerate materials discovery, although it must be mentioned that applications in structure prediction such as those of [208] are as yet based to chemistries much simpler than those required to make real progress in PIB electrodes and are sensitive to the choice of DFT functional used in the generation of reference data. Alternative structure prediction methods that employ more substantial input from known structural chemistry relationships are also available, e.g. [210], and have been successfully applied to materials with multiple elements using DFT calculations to rank energies. At the other extreme, machine

learning analysis of MOFs can be employed to predict the likelihood of given metal and complex anion compositions to yield structures with the desired porosity [211] and could be employed to identify less commonly used anions of potential interest. Useful prediction of new stable K intercalation hosts will require a confluence of components from all the above approaches into a single chemically driven tool.

Concluding remarks

The continuous development of more accurate quantum chemistry techniques, allied to large improvements in high performance computing architectures has made property prediction for battery systems more and more reliable. To advance the field further, and to support true theory-experiment studies of new/existing PIB, the field needs to fully embrace and explore the potential advances enabled by the use of machine learning, both in terms of materials discovery, and property prediction. *Ab initio* modeling of batteries under realistic operation conditions is moving tantalizingly closer and closer.

12. Organic electrolytes—salts

Lei Qin and Yiyang Wu

Department of Chemistry and Biochemistry, The Ohio State University, Columbus, Ohio, United States of America

Status

PIBs are recognized as one powerful competitor to current LIBs as the large-scale energy storage solution due to their cost-effectiveness and high-voltage operation. Nevertheless, compared to LIBs adopting 1.0 M lithium hexafluorophosphate (LiPF_6) in ethylene carbonate/dimethyl carbonate as the standard electrolyte recipe, an advanced electrolyte is yet to be explored for PIBs [212]. As the bridge to connect anode and cathode, the electrolyte is crucial in affecting the PIBs performance in terms of rate capability, lifespan, reversible capacity, and safety. This is controlled by the stability and properties of the SEI and cathode electrolyte interphase (CEI) at the anode and cathode, resulting from the degradation of the solvent and/or salt during the battery cycling process [213]. Although extensively studied and well characterized in LIBs, the SEI/CEI components for PIBs are ambiguous and remain one of the most critical fields for future research.

Organic electrolytes contain salts and solvents with/without functional additives. The ideal potassium salt must adhere to some criteria: (1) high ionic conductivity; (2) (electro)chemical and thermal stability; (3) low cost with scalable syntheses with high purity; and (4) low toxicity/environmental benignity. The high ionic conductivity of the electrolyte is essential for rapid ions transport between electrodes. In addition, a low HOMO and a high LUMO of electrolyte ensure superior electrode/electrolyte interfacial stability. Such strict requirements naturally limit the available salt options.

Notably, there exist obvious differences in ionic conductivity, solubility, and solvation/de-solvation behavior of potassium-based electrolytes compared with the lithium-based counterpart. As is known that both solvents and salt anions possess the ability to coordinate the cations [214]. Generally, the weaker Lewis acidity of potassium ions results in a weaker interaction with anions/solvents, thus promoting potassium ions' diffusion rate and conductivity with reduced electrolyte viscosity [212].

Current and future challenges

Among the salt anions illustrated in figure 16, tetrafluoroborate (BF_4^-) and perchlorate (ClO_4^-) have received less attention due to their low solubilities and disappointing ionic conductivities in conventional organic solvents [215]. Like LIBs, PF_6^- is still the most promising salt option for PIBs due to its superb ionic conductivity and electrochemical stability, especially for the passivation of Al foils. Nevertheless, it suffers from intrinsic sensitivity to moisture and low thermal stability. The HF formation via hydrolysis or the toxic gas components via thermal decomposition could lead to electrolyte degradation with severe safety concerns [216]. In comparison, the hydrolytically stable trifluoromethanesulfonate (OTf^-) has shown promising results as it possesses high thermal stability, good electrochemical stability, and low viscosity when applied in ILs [217].

An interesting emerging class of imide-based salts is attractive owing to the high solubilities in conventional carbonate- and ether-based solvents [215]. The typical examples are the KFSI and potassium bis(trifluoromethane)sulfonimide (KTFSI). Notably, the KFSI-based electrolytes have higher conductivities with superior electrode compatibility than the KPF_6 counterpart. The stabilization effect of KFSI on various anodes is mainly due to the formation of durable KF-rich SEI derived from FSI-decomposition [218]. Therefore, KFSI-based electrolytes enable highly reversible K metal plating/stripping [97], K^+ intercalation/deintercalation [219], or alloying/dealloying [220] for PIB anodes. However, its high cost and incompatibility with Al foil may impede the potential application in high-energy-density PIBs [145]. Additionally, KFSI cannot be used in emerging K- O_2 batteries due to the nucleophile nature of the superoxide intermediate [221]. Despite possessing a lower ionic conductivity of the electrolyte and formed SEI than KFSI, KTFSI is a potential salt option for K- O_2 batteries because of its higher stability when exposed to superoxide species. Admittedly, it is still challenging to develop a salt that can meet all the requirements abovementioned. Future research efforts should focus on molecularly designing anions with tunable groups, which allows for easy modification on the fundamental properties of salt.

It is highly challenging but more prominent to characterize the SEI/CEI for PIBs due to the reactive K and more dynamic changes of the electrode structures upon cycles. X-ray photoelectron spectroscopy (XPS) and time-of-flight secondary-ion mass spectrometry (SIMS) analyses have probed the existence of organic (such as alkoxide, alkyl carbonate) and inorganic (such as KF , $-\text{SO}_x\text{F}$) species in SEI components [8]. These organic potassium-based compounds are usually more soluble than their lithium counterparts, resulting in higher fractions of inorganic fragments formed on the PIB anode surface.

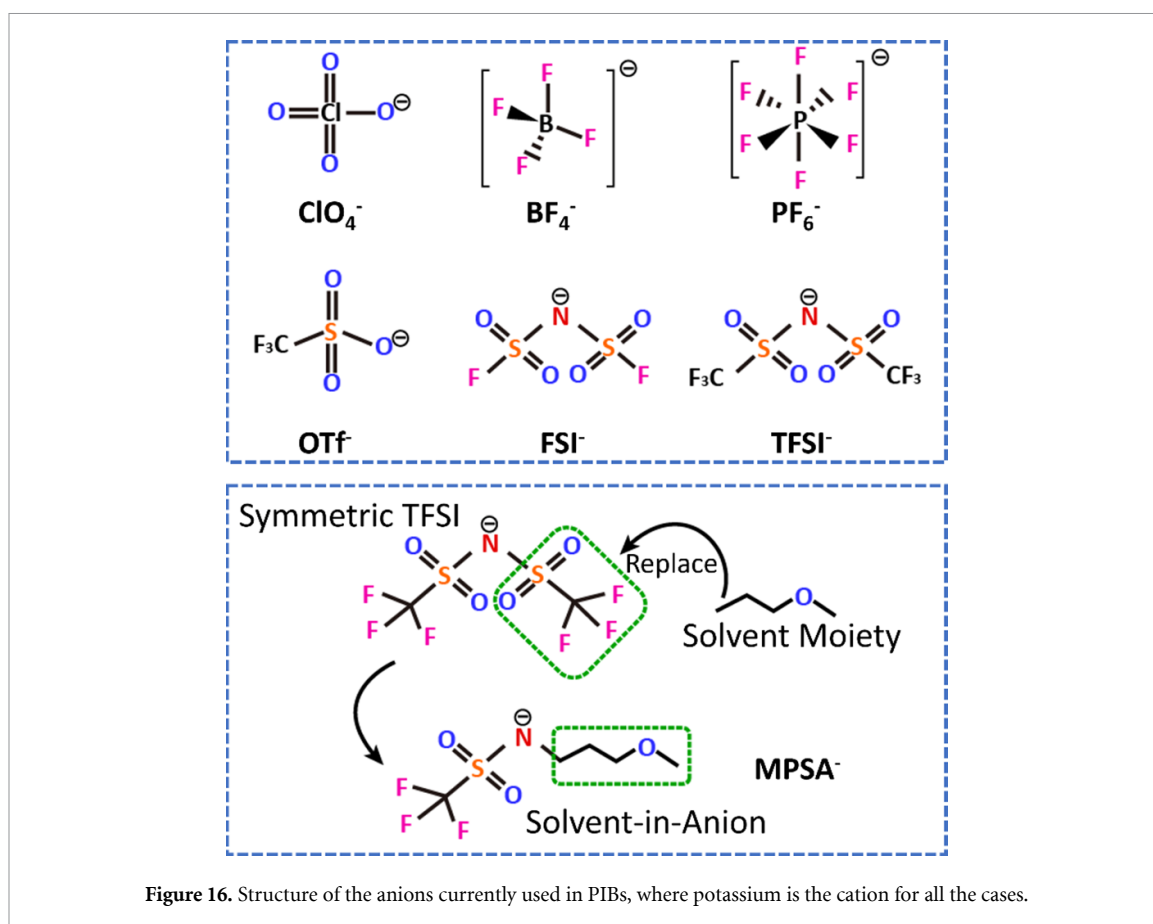


Figure 16. Structure of the anions currently used in PIBs, where potassium is the cation for all the cases.

Another challenge is to reduce the safety hazard, which is crucial for PIBs because of the reactive K with atmospheric oxygen and moisture. Few studies address this, but KFSI has been verified to be a non-flammable electrolyte when used in the fire-retardant phosphates [222]. Nevertheless, the dilute KFSI/phosphate electrolyte cannot form a superb passivation layer on the anode, and more efforts are required to achieve satisfactory electrochemical performance.

Advances in science and technology to meet challenges

Functional salt additives are explored to resolve the K metal or K^+ insertion/extraction inefficiency. Yang *et al* utilized potassium difluorophosphate as the effective SEI-forming additive (0.2 wt%) to improve the depotassiation kinetics and capacity retention in graphite anode [223]. Kang's current work demonstrated that a small amount of potassium nitrate (50 mM) into KFSI/ether-based electrolyte could contribute to the formation of a more stable SEI layer enriched in N/F species on the K metal surface [224].

Cation solvation structure plays a crucial role in dictating interfacial chemistry. A general principle was unraveled in prior studies that the competitive coordination between anions and (solvating) solvents to cations is the origin of different interfacial chemistries since the primary solvation sheath is the precursor of SEI and CEI. It is generally accepted that the anion-derived inorganic-rich SEI/CEI can provide good electrode stability and ion transport property [225, 226]. Besides solvents, functional salts could be introduced to tune the solvation structures. Wu group has recently conducted some pioneering research in this direction [227]. They utilized the concept of "solvent-in-anion" to synthesize the asymmetric K salts by grafting the ether solvent moiety onto the bis(trifluoromethyl) sulfonylimide (TFSI) motif. The typical example is the (3-methoxypropyl)((trifluoromethyl)-sulfonyl)amide (MPSA) anion with the structure shown in the lower panel of figure 16. One advantage of this salt design principle is that it allows easy tuning of the cation-anion/solvent interactions by attaching various ether side chains. In addition, such salt is proposed to possess the combined features of a TFSI anion and an ether solvent. Guided by the like-dissolves-like rule, the designed KMPSA possesses unprecedented solubilities in dimethoxyethane ($\sim 16.6 \text{ mol kg}^{-1}$). The resultant concentrated electrolyte shows a stable electrochemical window up to above 7 V vs. K^+/K , which offers a possibility to realize the high-voltage operation of PIBs. Notably, KMPSA salt features a low melting point of around 50 °C, making it interesting for developing low-temperature single-cation ILs [228].

Owing to the complexity of the electrode/electrolyte interface layer, there is massive uncertainty about its composition, components' spatial distribution, solubility, ionic conductivity, as well as chemical, mechanical and thermal stability. Modern advances in emerging and powerful characterization techniques, such as cryogenic TEM, time-of-flight SIMS, neutron scattering spectroscopy, dynamic nuclear polarization-enhanced NMR spectroscopy, and operando testing methods, could be readily applied to PIBs to offer further insights into the formation or even dynamic evolution of interface layer. With advances in computer technology, computational methods based on DFT calculation and molecular dynamics (MD) simulation would facilitate a better understanding of the SEI/CEI formation mechanism. Although there have been several investigations on the SEIs/CEIs for PIBs, more research is still required to understand the interplay between electrolyte chemistry, SEI/CEI formation, and electrode stability.

After replacing the flammable organic solvents with non-flammable ones (e.g. phosphates [222], fluorinated phosphazenes [229], ILs [229], water [34]), it is promising to use the moderately concentrated or localized concentrated recipes to ensure that the anode is protected by the salt anion-derived SEI passivation layer. In this regard, the battery is expected to possess the combined advantages of nonflammability and superb electrochemical performance.

Concluding remarks

Compared to the mature LIBs technology, many efforts are still needed to explore the full potential of infancy PIBs for commercial use. Electrolytes are crucial, as unwanted side reactions on electrodes can significantly deteriorate the overall battery performance and calendar life. The current potassium electrolytes possess significant shortcomings, such as moisture sensitivity, thermal instability, flammability, and cost, indicating an urgent need to develop advanced electrolytes to overcome the above drawbacks. The emerging big data analysis technique can assist in conducting high-throughput screening and even precise predicting of electrolyte properties. This could, in turn, accelerate the discovery of high-performance electrolytes for PIBs. This roadmap emphasizes critical areas where efforts should be put. Principally, this is in characterizing the degradation by-products of SEI/CEI as well as developing the novel salts whose molecular structure can be easily tailored for further tuning their fundamental properties in this chapter. Undoubtedly, PIBs would have a prosperous future and rival LIBs counterpart with an increased research focus.

Acknowledgments

This research is funded by the U.S. Department of Energy (Award No. DE-FG02-07ER46427). The authors are also grateful for the partial support of this work from the Ohio State University.

13. Organic electrolytes—solvents

Dengyun Zhai, Junyang Hu and Feiyu Kang

Shenzhen Geim Graphene Center, Institute of Materials Research, Tsinghua University, Shenzhen, People's Republic of China

Status

The organic solvents used for PIBs could be classified into three kinds, i.e. carbonate ester, ether, and phosphate ester (figure 17). They are all invented for LIBs first and are introduced into PIBs afterwards. However, none of them can function well enough to commercial level in PIBs, not like carbonate ester solvents in LIBs. Much effort should be put into this field in the future.

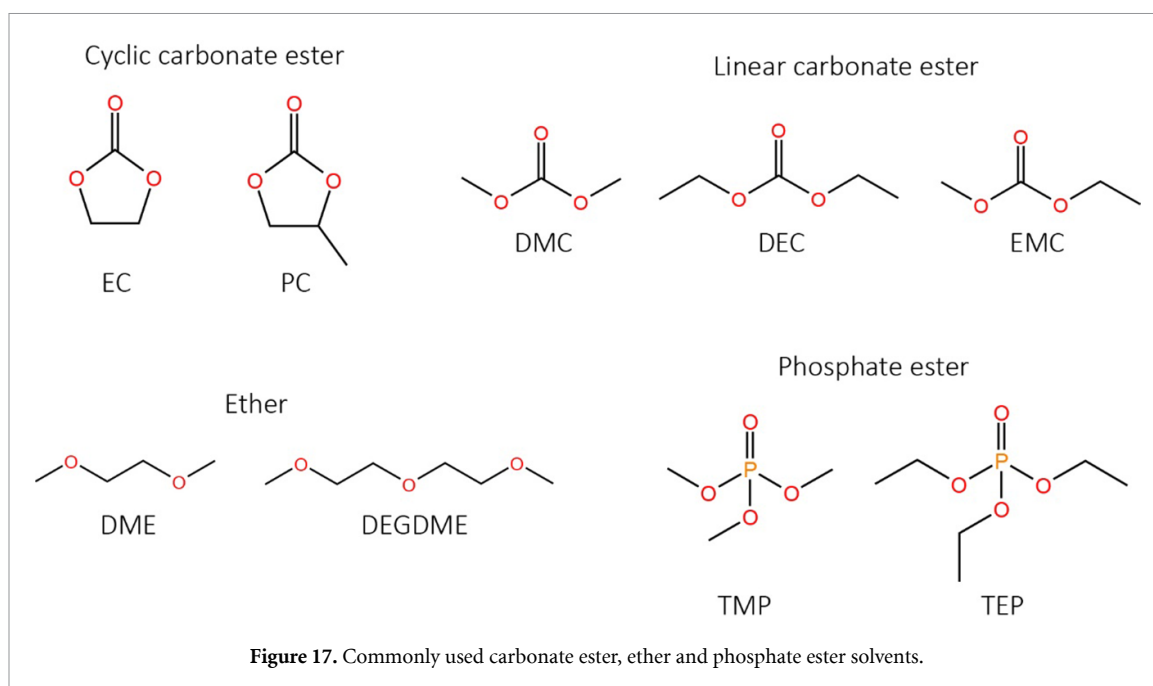
The first PIB with organic electrolyte was proposed by Ali Eftekhari in 2004, learning the successful ethylene carbonate (EC)-based electrolytes of LIBs [29]. In 2015, graphite was found as a promising anode material for PIBs in a classical EC-based electrolyte (0.5 M KPF₆ EC:diethyl carbonate(DEC)), which aroused great enthusiasm for PIBs [92]. However, in next studies the classical EC-based electrolytes with cyclic and linear carbonates mixed solvents were reported to be not stable [230]. In 2019, Naylor *et al*, found that thick and unstable SEI is generated on graphite anode during cycling in the classical EC-based electrolyte (0.8 M KPF₆ EC:DEC), which should be the reason for the rapid capacity fading of graphite anode [231]. Recently, our group revealed that the thick and unstable SEI should be accumulated oligomers [232]. Apparently, the classical EC-based electrolytes are not able to form stable SEI and exploit the full capability of graphite anode. Additionally, the classical EC-based electrolytes were found unfavorable to other anodes and cathodes in PIBs as well [97, 222, 233].

In recent years, researchers have investigated numerous electrode materials and electrolyte formulas for PIBs. Several carbonate-ester-, ether- and phosphate-ester-based electrolytes exhibited superior performance in half-cell or full-cell tests. Pure cyclic carbonates EC: PC-based electrolyte and pure linear carbonate EMC-based electrolyte are surprisingly better than the classical EC-based electrolytes in graphite anode tests [90, 234]. Ether solvent DME shows excellent stability in anode half-cell experiments [94, 97]. And high concentration ether electrolytes further show long cycling performance in cathode tests [97, 215, 219]. Moreover, phosphate-ester-based electrolytes were found to have the most excellent performance in anode and cathode half-cell and full-cell tests [37, 222, 235]. These successful electrolyte formulas make practical PIBs extremely promising now. However, there is still a gap from lab-scale PIBs to commercial PIBs. And more effort should be filled up this gap.

Current and future challenges

The three kinds of electrolyte solvents carbonate ester, ether and phosphate ester are facing different challenges now.

1. Carbonate ester solvents. Through years of study, the cyclic and linear carbonate mixed solvents are found not stable and detrimental to PIBs. However, interestingly, the pure cyclic carbonate EC: propylene carbonate (PC)-based electrolytes (1 M KPF₆ EC:PC) exhibits much better performance in the graphite anode half-cell test [234]. And pure linear-carbonate-based electrolyte (concentrated KFSI EMC) show extraordinary long cycling stability in the graphite half-cell test and promising performance in the full-cell test [90]. Therefore, carbonate ester solvents are still promising candidates for PIBs. In this context, the key issue is what makes the classical EC-based electrolyte unstable, and whether it is possible to modify it. This might also be the key to improve the performance of pure cyclic- or linear-carbonate-based electrolytes.
2. Ether solvents. Owing to the reduction stability of ether solvents, ether-based electrolytes generally show excellent long cycling stability in half-cell tests on anode materials. However, the ether solvents have low oxidation stability, resulting in poor performance in half-cell tests on cathode materials [236]. Fortunately, researchers found high concentration and localized high concentration ether-based electrolytes could minimize the amounts of free ether solvents, and therefore improve the oxidation stability of ether-based electrolytes [215, 237]. Additionally, with low-polarity cosolvent diluted, the localized high concentration ether-based electrolytes can avoid the poor rate performance caused by high viscosity [219]. Therefore, the remaining issue is the imperfection of CE. In the first few cycles, the CE of graphite anode is relatively low. And in the afterwards stable cycles, the CE is also around 99.7%, not reaching 99.9% [219]. This imperfection will be enlarged in practical PIBs, and thus should be resolved in the future.



3. Phosphate ester solvents. Among the three kinds of solvents, phosphate esters are the most promising ones. The concentrated trimethyl phosphate (TMP)- and triethyl phosphate (TEP)-based electrolytes show extraordinary long stability and acceptable rate performance in anode and cathode half-cell tests. In the full-cell tests, they also show considerable long life. With the merit of nonflammability, TMP- and TEP-based electrolytes seem most suitable for commercial PIBs. However, the imperfection of CE is also a problem for this kind promising electrolyte.

Advances in science and technology to meet challenges

Considering the excellent performance of ether- and phosphate-ester-based electrolytes, the following research on electrolyte solvents should first pay more attention to practical PIBs, which means employing high enough mass-loading and fair rate in tests. Through those approaches, the research community could amplify the problems of electrolytes, and thereby make real progress toward practical PIBs;

1. Carbonate ester solvents. On the way to modifying the carbonate ester solvents, two key questions should be answered. One is why the classical EC-based electrolytes fail in PIBs, the other is why pure cyclic carbonates and pure linear carbonate function better than the classical EC-based electrolytes. We believe these two questions are the keys to understanding the instability of carbonate ester solvents and then modifying them.
2. Ether and phosphate ester solvents. These two kinds of electrolytes both have shown promising performance in lab-scale tests. And the problem is the same, which is the imperfection of CE. This should be a result of parasite reactions in the battery system. However, in a complicated electrochemical system, it is not easy to identify the parasite reactions and eliminate them. A finer analysis of the change in SEI and electrolyte composition may be the key to resolving it.
3. Electrolyte additives. Electrolyte additives could be another way to solve the problems of electrolytes. With low content, the additives can alter the viscosity, wettability, SEI formation process, and solvation structure of electrolytes. By specific alterations, the performance of the electrolyte can be improved. Fluoroethylene carbonate (FEC) is one of the most widely reported and used additive in LIBs [238]. However, the introduction of FEC into EC-based electrolytes demonstrated distinctly different results for PIBs [239, 240]. As to the ether and phosphate ester solvents, the adding of additives in lower concentration electrolytes can achieve the excellent performance of highly concentrated electrolytes. Our group has reported that the KNO_3 additive can make the moderate concentration (2.3 M) KFSI DME electrolyte comparable to the high concentration (normally, >3 M) electrolytes in 4 V-class cathode half-cells [224]. Liu *et al.*, found that the ethylene sulfate (DTD) additive can make 1.0 M KFSI TMP electrolyte compatible with graphite anode, without the need of concentrated electrolyte strategies [241]. Therefore, the study on the electrolyte additives may also be a viable path to practical PIBs.

Concluding remarks

After years of study, localized high concentration ether and concentrated TEP are the most optimized electrolyte for PIBs for now. These two kinds of electrolytes show much better performance than the classical EC-based electrolyte and should be the preferred choices to evaluate anode and cathode material in the following research. And to realize the commercialization of PIBs as soon as possible, resolving the imperfection of CE of these two kinds of electrolytes should be in top priority for the community. Yet the carbonate-based electrolytes are still promising. Figuring out why the classical EC-based electrolyte is unstable may be the key to making them competitive again.

Acknowledgments

This work is financially supported by National Key R&D Program of China (2021YFA1202802), the National Natural Science Foundation of China (No. 52072206), Local Innovative and Research Teams Project of Guangdong Pearl River Talents Program (2017BT01N111) and Shenzhen Stable Supporting Project (WDZC20200818155913001).

14. IL electrolytes for potassium ion batteries

Tianyi Shi and Robert G Palgrave

Department of Chemistry, University College London, 20 Gordon Street, London WC1H 0AJ, United Kingdom

Status

ILs are compounds composed only of ions that are liquid at or near room temperature and can also be described as molten organic salts. They have excellent potential as electrolytes for many applications, due to their high ionic conductivity, wide electrochemical stability window, and powerful, and sometimes unusual solvating properties. Further characteristics make ILs especially suitable for use in batteries. Firstly, they are almost completely involatile, and as such, despite commonly comprising organic molecular ions, their flammability is very low, making them safer than organic battery electrolytes. Secondly, they are highly tunable, as the molecular structure of cation and to some extent the anion can be altered incrementally, allowing fine tuning of chemical and physical properties. Thirdly, due to their very low vapor pressure, additional possibilities open up for analysis—for example, vacuum techniques such as XPS can be carried out on ILs, or on electrochemical devices containing ILs as electrolytes. This may allow new insights into interaction between IL and electrode, SEI formation, or degradation pathways and products; such *operando* and *in situ* analysis is considerably more difficult with traditional battery electrolytes.

Compared with the situation with Li and Na batteries, there have been far fewer ILs studied for use in PIBs. Table 2 shows a summary of the reported ILs for use in PIBs, either in full cells or half cells. The structures of the ILs are displayed in figure 18. ILs for PIBs have been recently reviewed [212], and only a summary will be presented here.

Perhaps unsurprisingly, many of the currently researched PIB IL electrolytes have previously been used for SIBs and LIBs. However, there are significant differences between solubility, ionic conductivity and solvation properties of potassium electrolytes and that of lithium electrolytes due to the lower electronegativity and large size of the potassium ions [212]. In addition, since potassium metal has higher chemical reactivity, the interfacial chemistry controlled by the stability of electrolytes will become more important.

Imide anions, namely bis (fluorosulfonyl) imide (FSI) and TFSI, are almost exclusively used as the anions for PIB IL electrolytes. These anions have several advantages over alternatives, such as halides, PF₆ or BF₄; the charge delocalization of the imide is such that it reduces the intermolecular ionic interaction, making imide based ILs of lower melting point and viscosity, and high conductivity than the most closely corresponding non imide analogues [247, 248]. These factors also make them popular for Li and Na battery electrolytes [249].

The large majority of the work has been using di N-alkylated pyrrolidinium based cations, denoted Pyr_{x,y}, where x and y are numerals representing the alkyl chain lengths. The N,N-dimethylpyrrolidinium cation (Pyr_{1,1}) forms only solid ionic compounds with melting points over 100 °C [250]. Lengthening one of the alkyl chains depresses the melting point, as the cation becomes less symmetric and bulkier. While Pyr_{1,2} TFSI is also a solid at room temperature, Pyr_{1,3} TFSI and Pyr_{1,4} TFSI have melting points of 12 °C and −18 °C respectively [250]. The electrochemical stability window for such compounds is around 5.5–6 V and is largely unaffected by the cation alkyl chain length [251]. Longer alkyl chain length have higher viscosity and are unsuitable as electrolytes.

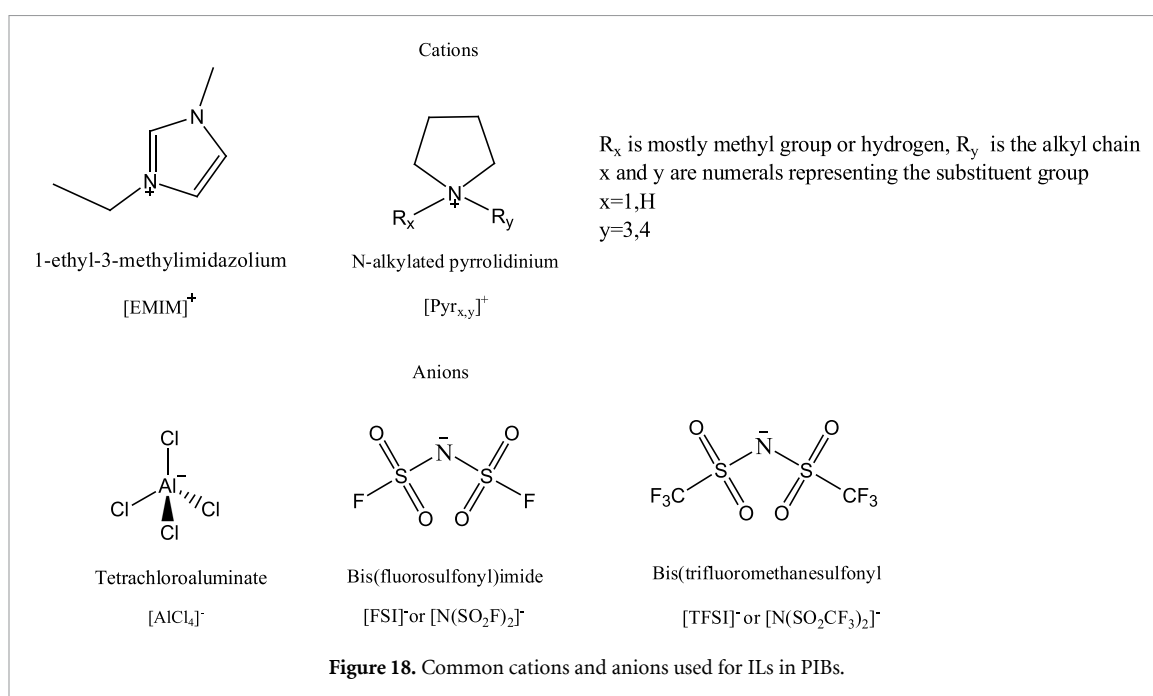
Morozova *et al*, recently called into question the stability of some commonly used TFSI derived ILs, when used with Al/Al₂O₃ electrodes [252]. They found that imidazolium based cations, as well as Pyr_{1,2}, Pyr_{1,3}, and Pyr_{1,4} cations, each with TFSI anion, showed pronounced Al corrosion when KTF SI salt was used. Much of this could be avoided by using a mixture of KTF SI and KPF₆, the latter known to pacify Al surfaces through formation of aluminum fluoride. Even with KPF₆, each electrolyte showed evidence of oxidation.

Addition of a K containing salt additive is of course necessary. Typically K TFSI or K FSI is chosen, in each case to match the anion of the IL electrolyte. These potassium sulfonimide salts offer several advantages over alternatives, such as KPF₆ or KClO₄: they are lower toxicity, and, as is the case with organic electrolytes, they tend to have higher solubilities in ILs. However, the solubilities in ILs are much lower than organic electrolytes. KTF SI and KFSI can typically be dissolved up to around 1 mol kg^{−1}, much lower than can be achieved in propylene carbonate. Addition of the potassium salt causes a slight increase in both density and viscosity, as the K⁺ ion is considerably smaller than the organic IL cation, so increases the strength of ionic interactions. Ionic conductivity typically decreases upon salt dissolution, this is of course because the pure IL has considerable ionic conductivity even in the absence of the potassium salt, and the increase in viscosity causes this to fall.

Table 2. Summary of reported IL electrolytes for PIB applications.

Ionic liquid	K salt (concentration)	Conductivity (room temp) (mS cm ⁻¹)	Decomposition temperature (°C)	Electrochemical stability window width (V)	References
EMIM Cl/AlCl ₃	KCl/KFSI (0.96 M)	13.1	330		[242]
Py _{r13} TFSI	KTFSI (0.6 M)	2.1	417	6.01	[243]
Py _{r13} FSI	KFSI (1.0 M)	4.8	307	5.72	[243, 244]
Py _{r13} FSI	KFSI (1 M)	3.31	Not reported	Not reported	[46]
Py _{r14} TFSI	KTFSI (0.5 M)	7.96	350	6	[245]
Py _{r14} TFSI + ethylene sulfate	KTFSI (0.3 M)	Not reported	Not reported	Not reported	[246]
Py _{rH4} TFSI	KTFSI (0.5 M)	1.49	300	4	[245]

Key: TFSI: bis(trifluoromethane) sulfonimide, FSI: bis (fluorosulfonyl) imide, EMIM: 1-ethyl-3-methylimidazolium, Py_{r_xy} is defined in the text.

**Figure 18.** Common cations and anions used for ILs in PIBs.

Current and future challenges

The nascent state of research into ILs for PIBs mean there are many fundamental challenges to be overcome. While some of these are shared with Li and Na battery fields, some are unique to the PIBs.

Perhaps the most important issue to be dealt with is high viscosity of currently used ILs. While in theory, ILs offer great tunability of ion molecular structure, which should allow creative approaches to improve solvation and electrode interface chemistry, in practice the need for low viscosity to achieve sufficient ionic conductivity and transference numbers limits most current research to a small selection of anions (chiefly imides) and cations (Py_{r_{1,n}} n = 3,4). Commonly, small deviation from these choices leads to higher viscosity, which will negate any other benefits. A current challenge is therefore to find new ILs with lower, or at least equal viscosity to those already well used, whilst maintaining the necessary solubilizing power, electrochemical stability and surface chemical properties for PIB applications. Viscosity in ILs has been extensively studied [253], and there is a good understanding of underlying physics and how to apply this in chemical design [254]. One approach is to functionalize the alkyl chains in the cation; for example, use of ether [255, 256] or alkene functional groups [257] reduce viscosity, but likely will increase the reactivity of

the IL, reducing the electrochemical stability window. Alternative cations such as sulfonium [258], phosphonium and ammonium have all been demonstrated to display low viscosities. For anions, the dicyanamide anion has been used successfully of low viscosity liquids [259, 260]. Adaptation of these chemistries, used successfully in other fields, to produce useful PIB electrolytes with lower viscosities than those listed in table 2, will be an important future challenge.

Strongly linked with the issue of viscosity is that of potassium ion conductivity. Ionic conductivities of ILs are high compared with organic electrolytes, but potassium ion transference numbers are likely lower in most cases. Solubility limits of potassium salts are also currently rather low (table 2), and so development of electrolyte chemistry to allow higher concentrations to be stabilized is an important goal. Indeed, ILs have proven to be much more effective electrolytes at high salt concentration in LIBs, and a similar benefit may be found in PIBs. However, understanding atomistically the interactions between salt and IL electrolyte during cycling is still at an early stage even for LIBs, and is non-existent for PIBs. Progress in this area will come from combined experimental and computational studies and may be necessary for driving rapid progress in electrolyte-salt chemistry.

Characterization of electrolyte–electrode interface chemistry is a third challenge. An extensively studied topic for other battery chemistries that is recognized as central to developing new electrode and electrolyte chemistries, the work on PIB IL-electrode interfaces is extremely limited. However, use of ILs offers opportunities for *in situ* and operando studies of electrolyte surfaces that are difficult or impossible with organic electrolytes [261]. Use of such methodologies (most prominently XPS, but other surface methods are applicable too) may offer a short cut to understanding of surface phenomena in PIBs with ILs.

Further ahead, an important challenge to be faced is the high cost of ILs. Progress can be made through development of cheaper reaction pathways, such as use of ion exchange resins rather than traditional batch metathesis reactions [262], and scale up of manufacture is expected to significantly drive down costs. Such an approach has led to more economic use of ILs in areas such as timber processing, and may also apply to battery electrolytes.

Concluding remarks

In summary, the field of ILs for PIB electrolytes is very new, with much work still to do in fundamental materials design and characterization. Challenges of improving viscosity, conductivity, understanding interfaces and reducing costs will need to be overcome, but rapid progress may be made by using the principles developed in other metal ion battery chemistries.

15. The SEI in potassium ion batteries

Pengcheng Liu and David Mitlin

Materials Science and Engineering Program & Texas Materials Institute (TMI), The University of Texas at Austin, TX, United States of America

Status

As well known, the SEI is essentially significant for the success of non-aqueous batteries [263–267]. In general, when the anode contacts with the electrolyte, SEI forms instantaneously through the chemical and electrochemical reactions. The thin films formation on electrodes between electrolytes and Li metal anode was first discovered by Dey in 1970s [268]. In 1979, Peled *et al* named this thin film as SEI, and proposed that this SEI model is valid for all alkali metals and alkaline earths-based batteries [263]. In 2010, the theoretical foundation for SEI formation, where the operating voltage window surpasses the thermodynamic stability of the electrolyte, was outlined by Goodenough and Kim, based on the classic LUMO—HOMO energy diagram [269]. If the LUMO of the anode lies above that of the electrolyte, electrons would transfer from the anode to the LUMO of the electrolyte, resulting in the reduction of the electrolyte until a passivation SEI layer is created. Insoluble and partially soluble reduction products from electrolyte constitute the SEI. The electron-tunneling range determines the thickness of the initial formed SEI. The SEI is an interphase between the anode and the electrolyte with the similar properties of a solid electrolyte showing the high electronic resistivity and high ion conductivity. SEI is the key electrochemical interface to determine the rate performance, cycle life, anode stability, and safety for batteries [270, 271]. An ideal SEI should meet the following requirements: high cation selectivity and conductivity, high electrical resistance, high mechanical strength, high tolerance to the change of strain and stresses caused by the expanding and contracting sub-surfaces of anodes during charging and discharging, and stability in the electrolyte and in a wide range of temperatures and voltage. While research in SEI fields is rapidly accelerating, to date, the depth of understanding of the SEI in PIBs lacks far behind that of LIBs or even SIBs. Therefore, understanding and ultimately controlling the K-based SEI remains the primary challenge for achieving stable K electrochemical interfaces and PIBs.

Current and future challenges

High reactivity of K-based anodes and the instability of formed SEI

Due to the electron structure of K ($1s^2, 2s^2 2p^6, 3s^2 3p^6, 4s^1$), K-based anodes show the extremely high reactivity, much higher than those of Li ($1s^2, 2s^1$) and Na ($1s^2, 2s^2 2p^6, 3s^1$). So that, when electrolyte contacts with the K-based anodes, the electrolyte will be extremely reduced into the decomposition. Also, as-formed SEI passivation layer is much less stable than the Li-based or even Na-based SEI with comparable electrolyte—solvent combinations. So, the high reactivity of K-based anodes is the intrinsic reason to cause the instability of formed SEI. The high reactivity of K-based anodes will also cause the inhomogeneity of geometry structure, chemical composition, and physical & mechanical properties for the SEI, which will result in the serious influence on the K ions transfer through the SEI and the thereby electrochemical performance.

Uncertainty of the chemical components

A classic model for Li-based SEI in LIBs is so called “mosaic structure”, consisting of multiple organic and inorganic layers [272]. In the mosaic structure, the thin compact layers close to the electrode surface are composed of inorganic lithium compounds, such as Li_2O , Li_2CO_3 and LiF . On the outside of the SEI are multiple organic species, comprising mainly oligomer organic compounds, such as semi carbonates and polyolefins [273]. However, the composition and structure of K-based SEI in PIBs remain unknown. Moreover, the function of some specific components in K-SEI, such as KF , is still not clear, to some extent, shows the opposite effect compared to Li-analogy. For example, FEC, one electrolyte additive, is a known strategy to stabilize the SEI layers of Li and Na metals, which forms a stable and mechanically strong LiF or NaF layer on metal anodes [274]. However, FEC does not appear to be effective for K metal anodes, showing the higher polarization and increased resistance [275]. One hypothesis is that the KF -contained SEI is not so favorable for K metal anode. Another hypothesis is that it may just be thicker or of composition that gives more resistance. More work is needed to understand the composition and structure of K-based SEI in PIBs, and their role and function.

Limitation of the modification

The melting point of K metal are 64 °C, and the reactivity of K-based anodes is high, which brings the difficulty of sample prep and limits how the post-mortem electrode is handled. For example, low temperature atomic layer deposition (ALD) or other chemical vapor deposition (CVD) are the useful techniques to fabricate a modification coating layer on the surface of Li metal to stabilize the SEI, but they are difficult for K metal owing to its low melting point [264]. Furthermore, the intrinsic reactivity of K-based anode with air and with water vapor creates difficulties in performing artifact-free analytical studies. Any transfer operation to an inert or vacuum environment after cell disassembly becomes more sensitive to ambient exposure.

Advances in science and technology to meet challenges

Promising evolution to stabilize SEI in PIBs has been achieved, such as the ether-based electrolyte with the LUMO close to K-based anode, high-concentration electrolyte [97]. To achieve a more stable SEI and the thereby PIBs, the following aspects need to be further and more researched.

Structure-properties relationship

One main principle for designing a desirable SEI is to keep their chemical components & distribution and physical & mechanical properties uniform. If not, it will cause the non-uniformity of ions flux when passing through SEI. Thus, the effective current density will be increased, and also shorten the “Sand’s time” [276, 277]. Therefore, to explore and reveal the structure-properties relationship for SEI from the different aspects is the key to develop the high-performance PIBs. For example, as shown in figure 19(a), Liu *et al* [265] for the first time revealed the structure-property relationship and the interaction mechanism for the electrolyte wettability on substrate—uniformity of SEI (especially for the initially formed one)—stability of anodes (especially the plated metal anode). The key fundamental takeaway is that the complete electrolyte wetting will lead to the uniformity and stability of SEI, beneficial to the uniform ion flux and transfer in SEI, and the following electrochemical reaction with anodes and/or metal plating, vice versa.

Mechanical properties

A desirable SEI should have the robust mechanical strength and good elastic/plastic properties, so that it cannot only endure the stress/strain change of the anodes during charging and discharging, but also to some extent have a shear modulus to stop the dendrite growth [278]. As shown in figure 19(b), a recent study showed that despite a decrease in ionic conductivity for both electrolyte and SEI, exceptional cycling performance of K-metal batteries is achieved in a low concentration carbonate electrolyte by optimizing the mechanical stability of the SEI [279]. The inorganic content in SEI increases with increasing electrolyte concentration and corresponds to an increase in Young’s modulus (E) and ionic conductivity of SEI and a decrease in elastic strain limit (ε_Y). SEI with low either E or ε_Y inevitably triggers dendrite growth. The maximum elastic deformation energy combines effects of E and ε_Y , achieving a maximum in 0.5 M electrolyte.

Advanced characterization

Better understanding the composition and structure of SEI in PIBs and their functions will pave the way to propose more promising approach to stabilize the anode and achieve high-performance PIBs. So, for this aspect, the advanced characterization technologies will play the dominant role. For example, researchers used the site-specific cryo-TEM to image Li_2O and LiF particles within the SEI, and identified their orientation relative to the underlying metal anode [281]. Recently, a dynamic picture of the SEI formation in LIBs was established by using an *in-situ* liquid-SIMS technique in combination with MD simulations [282]. As shown in figure 19(c), Nanda group reported the first observation of nanoscale chemical and topographical mapping heterogeneity of a SEI formed on amorphous silicon (a-Si) using Tip-Enhanced Raman Spectroscopy (TERS) [280]. Fang *et al* established the analytical method of titration gas chromatography to quantify the contribution of unreacted metallic Li^0 to the total amount of inactive (‘dead’) lithium (consisting of both (electro)chemically formed Li^+ compounds in SEI and electrically isolated unreacted metallic Li^0) [283]. No akin analysis exists for SEI in K-based batteries, representing a promising direction for future research.

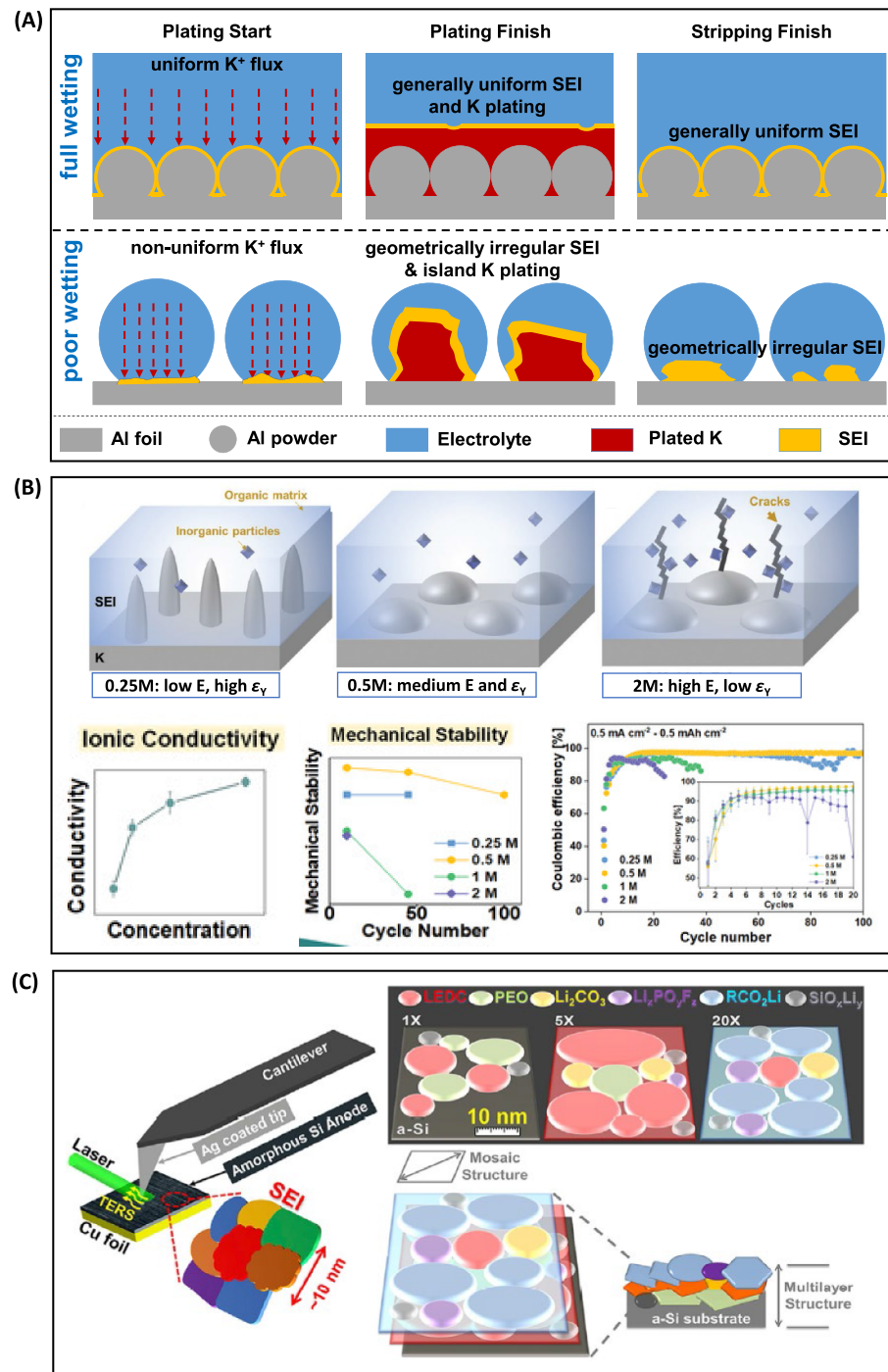


Figure 19. Advances in science and technology for SEI in PIBs. (A) Structure-property relationship for the electrolyte wettability on substrate—uniformity of SEI—stability of anodes. [265] John Wiley & Sons. © 2020 Wiley-VCH GmbH. (B) Mechanical properties and stability of SEI combining effects of Young's modulus (E) and elastic strain limit (ϵ_y). [279] John Wiley & Sons. © 2022 Wiley-VCH GmbH. (C) Advanced characterization of TERS. Reprinted from [280], Copyright (2019), with permission from Elsevier.

Concluding remarks

Because the cost considerations for stationary energy storage systems are paramount, K-based battery technologies are potentially superior to LIBs, in terms of abundance and wide distribution of precursors resources. As one of the most important electrochemical interfaces, SEI will have the significant effect on

every aspect of the anode and the thereby electrochemical performance of PIBs. To overcome the challenges of K-based SEI and achieve a high-performance PIB, more work and effort deserve to focus on further revealing the structure-property relationship of SEI, researching the mechanical properties of SEI, establishing the SEI model by using the advanced characterizations, developing more promising artificial SEI, etc. In parallel, the aid from the machine learning and artificial intelligence will also be beneficial to accelerating the research and development of SEI for PIBs.

Acknowledgments

D M and P L were supported by the Office of Science, U.S. Department of Energy, Award: DE-SC0023260.

16. X-ray absorption spectroscopy (XAS)

Jingyu Feng and Patrick L Cullen

School of Engineering and Materials Science, Queen Mary University of London, London, United Kingdom

Status

XAS is a powerful tool to characterize materials to give nanoscale insights. X-rays are directed at the samples, and some x-rays are absorbed by the atoms in the sample, causing the excitation or ejection of a core electron, resulting in a sharp increase in absorption that can be identified as the absorption edge [284]. XAS can be classified into hard/soft XAS based on the incident photon energy, where hard XAS typically have incident photon energies above 2 keV, and soft XAS have incident photon energies lower than 2 keV [285, 286]. There are two typical measurement geometries for XAS (figure 20(a)), transmission and fluorescence, both of which have advantages and disadvantages. Transmission is a more direct measurement as it is truly absorption, whereas fluorescence can suffer from complications in data processing due to self-absorption of the fluorescence photon. The fluorescence geometry, however, is more useful than transmission geometry in lower atomic percentage concentrations.

Typical XAS spectra consist of two parts, which are x-ray absorption near edge structure (XANES) and Extended x-ray absorption fine structure (EXAFS) (figure 20(b)). XANES, less commonly known as near-edge x-ray absorption fine structure, is sensitive to the polarization of the central atom and thus can provide information such as oxidation and phase of materials. EXAFS results from the interaction between the central and the neighboring atoms, thus giving information about bond lengths and coordination numbers. The theory of the XAS was established by the 1940s, but the practical development of XAS was only realized in the 1970s due to the simplification of the EXAFS equation and the development of synchrotron x-ray sources [287].

So far, XAS has been widely applied to metal ion batteries and has made significant progress in monitoring redox reactions, probing structure evolution, studying high-rate operating conditions, monitoring surface chemistry, and studying the behavior of the SEI [285]. XAS is an elementally specific technique that can differentiate between the selected elements. In addition, it can provide information such as bond length, coordination numbers, and oxidation states for materials in gas, liquid, or solid states with or without long-range ordering [288].

When using potassium as an alternative charge carrier to lithium, many differences between the ions make this a difficult challenge, including but not limited to; the larger potassium ion size and resultant larger volume changes upon charge/discharge and the typically lower diffusivity of K^+ within the solid electrode materials [289, 290]. With the assistance of XAS, atomic local structure-performance relationships can be established, thus enabling a better battery design.

Current and future challenges

Significant progress has been made using XAS for battery research, with most XAS studies focusing on LIBs. However, there are tremendous opportunities for the use of XAS in PIB which are functionally similar to LIBs. Potassium itself is a heavier element than lithium, and the potassium K-edge is in the hard x-ray region as opposed to the lithium K-edge being in the soft x-ray region. This means that there is potentially more opportunity to measure XAS of the charge carrier in PIB than in LIB. There are still challenges that hinder the XAS techniques [289, 291, 292]:

In-situ XAS: To fully understand the behavior of materials within a battery it is important to probe them during operation. *In-situ* or *operando* measurements; eliminate the spontaneous relaxation or contamination of highly reactive and transient species, make the identification of short-lived intermediates and subtle nonlinearities in behavior possible and allow for time-resolved investigation of electrochemical reactions. *In-situ* and *operando* electrochemical cells are needed to be carefully designed to ensure the quality of obtained data. As XAS spectra are averaged within the measured spot, inhomogeneous reactions caused by non-ideal cell design or poor electrode preparation could effect the accuracy of XAS spectra. Measurements of XAS under long-time battery cycling can incur a high exposure of electrode materials under x-rays, which may cause sample damage such as phase reconstruction and thus influence obtained results. It is therefore important to make sure that the beam used for EXAFS does not damage the probed material and that cell design is as representative as possible of laboratory based cells for fair comparison.

Correlating the current XAS with other materials characterization techniques: XAS techniques cannot stand alone to explain structure-performance relationships as this endeavor requires a combination of characterization techniques. Correlating XAS results with other chemical and physical structure characterization methods, DFT modeling, and electrochemical performance characterization is challenging as it involves data interpretation/analyses and cross-disciplinary knowledge. Here, we provide brief steps to

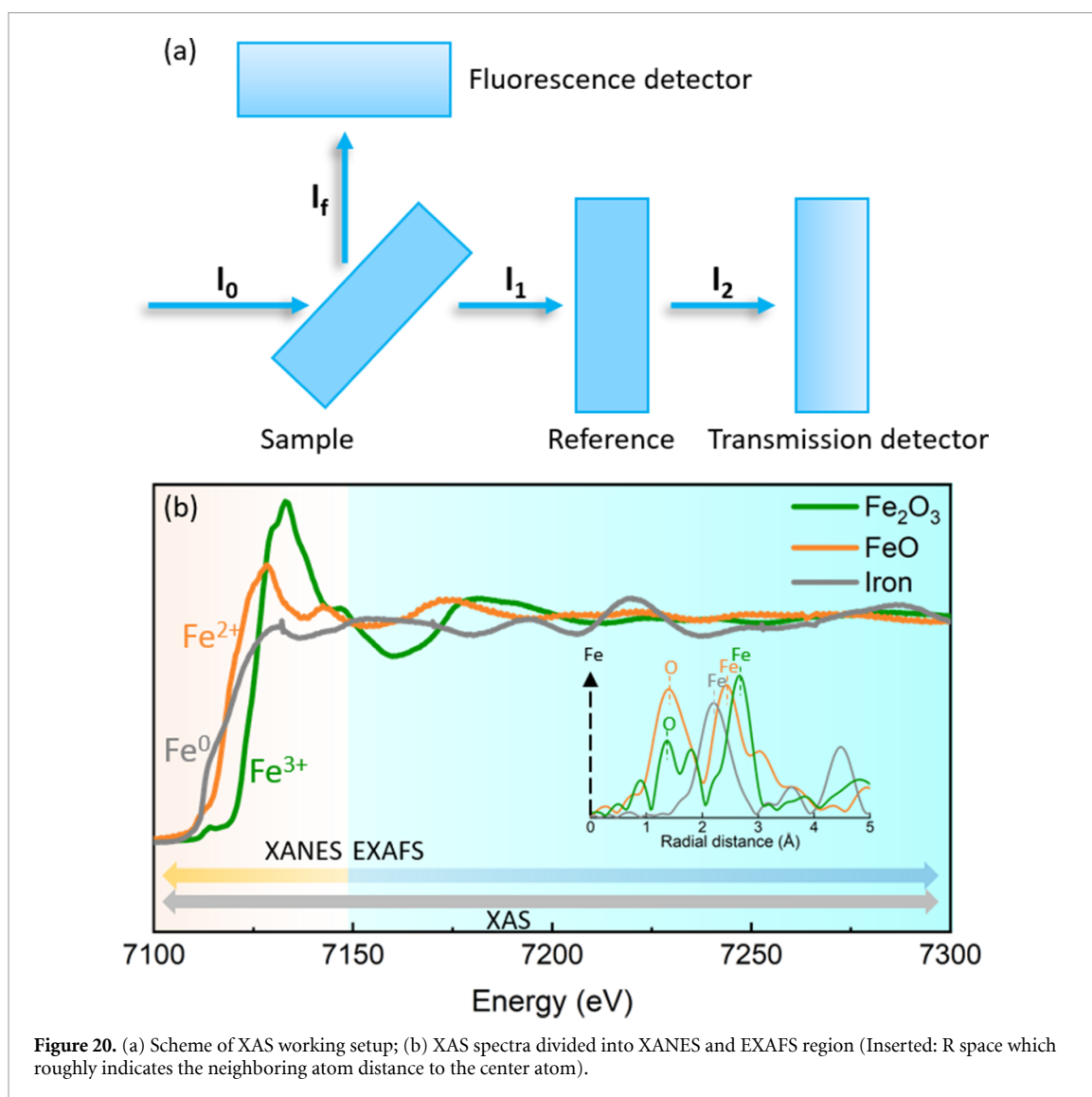


Figure 20. (a) Scheme of XAS working setup; (b) XAS spectra divided into XANES and EXAFS region (Inserted: R space which roughly indicates the neighboring atom distance to the center atom).

correlate the XAS with other characterization techniques and note that these steps could differ on a case-to-case basis. Firstly, the researcher needs to be clear as to what information is required from XAS, such as local structure in ambient conditions or how local structure evolves with the temperature. It is also important to select appropriate absorption edges for the XAS experiment, and ideally more than one edge per sample. Secondly, several methods of materials characterization to probe physical and chemical structures (XRD, XPS, ICP-MS, etc) should be conducted before the XAS experiment in order to have some idea of potential atomic structures. The subsequent XAS experiment can then be used help confirm an atomic structure. This approach gives the best chance of success for an XAS experiment, and atomic percentages are required for ideal sample preparation. Thirdly, fitting XAS to reveal the atomic structure should match information from the methods of physical and chemical structure characterization and, ideally, DFT modeling results.

XAS experiment feasibility: high brilliance high energy synchrotron XAS are highly effective and make time-resolved experiments possible. However, it is currently competitive to apply for beamtime due to the small number of XAS instruments globally. For *in-situ* or *operando* experiments, it is difficult to develop reliable electrochemical cells and to be awarded enough time for thorough studies due to this limited, competitive time. Whilst there are benchtop x-ray absorption spectrometers on the market, to the best of our knowledge, they are not yet well adopted globally.

Advances in science and technology to meet challenges

Intensive research efforts have been made to address the challenges, even though the development of PIB is far behind the ubiquitous LIB, similar experiment design/methods/electrochemical cells from LIB could also be adapted for PIB research.

PIB Cathodes often include TMs such as Fe, Co, Ni, Mn, which are ideal for hard XAS characterization [27, 293, 294]. For example, $\text{KFeC}_2\text{O}_4\text{F}$ has been applied as a cathode for PIB with a soft carbon anode yielding a full cell with an energy density of 235 Wh kg^{-1} and negligible capacity decay within 200 cycles [294]. In this study, *in-situ* XAS on Fe K-edge was performed to probe the structural evolution of the cathode during charge and discharge. The XANES region showed the oxidation state of Iron increasing from Fe^{2+} to Fe^{3+} during charge and vice-versa during discharge. In the EXAFS region, the length between Iron and Oxygen atoms decreased during charge and increased during discharge. DFT calculations were performed to reveal the role of Fe, O and F elements in the charging and discharging states, which showed good agreement with the *in-situ* XAS data.

In another study, *Ex-situ* soft XAS measurements were performed on a $\text{K}_2\text{Ni}_2\text{TeO}_6$ cathode for Ni, Te and O—K edge, where the O—K edge was measured at different charge states [27]. Using the O—K edge data, corroborated by *a priori* DFT calculations, the authors were able to suggest the degree of oxygen hybridization or covalency with potassium extraction from $\text{K}_2\text{Ni}_2\text{TeO}_6$ (and vice-versa) was relatively large.

For PIB anode materials, XAS studies have also been performed to obtain information on the local structure of materials as well as to elucidate the charge/discharge mechanism [289, 295–298]. For example, in one study *in-situ* XANES was performed on $\text{Bi}_2\text{O}_2\text{Se}$ and $\text{Bi}_2\text{O}_2\text{Se}/\text{graphite}$ samples at both the Bi—L_{III} edge and the Se—K edge versus lithium metal. Together with *ex-situ* XANES data of the same $\text{Bi}_2\text{O}_2\text{Se}$ and $\text{Bi}_2\text{O}_2\text{Se}/\text{graphite}$ samples versus potassium, the authors were able to compare the mechanism for potassium insertion into $\text{Bi}_2\text{O}_2\text{Se}$ anodes against the mechanism for lithium insertion for the same anodes. We note that the mechanism of K-ion could have been directly probed with the use of *in-situ* XAS measurements versus potassium metal, but that likely this was beyond the scope of the authors work [296]. In another study, by combining *ex-situ* XANES and *operando* XRD results, the authors were able to examine the relationship between the nanostructuring of bismuth in the form of carbon-coated double-shell hollow box bismuth samples (synthesized from ZIF-8 MOFs), and the subsequent improvement in reversible capacities for PIBs relative to microsized bismuth [295].

To accelerate the development of metal-ion batteries, many beamlines have built the capability to perform *in-situ/operando* tests where electrochemistry and XAS intersect. In addition, lab-based XAS has shown promising capabilities to obtain results for probing the atomic structure of battery electrodes [299].

Concluding remarks

In summary, XAS as a tool for studying materials within PIBs is in a nascent phase, but it has shown potential in probing the PIB local structure of electrode materials and revealing mechanisms for potassium incorporation in electrodes. While XAS is an interesting method for the characterization of materials within PIBs, several challenges remain. Conducting *in-situ/operando* measurements, correlating XAS results with other materials characterization techniques, and DFT are recommended to deepen understanding of how PIBs electrodes incorporate the potassium ion. Furthermore, increasing the amount of time available at synchrotron XAS facilities and/or benchtop XAS kits is likely to make this characterization tool more accessible to PIB researchers.

Acknowledgments

P L C would like to thank the EPSRC for funding this work (EP/S001298/2).

17. X-ray pair distribution function (XPDF)

Gopinathan Sankar¹ and Timothy I Hyde²

¹ Department of Chemistry, University College London, 20 Gordon Street, London WC1H 0AJ, United Kingdom

² Johnson Matthey Technology Centre, Sonning Common, Reading, United Kingdom

Status

Total x-ray/neutron scattering also known as PDF method or High energy x-ray diffraction/scattering (HEXRD or HEX) is widely used for the study of range of functional solids to gain atomic architecture of the material. The method is the measurement XRD at a shorter wavelength typically below 0.4 Å so as to yield a large q-range ($q = 4\pi \sin(\theta) / \lambda$) and subsequently converted to real space through Fourier Transform resulting in the PDF; XRD data including Bragg (if present) and non-Bragg (diffuse) scattering are taken in to account to process the data to obtain real space information [300, 301]. Although this methodology was described around 70 years ago [301], it has only been possible to conduct reliable measurements at short wavelengths since the establishment of dedicated synchrotron radiation sources (SR) where it is now almost a routine technique. Therefore, SR is ideal (although lab-based x-ray systems employing Ag as target are used in several laboratories) as one can select a wavelength sufficiently low (for example 0.2 Å) to yield good quality data of up to a q value of ca 25 Å⁻¹. Furthermore, the use of modern SR sources provides a distinct advantage that they provide higher penetration of the sample/system and more importantly offer a good time-resolution due to the use of low emittance and high coherence and brilliance through upgrades coupled with advanced detector technologies such that entire total scattering data can be collected in a minute or less. There are several dedicated beamlines for x-ray total scattering (XTS) measurements for both static and time-resolved *in situ*/operando experiments and some of them are listed here: I15-1 XPDF at Diamond Light Source, ID11 and ID15A at ESRF, P02.1 and P07 at PETRA III, 11-ID-B at Advanced Photon Source, 28-ID-1 at NSLS-II, and BL04B2 at Spring8. In addition, advances in *in situ* capabilities that can accommodate sample preparation in special chambers or operations during the measurement have contributed enormously for the study of functional materials, including energy storage systems. One of the developments for operando measurement is the utilization of the so-called AMPIX, DRIX and RATIX cells [302, 303] for battery materials. (see figure 21). These *in situ* cells have been deployed for a range of x-ray scattering (and spectroscopic) techniques enabling successful measurements under operando conditions. Furthermore, data analysis procedures are well-established and now there are several dedicated software's that are available for processing the data, for example, PDFGET and PDFGUI packages [304] are used widely to gain structural information. Details of a typical experiment and the analysis of XTS data are beyond the scope of this article.

Current and future challenges

One of the current challenges is to determine the atomic-architecture of the energy storage materials, preferably under operando conditions, to determine a clear structure-function relationships which will enable a fuller understanding of the performance of these solid-state systems. Through the understanding of structure-function relationships, there is always a desire to search for new materials that will outperform the existing systems providing better or improved solutions. Although atomic arrangements determined through crystallographic techniques have enabled the determination of structure which are correlated with functional properties, there are many other factors that can contribute to the performance, for example, presence of defects, size and shape of nano materials, heterogeneities etc. A single technique, specifically, XRD, alone cannot provide all these information as there may be disordered or non-crystalline components present in a given system. Similarly, XAS is not completely adequate to provide the missing information from diffraction studies, although element specific and applicable to any type of system whether they are crystalline or not, can provide information about the local geometric structure and in addition information on the oxidation states of metal ions can be gained through this technique. The combined information from both XRD and XAS is not sufficient in the majority of the cases where medium range disordered structures may exist. Here, in such a situation the PDF technique [285, 305] has played an important role as it does not depend on the presence of long-range order in a given material. Whilst current issues are met either by the use of one of the techniques or combining through individual measurements, the challenge is to measure in a single beam line on the same sample using all these techniques with adequate spatial, energy and time resolution to advance

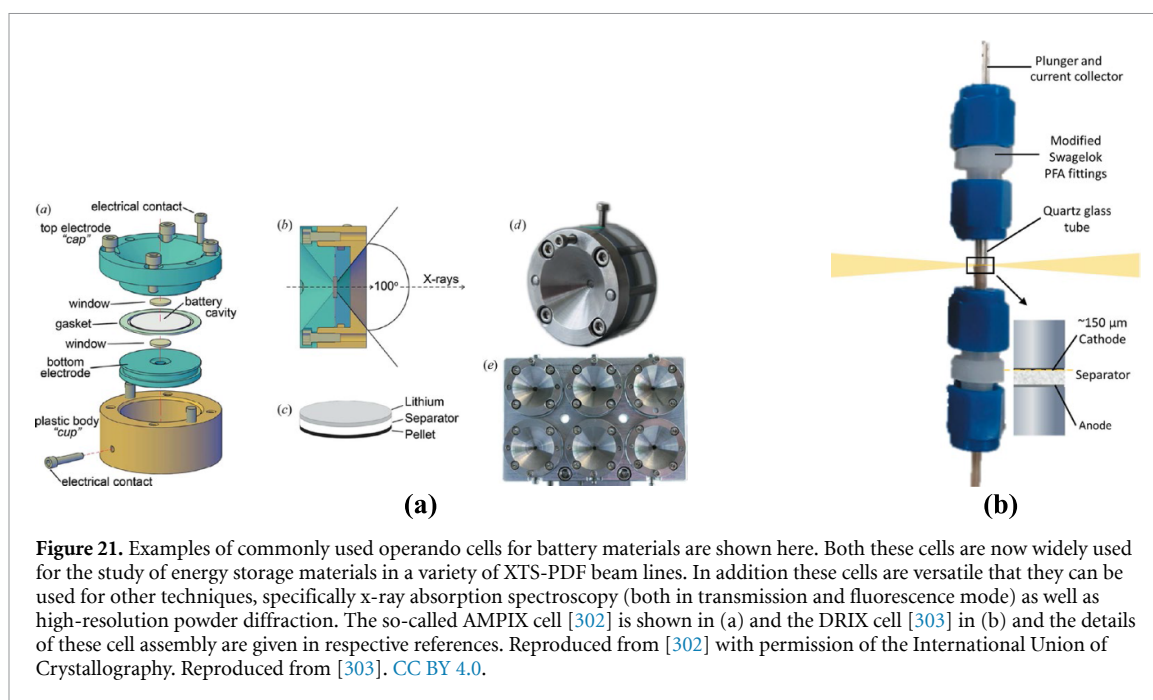


Figure 21. Examples of commonly used operando cells for battery materials are shown here. Both these cells are now widely used for the study of energy storage materials in a variety of XTS-PDF beam lines. In addition these cells are versatile that they can be used for other techniques, specifically x-ray absorption spectroscopy (both in transmission and fluorescence mode) as well as high-resolution powder diffraction. The so-called AMPIX cell [302] is shown in (a) and the DRIX cell [303] in (b) and the details of these cell assembly are given in respective references. Reproduced from [302] with permission of the International Union of Crystallography. Reproduced from [303]. CC BY 4.0.

our determination of evolving electronic and geometric structures of energy storage materials. With the currently available state-of-the-art XTS technique several studies have used XTS on its own or in combination with other methods including computational techniques and investigated energy storage materials containing Li or Na as the migrating cations. To our knowledge K based systems have only recently been investigated by XTS-PDF [306]. The use of this technique will significantly advance the understanding of many future K-based battery materials.

Advances in science and technology to meet challenges

PDF obtained from a XTS and Neutron scattering are widely used for the study of range of systems from liquids, to amorphous to nano systems and crystalline solids. Here the focus is primarily on the use of XTS-PDF methods and on energy storage materials. PDF data obtained from XTS have played a vital role in understanding the short, medium and long-range structures of Li and Na based energy storage materials. An example of this is the work by Hartman *et al* [307], utilized XTS-PDF methods (in addition to XRD and XAS) to unravel the sodium storage properties in Fe_3S_4 nano particles. Based on the XTS-PDF investigation (see figure 22(a)), they propose models at four different stages of the electrochemical reaction. XTS-PDF data were found to be valuable to interpret the various transformations that occurred during the electrochemical process. Another study by Stratford *et al* [308], wherein XTS-PDF, solid state NMR and other complementary methods were used to determine the structure of sodium storage in hard-carbon which are a leading system as anode materials. Here they employed the so-called differential PDF (dPDF) methodology to determine the structure of evolving electrochemical process (see figure 22(b)). It was illustrated, based on a structural model taking into account Na–C and C–C interactions to account for the short and medium range distances and the Na–Na interactions is suggested for peaks above 7 Å in dPDF data, consistent with an earlier operando study by Mathiesen *et al* [309]. Very recently Xu *et al* [306], aimed at elucidating the structure of carbon and potassium storage mechanism. The PDF data obtained from XTS measurements (laboratory-based system) of a range of samples obtained from pyrolysis at various temperatures, between 800 °C to 2900 °C (see figure 22(c)). The authors propose that a three-stage process takes place wherein an amorphous material is formed at 800 °C (stage 1), between 1000 °C to 1500 °C (stage 2) amorphous and pseudographite like phases coexist and between 1800 °C and 2900 °C (Stage 3) both pseudographite and graphite phases are present. These recent studies clearly demonstrated the power and need for XTS-PDF methods to unravel various stages of structural changes during uptake of Na/K ions into respective materials present in the energy storage systems.

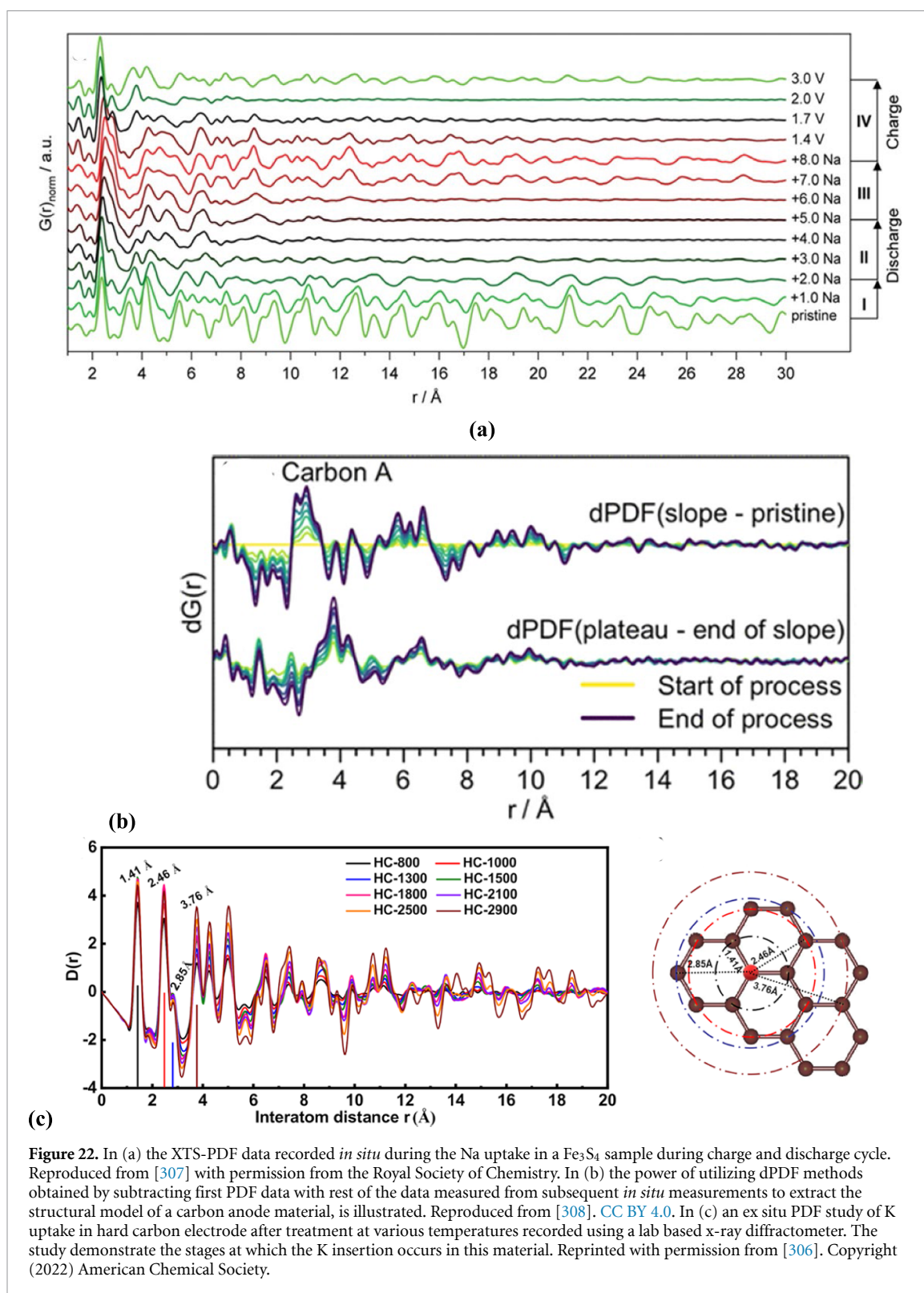


Figure 22. In (a) the XTS-PDF data recorded *in situ* during the Na uptake in a Fe_3S_4 sample during charge and discharge cycle. Reproduced from [307] with permission from the Royal Society of Chemistry. In (b) the power of utilizing dPDF methods obtained by subtracting first PDF data with rest of the data measured from subsequent *in situ* measurements to extract the structural model of a carbon anode material, is illustrated. Reproduced from [308]. CC BY 4.0. In (c) an ex situ PDF study of K uptake in hard carbon electrode after treatment at various temperatures recorded using a lab based x-ray diffractometer. The study demonstrate the stages at which the K insertion occurs in this material. Reprinted with permission from [306]. Copyright (2022) American Chemical Society.

Concluding remarks

XTS and associated PDF provide a powerful means of extracting structural information of both short, medium, and long-range structures; the crystalline component can be analyzed to extract detailed structural information through conventional crystallographic methods. As this method is not limited to crystalline solids, the structural studies have much wider scope from studies on synthesis of battery materials from solution processing, including *in situ* investigation of solvo/hydrothermal processes, post synthetic treatments over a wide temperature range and during battery operations. Continued effort in the development of *in situ*/operando techniques enable further advancement in understanding the structural

changes during operations. Small beam size, high-brilliance and high-temporal and spatial resolution enable the study of small volume of sample and bulk energy storage systems. Furthermore, the advancement in detector technologies has enable very fast measurements in the order of milli seconds achievable. This facilitates practical PDF computed tomography measurements, where larger volumes can be probed which will enhance our understanding and performance (including failures) of these energy storage materials [310, 311]. Some SR facilities have additional capability of combining XTS-PDF methods with XAS and XRPD (collected at nominal wavelengths) which makes it even more powerful for determine electronic and geometric structures of these materials under identical operating conditions on the same sample [312]. However, improvement in both temporal, spatial resolutions can enhance their capabilities to advance further in the study of battery materials.

18. *In-situ* characterization

Jingwei Chen, Fanlu Meng and Huanlei Wang

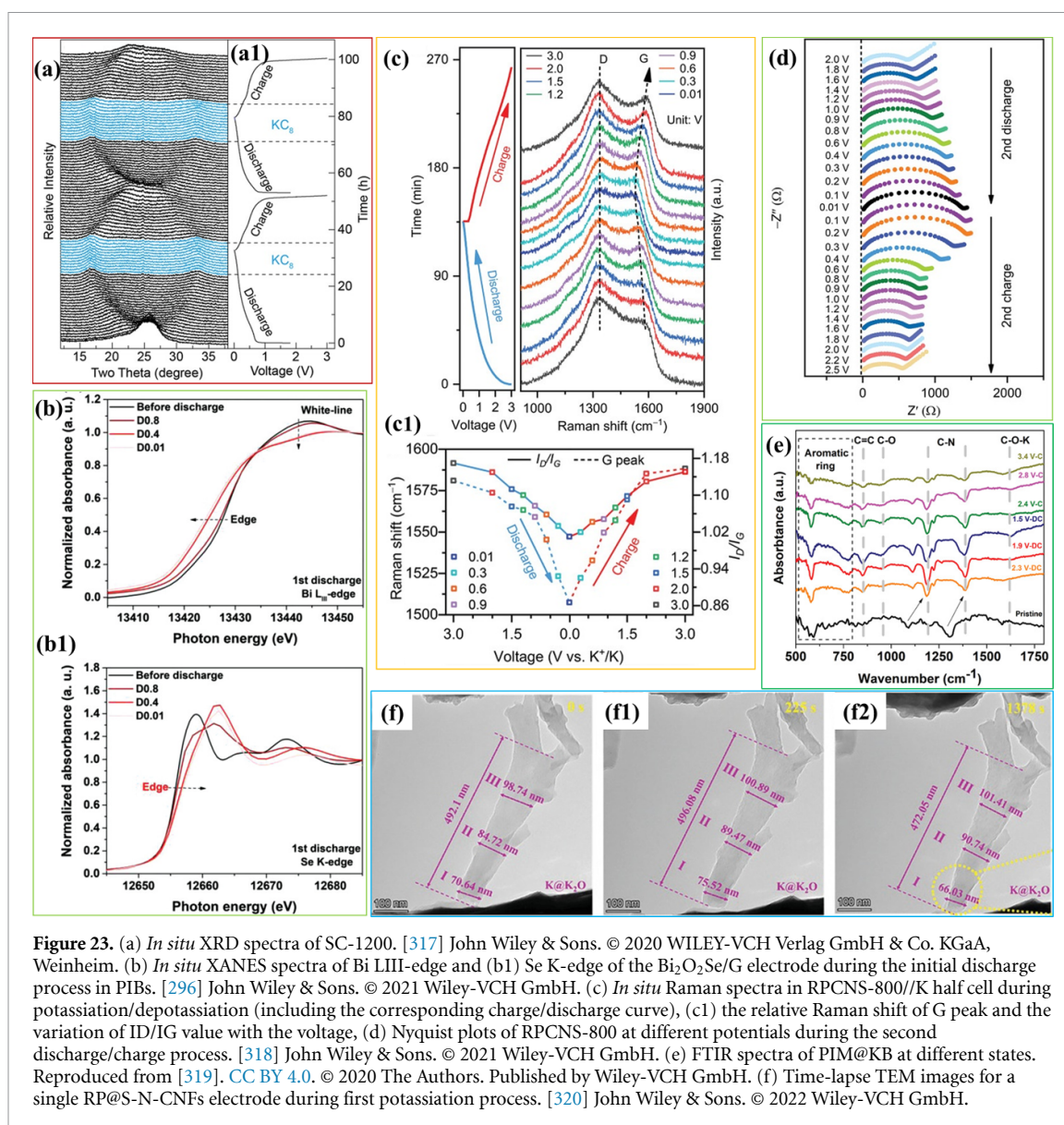
Ocean University of China, Qingdao, People's Republic of China

Status

Similar to other metal ion batteries, charge/discharge of PIBs are accompanied by variation of electrode morphology, crystal structure, molecular structure, etc [313, 314]. Compared to ex-situ methods, *in-situ* characterization techniques are more accurate in capturing intermediate states and formation of possible intermediate phases, thus advancing the understanding of PIBs' electrochemical mechanism [315, 316]. As shown in figure 23, multiple *in-situ* characterization techniques have been employed to deconvolute the dynamic structural and chemical evolution of PIB electrodes during charge/discharge. Along with charge/discharge (figure 23(a1)), *in-situ* XRD revealed the different staging behavior between pitch-derived soft carbon (SC-1200) and graphite. While potassiation of graphite involved formation of various potassium intercalation compounds (KC_{48} , KC_{36} , KC_{24} and KC_8), SC-1200 with turbostratic lattices and wide interlayer spacing only experienced formation of KC_8 (figure 23(a)) [317]. Figures 23(b) and (b1) present the *in-situ* XANES spectra of Bi L_{III}-edge and Se K-edge during Bi_2O_2Se/G potassiation. The obvious Bi L_{III}-edge downshift, decreased white-line intensity and Se K-edge upshift were ascribed to Bi^{3+} reduction, Bi potassiation, break of Bi–Se and formation of K–Se intermediate phases [296]. *In-situ* Raman spectra evidenced the redshift of G peaks and increased I_D/I_G values in radially porous carbon nanospheres (RPCNSs) during potassiation (figures 23(c) and (c1)), suggesting that successful K^+ intercalation lead to improved graphitization degree and enhanced stretching vibration of in-plane C–C bonds. Depotassiation allowed the restoration of G peak position and I_D/I_G values [318]. Concurrently, *in-situ* electrochemical impedance spectroscopy (EIS) quantified the charge transfer resistance (R_{CT}) variation during second cycle potassiation/depotassiation (figure 23(d)). The sharp increase of R_{CT} at voltage <0.9 V indicated the hindered kinetics in reconstructed RPCNSs. The restored R_{CT} during charging demonstrated the high reversibility in RPCNSs anode, synchronizing with the *in-situ* Raman analysis [318]. *In-situ* Fourier transform infrared spectra were employed to unveil the K storage behavior in polyimide@ketjenblack (figure 23(e)). The increased intensity of C–O–K and C–O peaks during discharging indicated the oxygen coordination with K^+ . During K^+ insertion/extraction, the polymer molecular chains will be rearranged, leading to the peak shift of rotatable C–N peaks [319]. *In-situ* TEM was adopted to visualize the volume variation in red phosphorous in sulphur, nitrogen co-doped carbon nanofibers (RP@S–N–CNFs) (figures 23(f)–(f2)). Initial potassiation (225s) resulted in slight expansion in RP@S–N–CNFs, however, further potassiation lead to drastic shrinkage in both longitudinal and transverse directions due to the strong adhesion between potassiated RP nanocrystals at the tip and S–N–CNFs [320].

Current and future challenges

The above examples have showcased the application of multipronged *in-situ* characterization techniques in unveiling the electrochemical mechanism of PIB electrodes. To fulfill the requirements of *in-situ* characterizations (e.g. allowing x-rays, lasers, and light transmission), different set-ups have been developed as displayed in figure 24. However, there are still several factors that hinder the advancement of *in-situ* techniques in PIBs. (1) Limited information revealed by a single *in-situ* technique. *In-situ* XRD is powerful in tracking crystal structure variation, yet less sensitive to morphological or chemical changes in electrodes [316]. *In-situ* EIS can quantify the charge transfer resistance fluctuation during electrochemical reactions, yet it can hardly reflect physical or chemical structure variation of electrodes. It is thus necessary to combine several *in-situ* techniques to provide complementary understanding of PIBs electrochemical mechanism. (2) Limited applicability for each *in-situ* technique. *In-situ* XRD is more suitable for crystalline electrodes, samples with low crystallinity will result in limited signal intensity [317], excluding the application of *in-situ* XRD for amorphous electrodes. Thus, the selected *in-situ* methods should match with electrode properties [316]. (3) non-standardized set-up. Different set-ups have been reported among various literature. Both lab-based x-ray diffractometer [321] and synchrotron beamline x-ray sources [322] have been adopted for *in-situ* XRD characterizations [315]. While some researchers collect *in-situ* XRD signals in reflection mode (figure 24(a)) [323], the others employs transmission mode instead [324]. Furthermore, both Swagelok-type cell [325] and coin cell [324] were employed for *in-situ* XRD analysis. Three-electrode cell, coin cell and pouch cells were all constructed for *in-situ* Raman analysis [315]. (4) Deviated cell configuration from practical cells. *In-situ* XAS, *in-situ* Raman and *in-situ* visualization often require construction of home-built cells (with holes/windows) that allow the transmission of x-rays (figure 24(b)), lasers (figure 24(c)) and light (figures 24(d) and (e)) to interact with electrodes, and reduce the interference from other components



[317, 324]. Unlike coin cells that use liquid electrolyte, *in-situ* TEM often adopts solid state electrolyte (K₂O) to operate in the vacuum environment (figure 24(f)) [127, 320]. However, this can lead to gradient potassiation and different degrees of volume change, especially in 1D electrodes [320]. (5) Further *in-situ* characterization techniques to be explored in PIBs. Aside from the above-discussed techniques, there are several emerging *in-situ* methods that were seldom reported for PIBs. For example, *in-situ* NMR, *in-situ* electrochemical quartz crystal microbalance (EQCM), *in-situ* scanning electrochemical microscopy (SECM), etc are capable of monitoring the local chemical environment of elements of interests, mass/geometrical changes, and localized heterogeneous charge transfer coefficient [316].

Advances in science and technology to meet challenges

Given the limited applicability and limited information obtained from a single *in-situ* method, combination of two or more *in-situ* characterization techniques can often harvest complementary understanding of the electrochemical mechanism of PIB electrodes. *In-situ* Raman analysis (figure 23(c)) detected the G peak shifting and I_D/I_G fluctuation, while the *in-situ* EIS quantified the R_{CT} variation of RPCNS during charge/discharge. At voltage < 0.9 V, sudden redshift of G peak position and increase of R_{CT} value are concurrently noticed, evidencing the hindered K intercalation at low potential in rearranged RPCNS [318]. A home-made optical microscopy system (figure 24(e)) was employed to *in-situ* visualize the morphology variation of FeSe₂@RGO, confirming the homogeneous potassiation of FeSe₂@RGO without obvious morphology change. However, *in-situ* Raman analysis detected the transformation and structural

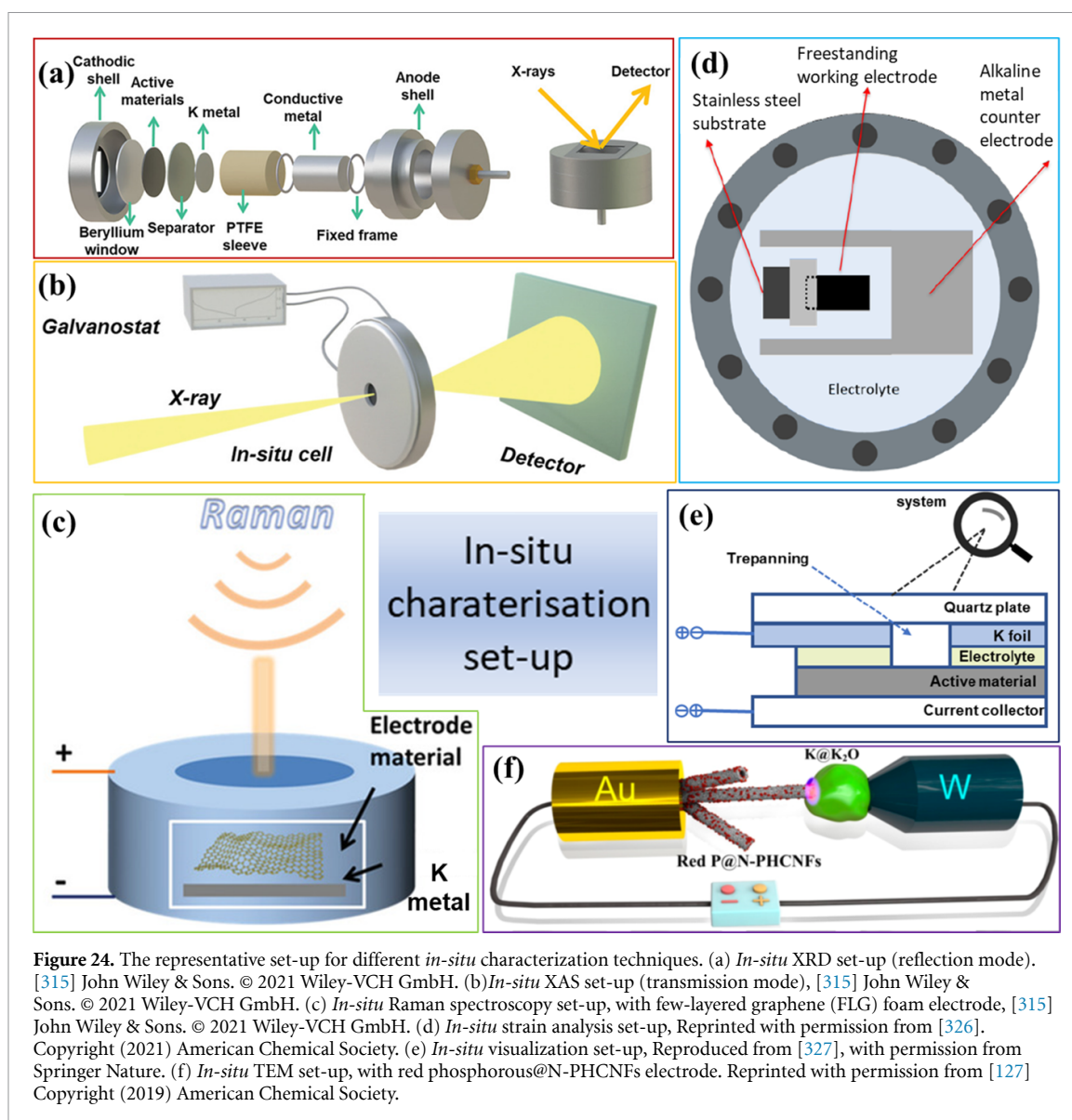


Figure 24. The representative set-up for different *in-situ* characterization techniques. (a) *In-situ* XRD set-up (reflection mode). [315] John Wiley & Sons. © 2021 Wiley-VCH GmbH. (b) *In-situ* XAS set-up (transmission mode), [315] John Wiley & Sons. © 2021 Wiley-VCH GmbH. (c) *In-situ* Raman spectroscopy set-up, with few-layered graphene (FLG) foam electrode, [315] John Wiley & Sons. © 2021 Wiley-VCH GmbH. (d) *In-situ* strain analysis set-up, Reprinted with permission from [326]. Copyright (2021) American Chemical Society. (e) *In-situ* visualization set-up, Reproduced from [327], with permission from Springer Nature. (f) *In-situ* TEM set-up, with red phosphorous@N-PHCNFs electrode. Reprinted with permission from [127] Copyright (2019) American Chemical Society.

remodeling of FeSe_2 during potassiation/depotassiation, as well as increased orderliness of the carbon components in the composite electrode [327].

Construction of proper set-ups are also very important for *in-situ* characterizations. As shown in figures 24(a), (b) and (c)–(e), x-ray transparent window (e.g. Beryllium window) and light transparent window (e.g. quartz window) were utilized to construct cells for *in-situ* XRD, XAS [315] and *in-situ* Raman [328] and *in-situ* optical microscopy [327]. An in-plane cell set-up (figure 24(d)) was built with a quartz window for analyzing the strain evolution in FePO_4 electrode during charge/discharge by digital image correlation, through tracking the speckle pattern position on the electrode surface. First cycle potassiation of FePO_4 lead to volume expansions, increased interplanar spacing and reduced crystallinity, as revealed by *in-situ* strain analysis and *in-situ* XRD characterization. However, in subsequent cycles, reversible volume expansion/shrinkage are still present, while the XRD patterns remain unchanged, indicating potassiation/depotassiation in an amorphized phase in the electrode.

Proper testing parameters are also suggested for *in-situ* characterization. Hard x-rays (5 to ~ 100 keV) with high penetration depth are often needed for *in-situ* XAS (transmission mode) analysis and can also be used for *in-situ* XRD characterization. Guo *et al*, employed synchrotron x-ray sources (wavelength 0.688273 \AA , transmission mode) to track the phases changes in few-layered Sb_2S_3 /carbon sheet (SBS/C) electrode. During initial potassiation, K^+ was inserted into Sb_2S_3 , which was then converted into K_2S and Sb. Further potassiation resulted in formation of K_2S_6 intermediate phase and the final discharge product of K_2S_3 and K_3Sb were also detected, revealing the multi-step intercalation, conversion, and alloying reactions in this SBS/C anode [322].

Concluding remarks

In-situ characterization methods are undoubtedly informative and constructive in analyzing the electrochemical mechanisms of PIBs. Albeit the fact that several *in-situ* methods have been adopted in PIBs, further efforts are still needed to advance the proliferation of more *in-situ* characterization techniques. First, it is suggested that proper *in-situ* methods should be selected to match with the electrode properties. Second, appropriate set-ups should be constructed for *in-situ* characterization, suitable testing parameters should also be considered to meet the testing requirements. Third, combination of different *in-situ* methods is suggested to harvest multidimensional and multimodal information, thus corroborating a more comprehensive understanding of PIB electrochemical mechanisms. What's more, aside from focusing on the structural variation of electrode (mostly anode) during charge/discharge, the electrochemical behavior of cathode and the effect of binders, separators and electrolytes on PIB electrochemical mechanism should not be neglected. Last, it is encouraged to explore more possibilities of *in-situ* methods in PIBs, including the emerging *in-situ* NMR, EQCM, SECM, atomic force microscopy etc. Through judicious adoption of the available *in-situ* characterization techniques and exploration of emerging *in-situ* methods, issues existing in PIBs will be resolved and the PIBs performance will be promoted, advancing the development and commercialization of PIBs.

Acknowledgments

This study was financially supported by the National Natural Science Foundation of China (Nos. 22179123 and 21471139), Shandong Provincial Natural Science Foundation, China (No. ZR2020ME038) and the Fundamental Research Funds for the Central Universities (No. 201941010).

19. Cost-effectiveness and techno-economic analysis of PIBs

Laura Lander and Jacqueline Sophie Edge

Imperial College London, London, United Kingdom

Status

While batteries have an important role to play in decarbonizing our energy and transport systems, they have environmental and social impacts across their lifecycle which need to be assessed and mitigated. These impacts include habitat destruction, pollution, displacement of communities, competition for freshwater and unethical labor practices. In addition, owing to the scarce minerals required in LIBs, there are supply chain risks, due to resource depletion and geographic localization. For this reason, alternative materials are sought to replace, for example, lithium with more abundant materials, such as potassium and sodium (table 3) [124, 329]. PIBs have the potential to outperform both LIBs and SIBs, because K^+ ions, unlike Na^+ ions, can intercalate reversibly into a graphite anode [330], K has a lower standard redox potential than Na and Li, resulting in a higher working voltage [330], and K electrolytes exhibit higher conductivity than Li and Na electrolytes [331].

Besides performance, an important criterion for the success of any new battery technology is its economic viability. Here, techno-economic analysis is an important tool to reveal economic benefits and drawbacks and to develop strategies on how to optimize the overall costs.

In this context, Yan and Obrovac conducted a techno-economic analysis of non-aqueous PIBs including current cathode materials (e.g. $K_2MnFe(CN)_6$, $KCrO_2$ and $KVPO_4F$) as well as a hypothetical $KNi_{0.6}Mn_{0.2}Co_{0.2}O_2$ (KNMC622) cathode [332]. The latter was then benchmarked against $LiNi_{0.6}Mn_{0.2}Co_{0.2}O_2$ (LNMC622). It was concluded that indeed costs can be reduced by \$2.2/kg cathode material using KNMC622 instead of LNMC622 due to the lower price of K compared to Li (figure 25(a), table 3). Further cost savings can be achieved on the anode current collector, which in PIBs, in analogy to SIBs is Al foil, whereas in LIBs Cu foil is used. However, the total PIB cost exceeds the cost of LIBs (\$7535.29 and \$7359.32, respectively; figure 25(b)). This stems from the lower volumetric capacity of graphite for PIBs compared to LIBs leading to larger amounts of material (i.e. graphite, binder and electrolyte) being required to achieve the set energy storage capacity [332, 334]. The study further evaluated the cost of a PIB over its cycle lifetime (\$/kWh-year). It was shown that for PIBs to become economically viable compared to LIBs an increase in battery lifetime to up to 1500 cycles (vs. 1000 for LIBs) is required.

Current and future challenges

Current and future challenges regarding the cost-competitiveness and techno-economic assessment of PIBs can be divided into three categories as described in the following:

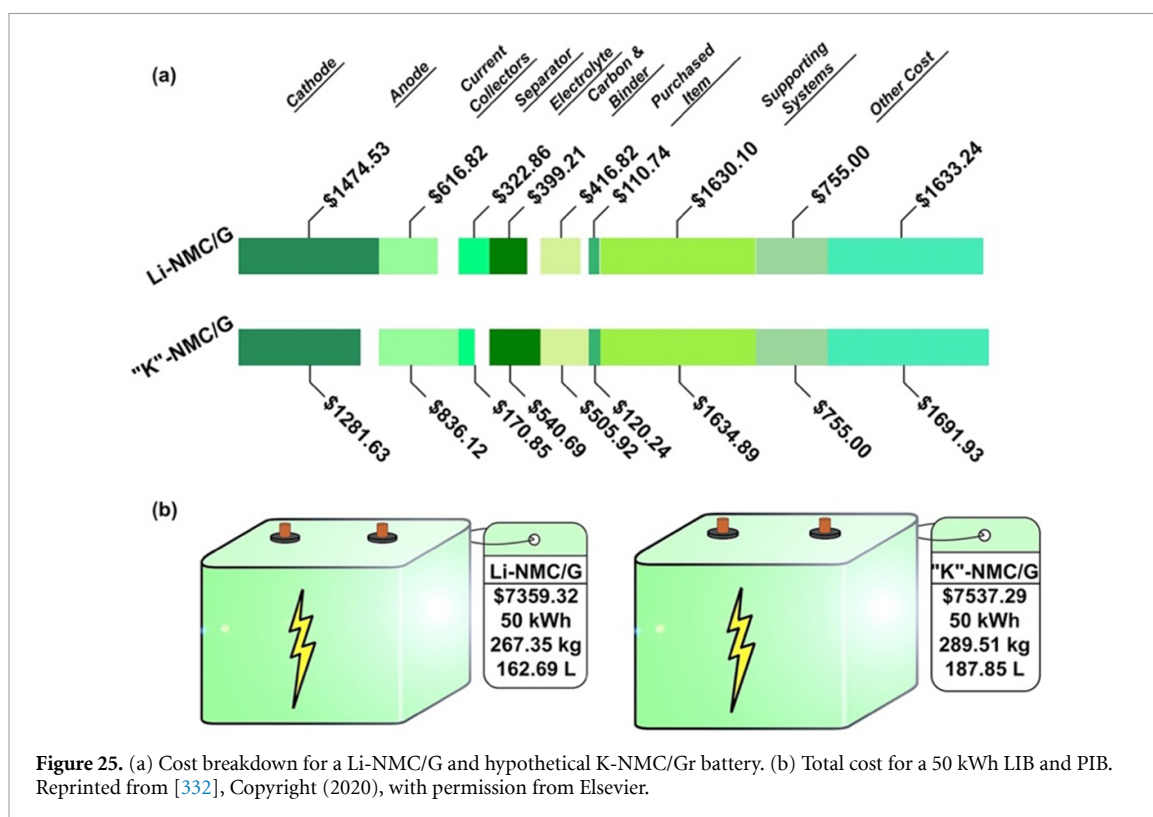
Technological challenges: economic drawbacks of PIBs stem primarily from currently low volumetric and gravimetric energies leading to higher materials demand as well as short cycle life [8, 332, 334–336]. PIBs are still in their early development stages and further intensive research efforts are needed to improve the overall battery performance. It should be noted, however, that also the performance and cost-efficiency of LIBs are going to be further optimized, which might make it even harder for PIBs to be a viable contender in the future [337].

Supply chain challenges: additional economic issues could arise from the availability and cost of the potassium source—potash. Potash is heavily used for fertilizers in the agricultural sector and its price is sensitive to geopolitical and global economic developments. It has been reported that the potash price has recently significantly increased from \$300 per ton in 2021 to \$1100 in 2022 [338, 339]. Similar fluctuations in the future would further compromise the cost-competitiveness of PIBs. Moreover, potential supply chain risks might occur for the PIB manufacturing industry as preference probably would be given to food production in case of potash shortages, for instance.

End of life processing challenges: like LIBs, spent PIBs will need to be processed, so that these still active, electrochemical devices do not pose an environmental hazard in landfill sites and so as not to waste their component materials. This goes especially for PIBs with critical, expensive and/or toxic materials such as cobalt, chromium, graphite or vanadium. LIBs can be recycled using three main processes: (1) pyrometallurgical, where the battery is shredded and melted down, so that standard metallurgical processes can be applied to extract the valuable materials; (2) hydrometallurgical, where the shredded battery undergoes lower temperature, chemical processes to extract materials and (3) direct recycling, in which component materials are first separated through various mechanical processes and then undergo a series of processes to restore their functionality, for direct use in manufacturing of further batteries. At the time of publishing, no specific research into the recycling of PIBs has been published, but it is expected that the processes will be largely similar to those for LIBs. There will be similar issues to overcome, such as the high

Table 3. Comparison between Li, Na and K. Reprinted from [332], Copyright (2020), with permission from Elsevier.

	Earth crust abundance (wt%) [329]	World reserves (ktonne ^a) [333]	Cost (\$/tonne ^a) [333]
Li	0.0017	22 000	17 000 (Li ₂ CO ₃) ^b
Na	2.36	25 000 000 (Na ₂ CO ₃)	155 (Na ₂ CO ₃)
K	2.09	35 00 000 (K ₂ O eq.)	980 (K ₂ O)

^a Refers to metric tonne.^b Battery grade Li₂CO₃.**Figure 25.** (a) Cost breakdown for a Li-NMC/G and hypothetical K-NMC/Gr battery. (b) Total cost for a 50 kWh LIB and PIB. Reprinted from [332], Copyright (2020), with permission from Elsevier.

cost and low resource efficiency of pyrometallurgical processing and the development of processes for recovery of a broader range of materials. First studies have reported the usage of graphite recycled from LIBs as anode in PIBs with promising electrochemical performance [340, 341]. This serves as a first proof-of-concept of the manufacturing of PIBs using recycled materials.

Methodological challenges: the techno-economic assessment of PIBs is currently facing several obstacles including: (1) lack of input data due to low technology readiness level, (2) unfair comparison between PIBs and LIBs as the latter are produced on industrial scale with optimized manufacturing processes and (3) incoherent assessment metrics [342].

Regarding the last point, it is crucial that a standardized assessment approach is used to be able to compare the costs across battery technologies. Here, cost needs to be paired with performance and results should be presented on a per kg, per kWh and per kWh-lifetime basis. To avoid misleading interpretation of results, economic analyses should consider single cell materials (the focus of interest is often on the electrode materials) as well as the whole battery pack with its defined performance metrics (e.g. kWh) [342]. Indeed, it was shown in several studies that while SIB and PIB cathode materials present lower costs than their LIB counterparts, the overall cell and battery pack costs are higher due to lower performance [332, 334–336].

Advances in science and technology to meet challenges

Materials

To improve the economic viability of PIBs, the implementation of low-cost materials should be envisaged. In this context, especially the production of anode materials from waste and biomass has attracted attention in recent years [124, 343]. This would not only have a positive impact on the economics of PIBs, but also on their sustainability as environmental impacts associated with mining activities and graphite manufacturing would be avoided. Moreover, the use of biomass-derived anodes could mitigate the use of graphite, which is

classified as critical material. This would increase the supply chain resilience for PIBs, which is one of the major weaknesses of LIBs.

Performance

An additional strategy to reduce the overall costs for PIBs is the improvement of their performance (i.e. cycling stability and energy density). This can be achieved by understanding the fundamental reaction mechanisms in PIBs, their performance bottlenecks and how to overcome them [343]. In this context, also the application purpose of PIBs should be well-defined to prioritize the correct performance metric for a specific use case and bundle research efforts.

Manufacturing

An increased efficiency of materials and energy use as well as waste reduction will reduce manufacturing and battery costs. Knowledge transfer from LIB production could accelerate upscaling and facilitate the establishment of optimized manufacturing processes [334]. Also already existing manufacturing lines for LIBs could be used for PIBs thus reducing initial capital expenses [344].

Techno-economics

Only few studies have dealt with the economics of PIBs due to their early development stages and lack of input data. Here, using the experience of battery manufacturers, for instance, could help overcome uncertainties in terms of battery costing and increase the accuracy of techno-economic models for this emerging technology. Therefore, close collaborations between industry and academia are highly desirable.

Concluding remarks

PIBs are handled as a promising battery technology and research efforts in this domain have significantly increased in recent years. However, PIBs also need to make a good business case to incentivize their commercialization. In this context, techno-economic analyses are crucial as they can reveal financially non-viable materials that should not be pursued further and highlight areas and metrics that need to be improved to bring down overall costs. Indeed, it was shown that PIBs are currently not cost-competitive to LIBs and further research is needed to achieve cost parity.

In addition to the techno-economics, also the environmental impacts of PIBs should be closely observed. For every technology, it is crucial to match performance and cost with sustainability to avoid environmental crises to the like we can observe currently with LIBs. Therefore, besides techno-economic analysis, also life cycle assessment should be an integral part of the fundamental research in the field of PIBs.














Acknowledgments

L L thanks the Faraday Institution for their support through the ‘Multiscale Modelling (MSM)’ project (Grant No. FIRG0025).

Data availability statement

No new data were created or analysed in this study.

ORCID iDs

Yang Xu  <https://orcid.org/0000-0003-0177-6348>
Magda Titirici  <https://orcid.org/0000-0003-0773-2100>
Jacqueline Sophie Edge  <https://orcid.org/0000-0003-4643-2426>
Jingyu Feng  <https://orcid.org/0000-0003-3181-4544>
Sumair Imtiaz  <https://orcid.org/0000-0001-7288-2987>
Laura Lander  <https://orcid.org/0000-0001-8128-126X>
Phuong Nam Le Pham  <https://orcid.org/0000-0001-7176-2449>
Laure Monconduit  <https://orcid.org/0000-0003-3698-856X>
Gopinathan Sankar  <https://orcid.org/0000-0001-5152-3424>
Lorenzo Stievano  <https://orcid.org/0000-0001-8548-0231>
Chengliang Wang  <https://orcid.org/0000-0002-1151-3122>
Qichun Zhang  <https://orcid.org/0000-0003-1854-8659>
Min Zhou  <https://orcid.org/0000-0003-2677-5472>

References

- [1] Marcus Y 1985 *Pure Appl. Chem.* **57** 1129
- [2] Matsuda Y, Nakashima H, Morita M and Takasu Y 1981 *J. Electrochem. Soc.* **128** 2552
- [3] U.S. Geological Survey 2020 *Mineral Commodity Summaries 2020* (U.S. Geological Survey) (available at: <https://pubs.er.usgs.gov/publication/mcs2020>)
- [4] Zhang J, Liu T, Cheng X, Xia M, Zheng R, Peng N, Yu H, Shui M and Shu J 2019 *Nano Energy* **60** 340
- [5] Potassium-ion battery startup Group1: "LFP is our benchmark" (available at: www.energy-storage.news/potassium-ion-battery-startup-group1-lfp-is-our-benchmark/)
- [6] Vacancy Engineering in Anode Materials for High-Power K-Ion Batteries (available at: <https://gow.epsrc.ukri.org/NGBOViewGrant.aspx?GrantRef=EP/V000152/1>)
- [7] "Free-from": transition metal-free and anode-free potassium batteries (available at: <https://gow.epsrc.ukri.org/NGBOViewGrant.aspx?GrantRef=EP/X000087/1>)
- [8] Hosaka T, Kubota K, Hamed A S and Komaba S 2020 Research development on K-ion batteries *Chem. Rev.* **120** 6358–466
- [9] Wu Z, Zou J, Chen S, Niu X, Liu J and Wang L 2021 *J. Power Sources* **484** 229307
- [10] Liu X, Ji T, Guo H, Wang H, Li J, Liu H and Shen Z 2022 *Electrochem. Energy Rev.* **5** 401
- [11] Zhao S, Guo Z, Yan K, Guo X, Wan S, He F, Sun B and Wang G 2020 *Small Struct.* **2** 2000054
- [12] Wu X, Chen Y, Xing Z, Lam C W K, Pang S, Zhang W and Ju Z 2019 *Adv. Energy Mater.* **9** 1900343
- [13] Imtiaz S, Amiin I S, Xu Y, Kennedy T, Blackman C and Ryan K M 2021 Progress and perspectives on alloying-type anode materials for advanced potassium-ion batteries *Mater. Today* **48** 241–69
- [14] Li L, Zhao S, Hu Z and Chou S 2021 *J. Chem. Chem. Sci.* **12** 2345
- [15] Vaalma C, Giffin G A, Buchholz D and Passerini S 2016 Non-aqueous K-ion battery based on layered $K_{0.3} MnO_2$ and hard carbon/carbon black *J. Electrochem. Soc.* **163** A1295–99
- [16] Delmas C, Fouassier C and Hagenmuller P 1980 Structural classification and properties of the layered oxides *Physica B* **99** 81–85
- [17] Kim H, Seo D-H, Urban A, Lee J, Kwon D-H, Bo S-H, Shi T, Papp J K, McCloskey B D and Ceder G 2018 Stoichiometric layered potassium transition metal oxide for rechargeable potassium batteries *Chem. Mater.* **30** 6532–9
- [18] Kim H, Seo D-H, Kim J C, Bo S-H, Liu L, Shi T and Ceder G 2017 Investigation of potassium storage in layered P3-type $K_{0.5} MnO_2$ cathode *Adv. Mater.* **29** 1–6
- [19] Hironaka Y, Kubota K and Komaba S 2017 P2- and P3-KxCoO₂ as an electrochemical potassium intercalation host *Chem. Commun.* **53** 3693–6
- [20] Toriyama M Y, Kaufman J L and Van Der Ven A 2019 Potassium ordering and structural phase stability in layered KxCoO₂ ACS *Appl. Energy Mater.* **2** 2629–36
- [21] Van der Ven A, Aydinol M K, Ceder G, Kresse G and Hafner J 1998 First-principles investigation of phase stability in LiCoO₂ *Phys. Rev. B* **58** 2975–87
- [22] Kim E J, Kumar P R, Gossage Z T, Kubota K, Hosaka T, Tatara R and Komaba S 2022 Active material and interphase structures governing performance in sodium and potassium ion batteries *Chem. Sci.* **13** 6121–58
- [23] Van Der Ven A, Bhattacharya J and Belak A A 2013 Understanding Li diffusion in Li-intercalation compounds *Acc. Chem. Res.* **46** 1216–25
- [24] Deng T, Fan X, Chen J, Chen L, Luo C, Zhou X, Yang J, Zheng S and Wang C 2018 Layered P2-Type $K_{0.65} Fe_{0.5} Mn_{0.5} O_2$ microspheres as superior cathode for high-energy potassium-ion batteries *Adv. Funct. Mater.* **28** 1–9
- [25] Wang X, Xu X, Niu C, Meng J, Huang M, Liu X, Liu Z and Mai L 2017 Earth abundant Fe/Mn-based layered oxide interconnected nanowires for advanced K-ion full batteries *Nano Lett.* **17** 544–50
- [26] Rudola A, Rennie A J R, Heap R, Meysami S S, Lowbridge A, Mazzali F, Sayers R, Wright C J and Barker J 2021 Commercialisation of high energy density sodium-ion batteries: Faradion's journey and outlook *J. Mater. Chem. A* **9** 8279–302
- [27] Masese T et al 2018 Rechargeable potassium-ion batteries with honeycomb-layered tellurates as high voltage cathodes and fast potassium-ion conductors *Nat. Commun.* **9** 3823
- [28] Li B et al 2022 Capturing dynamic ligand-to-metal charge transfer with a long-lived cationic intermediate for anionic redox *Nat. Mater.* **21** 1165–74
- [29] Eftekhari A 2004 Potassium secondary cell based on Prussian blue cathode *J. Power Sources* **126** 221–8
- [30] Zhang C, Xu Y, Zhou M, Liang L, Dong H, Wu M, Yang Y and Lei Y 2017 Potassium Prussian blue nanoparticles: a low-cost cathode material for potassium-ion batteries *Adv. Funct. Mater.* **27** 1604307
- [31] Bie X, Kubota K, Hosaka T, Chihara K and Komaba S 2017 A novel K-ion battery: hexacyanoferrate(II)/graphite cell *J. Mater. Chem. A* **5** 4325
- [32] Xue L, Li Y, Gao H, Zhou W, Lv X, Kaveevivitchai W, Manthiram A and Goodenough J B 2017 Low-cost high-energy potassium cathode *J. Am. Chem. Soc.* **139** 2164
- [33] Chapman K W, Chupas P J and Kepert C J 2006 Compositional dependence of negative thermal expansion in the Prussian blue analogues $M^{II}Pt^{IV}(CN)_6$ ($M = Mn, Fe, Co, Ni, Cu, Zn, Cd$) *J. Am. Chem. Soc.* **128** 7009
- [34] Jiang L et al 2019 Building aqueous K-ion batteries for energy storage *Nat. Energy* **4** 495–503
- [35] Ge J, Fan L, Rao A M, Zhou J and Lu B 2022 Surface-substituted Prussian blue analogue cathode for sustainable potassium-ion batteries *Nat. Sustain.* **5** 225
- [36] Liao J, Hu Q, Yu Y, Wang H, Tang Z, Wen Z and Chen C 2017 A potassium-rich iron hexacyanoferrate/dipotassium terephthalate@carbon nanotube composite used for K-ion full-cells with an optimized electrolyte *J. Mater. Chem. A* **5** 19017
- [37] Deng L et al 2021 Defect-free potassium manganese hexacyanoferrate cathode material for high-performance potassium-ion batteries *Nat. Commun.* **12** 2167
- [38] Li C, Wang X, Deng W, Liu C, Chen J, Li R and Xue M 2018 Size engineering and crystallinity control enable high-capacity aqueous potassium-ion storage of Prussian white analogues *ChemElectroChem* **5** 3887
- [39] Song J, Wang L, Lu Y, Liu J, Guo B, Xiao P, Lee J, Yang X, Henkelman G and Goodenough J B 2015 Removal of interstitial H₂O in hexacyanometallates for a superior cathode of a sodium-ion battery *J. Am. Chem. Soc.* **137** 2658
- [40] Hu J, Tao H, Chen M, Zhang Z, Cao S, Shen Y, Jiang K and Zhou M 2022 Interstitial water improves structural stability of iron hexacyanoferrate for high-performance sodium-ion batteries *ACS Appl. Mater. Interfaces* **14** 12234
- [41] Huang B, Liu Y, Lu Z, Shen M, Zhou J, Ren J, Li X and Liao S 2019 Prussian blue $[K_2FeFe(CN)_6]$ doped with nickel as a superior cathode: an efficient strategy to enhance potassium storage performance *ACS Sustain. Chem. Eng.* **7** 16659

- [42] Ishizaki M, Ando H, Yamada N, Tsumoto K, Ono K, Sutoh H, Nakamura T, Nakao Y and Kurihara M 2019 Redox-coupled alkali-metal ion transport mechanism in binder-free films of Prussian blue nanoparticles *J. Mater. Chem. A* **7** 4777
- [43] Morimoto Y, Igarashi K, Kim J and Tanaka H 2009 Size dependent cation channel in nanoporous Prussian blue lattice *Appl. Phys. Express* **2** 085001
- [44] Hosaka T, Fukabori T, Kojima H, Kubota K and Komaba S 2021 Effect of particle size and anion vacancy on electrochemical potassium ion insertion into potassium manganese hexacyanoferrates *ChemSusChem* **14** 1166
- [45] Cattermull J, Pasta M and Goodwin A L 2021 Structural complexity in Prussian blue analogues *Mater. Horiz.* **8** 3178–86
- [46] Fiore M, Wheeler S, Hurlbutt K, Capone I, Fawdon J, Ruffo R and Pasta M 2020 Paving the way toward highly efficient, high-energy potassium-ion batteries with ionic liquid electrolytes *Chem. Mater.* **32** 7653–61
- [47] Onuma H et al 2020 Application of ionic liquid as K-ion electrolyte of graphite//K₂Mn[Fe(CN)₆] cell *ACS Energy Lett.* **5** 2849
- [48] Padhi A K 1997 Phospho-olivines as positive-electrode materials for rechargeable lithium batteries *J. Electrochem. Soc.* **144** 1188
- [49] Masquelier C and Croguennec L 2013 Polyanionic (phosphates, silicates, sulfates) frameworks as electrode materials for rechargeable Li (or Na) batteries *Chem. Rev.* **113** 6552–91
- [50] Hosaka T, Shimamura T, Kubota K and Komaba S 2019 Polyanionic compounds for potassium-ion batteries *Chem. Rec.* **19** 735–45
- [51] Manthiram A and Goodenough J B 1989 Lithium insertion into Fe₂(SO₄)₃ frameworks *J. Power Sources* **26** 403–8
- [52] Gutierrez A, Benedek N A and Manthiram A 2013 Crystal-chemical guide for understanding redox energy variations of M^{2+/3+} couples in polyanion cathodes for lithium-ion batteries *Chem. Mater.* **25** 4010–6
- [53] Mathew V et al 2014 Amorphous iron phosphate: potential host for various charge carrier ions *NPG Asia Mater.* **6** e138
- [54] Sultana I, Rahman M M, Mateti S, Sharma N, Huang S and Chen Y 2020 Approaching reactive KFePO₄ phase for potassium storage by adopting an advanced design strategy *Batter. Supercaps* **3** 450–5
- [55] Zhang L et al 2019 Constructing the best symmetric full K-ion battery with the NASICON-type K₃V₂(PO₄)₃ *Nano Energy* **60** 432–9
- [56] Fedotov S S, Khasanova N R, Samarin A, Drozhzhin O A, Batuk D, Karakulina O M, Hadermann J, Abakumov A M and Antipov E V 2016 AVPO₄F (A = Li, K): a 4 V cathode material for high-power rechargeable batteries *Chem. Mater.* **28** 411–5
- [57] Chihara K, Katogi A, Kubota K and Komaba S 2017 KVPO₄F and KVOPO₄ toward 4 volt-class potassium-ion batteries *Chem. Commun.* **53** 5208–11
- [58] Fedotov S S, Luchinin N D, Aksyonov D A, Morozov A V, Ryazantsev S V, Gaboardi M, Plaisier J R, Stevenson K J, Abakumov A M and Antipov E V 2020 Titanium-based potassium-ion battery positive electrode with extraordinarily high redox potential *Nat. Commun.* **11** 1–11
- [59] Adams S and Rao R P 2011 High power lithium ion battery materials by computational design *Phys. Status Solidi a* **208** 1746–53
- [60] Melot B C, Scanlon D O, Reynaud M, L. Rousse G, Chotard J-N, Henry M and Tarascon J-M 2014 Chemical and structural indicators for large redox potentials in Fe-based positive electrode materials *ACS Appl. Mater. Interfaces* **6** 10832–9
- [61] Franco A A, Rucci A, Brandell D, Frayret C, Gaberscek M, Jankowski P and Johansson P 2019 Boosting rechargeable batteries R&D by multiscale modeling: myth or reality? *Chem. Rev.* **119** 4569–627
- [62] Wang J, Ouyang B, Kim H, Tian Y, Ceder G and Kim H 2021 Computational and experimental search for potential polyanionic K-ion cathode materials *J. Mater. Chem. A* **9** 18564–75
- [63] Ohara M, Hameed A S, Kubota K, Katogi A, Chihara K, Hosaka T and Komaba S 2021 A vanadium-based oxide-phosphate-pyrophosphate framework as a 4 V electrode material for K-ion batteries *Chem. Sci.* **12** 12383–90
- [64] Jun K, Sun Y, Xiao Y, Zeng Y, Kim R, Kim H, Miara L J, Im D, Wang Y and Ceder G 2022 Lithium superionic conductors with corner-sharing frameworks *Nat. Mater.* **21** 924–31
- [65] Wu Y, Cao Z, Song L and Gao J 2021 NaFe₂PO₄ (MoO₄)₂: a promising NASICON-type electrode material for sodium-ion batteries *ACS Appl. Mater. Interfaces* **13** 48865–71
- [66] Momma K and Izumi F 2011 VESTA 3 for three-dimensional visualization of crystal, volumetric and morphology data *J. Appl. Crystallogr.* **44** 1272–6
- [67] Nguyen T P et al 2021 Polypeptide organic radical batteries *Nature* **593** 61–66
- [68] Liang Y, Dong H, Aurbach D and Yao Y 2020 Current status and future directions of multivalent metal-ion batteries *Nat. Energy* **5** 646–56
- [69] Gibb B C 2021 The rise and rise of lithium *Nat. Chem.* **13** 107–9
- [70] Yu Y, Guo Z, Mo Y and Lei Y 2020 Post-lithium battery materials and technology *EcoMat* **2** e12048
- [71] Zhang W, Tian H, Wang J, Sun H, Wang J and Huang W 2022 Quinone electrode for long lifespan potassium-ion batteries based on ionic liquid electrolytes *ACS Appl. Mater. Interfaces* **14** 38887–94
- [72] Rajagopalan R, Tang Y, Ji X, Jia C and Wang H 2020 Advancements and challenges in potassium ion batteries: a comprehensive review *Adv. Funct. Mater.* **30** 1909486
- [73] Xu S, Chen Y and Wang C 2020 Emerging organic potassium-ion batteries: electrodes and electrolytes *J. Mater. Chem. A* **8** 15547–74
- [74] Zhang W, Huang W and Zhang Q 2021 Organic materials as electrodes in potassium-ion batteries *Chem. Eur. J.* **27** 6131–44
- [75] Wang C 2020 Weak intermolecular interactions for strengthening organic batteries *Energy Environ. Mater.* **3** 441–52
- [76] Pan Q, Zheng Y, Tong Z, Shi L and Tang Y 2021 Novel lamellar tetrapotassium pyromellitic organic for robust high-capacity potassium storage *Angew. Chem., Int. Ed.* **60** 11835–40
- [77] Hu Y, Tang W, Yu Q, Wang X, Liu W, Hu J and Fan C 2020 Novel insoluble organic cathodes for advanced organic K-ion batteries *Adv. Funct. Mater.* **30** 2000675
- [78] Obrezkov F A, Ramezankhani V, Zhidkov I, Traven V F, Kurmaev E Z, Stevenson K J and Troshin P A 2019 High-energy and high-power-density potassium ion batteries using dihydrophenazine-based polymer as active cathode material *J. Phys. Chem. Lett.* **10** 5440–5
- [79] Kato M, Masese T, Yao M, Takeichi N and Kiyobayashi T 2019 Organic positive-electrode material utilizing both an anion and cation: a benzoquinone-tetrathiafulvalene triad molecule, Q-TTF-Q, for rechargeable Li, Na, and K batteries *New J. Chem.* **43** 1626–31
- [80] Zhang Q, Wei H, Wang L, Wang J, Fan L, Ding H, Lei J, Yu X and Lu B 2019 Accessible COF-based functional materials for potassium-ion batteries and aluminum-ion batteries *ACS Appl. Mater. Interfaces* **11** 44352–9
- [81] Lin J, Chenna Krishna Reddy R, Zeng C, Lin X, Zeb A and Su Y 2021 Metal-organic frameworks and their derivatives as electrode materials for potassium ion batteries: a review *Coord. Chem. Rev.* **446** 214118
- [82] Chen Y and Wang C 2020 Designing high performance organic batteries *Acc. Chem. Res.* **53** 2636–47

- [83] Shi W, Tang M, Deng W, Li P, Yang X, Huang H, Du P, Liu J and Li C M 2022 11,11,12,12-tetracyano-9,10-anthraquinonedimethane as a high potential and sustainable cathode for organic potassium-ion batteries *J. Colloid Interface Sci.* **607** 1173–9
- [84] Zhou M, Liu M, Wang J, Gu T, Huang B, Wang W, Wang K, Cheng S and Jiang K 2019 Polydiaminoanthraquinones with tunable redox properties as high performance organic cathodes for K-ion batteries *Chem. Commun.* **55** 6054–7
- [85] Yu D, Wang H, Zhang W, Dong H, Zhu Q, Yang J and Huang S 2021 Unraveling the role of ion-solvent chemistry in stabilizing small-molecule organic cathode for potassium-ion batteries *Energy Storage Mater.* **43** 172–81
- [86] Duan J, Wang W, Zou D, Liu J, Li N, Weng J, Xu L, Guan Y, Zhang Y and Zhou P 2022 Construction of a few-layered COF@CNT composite as an ultrahigh rate cathode for low-cost K-ion batteries *ACS Appl. Mater. Interfaces* **14** 31234–44
- [87] Zhang L, Wang W, Lu S and Xiang Y 2021 Carbon anode materials: a detailed comparison between Na-ion and K-ion batteries *Adv. Energy Mater.* **11** 2003640
- [88] Wang W, Zhou J, Wang Z, Zhao L, Li P, Yang Y, Yang C, Huang H and Guo S 2018 Short-range order in mesoporous carbon boosts potassium-ion battery performance *Adv. Energy Mater.* **8** 1701648
- [89] Katorova N S, Luchkin S Y, Rupasov D B, Abakumov A M and Stevenson K J 2020 Origins of irreversible capacity loss in hard carbon negative electrodes for potassium-ion batteries *J. Chem. Phys.* **152** 194704
- [90] Fan L, Ma R, Zhang Q, Jia X and Lu B 2019 Graphite anode for a potassium-ion battery with unprecedented performance *Angew. Chem., Int. Ed.* **58** 10500–5
- [91] Jian Z, Luo W and Ji X 2015 Carbon electrodes for K-ion batteries *J. Am. Chem. Soc.* **137** 11566–9
- [92] Luo W et al 2015 Potassium ion batteries with graphitic materials *Nano Lett.* **15** 7671–7
- [93] Le Pham P N, Gabaudan V, Boulaoued A, Ávall G, Salles F, Johansson P, Monconduit L and Stievano L 2021 Potassium-ion batteries using KFSI/DME electrolytes: implications of cation solvation on the K^+ -graphite (co-)intercalation mechanism *Energy Storage Mater.* **45** 291–300
- [94] Cohn A P, Muralidharan N, Carter R, Share K, Oakes L and Pint C L 2016 Durable potassium ion battery electrodes from high-rate cointercalation into graphitic carbons *J. Mater. Chem. A* **4** 14954–9
- [95] Niu X, Li L, Qiu J, Yang J, Huang J, Wu Z, Zou J, Jiang C, Gao J and Wang L 2019 Salt-concentrated electrolytes for graphite anode in potassium ion battery *Solid State Ion.* **341** 1–6
- [96] Lei Y, Han D, Dong J, Qin L, Li X, Zhai D, Li B, Wu Y and Kang F 2020 Unveiling the influence of electrode/electrolyte interface on the capacity fading for typical graphite-based potassium-ion batteries *Energy Storage Mater.* **24** 319–28
- [97] Xiao N, McCulloch W D and Wu Y 2017 Reversible dendrite-free potassium plating and stripping electrochemistry for potassium secondary batteries *J. Am. Chem. Soc.* **139** 9475–8
- [98] Yuan F, Zhang D, Li Z, Sun H, Yu Q, Wang Q, Zhang J, Wu Y, Xi K and Wang B 2022 Unraveling the intercorrelation between micro/mesopores and K migration behavior in hard carbon *Small* **18** 2107113
- [99] Chong S et al 2022 Nitrogen and oxygen Co-doped porous hard carbon nanospheres with core-shell architecture as anode materials for superior potassium-ion storage *Small* **18** 2104296
- [100] Madec L, Gabaudan V, Gachot G, Stievano L, Monconduit L and Martinez H 2018 Paving the way for K-ion batteries: role of electrolyte reactivity through the example of Sb-based electrodes *ACS Appl. Mater. Interfaces* **10** 34116–22
- [101] Wu X, Xing Z, Hu Y, Zhang Y, Sun Y, Ju Z, Liu J and Zhuang Q 2019 Effects of functional binders on electrochemical performance of graphite anode in potassium-ion batteries *Ionics* **25** 2563–74
- [102] Hosaka T, Matsuyama T, Kubota K, Yasuno S and Komaba S 2020 Development of KPF6/KFSA binary-salt solutions for long-life and high-voltage K-ion batteries *ACS Appl. Mater. Interfaces* **12** 34873–81
- [103] An Y, Fei H, Zeng G, Ci L, Xi B, Xiong S and Feng J 2018 Commercial expanded graphite as a low-cost, long-cycling life anode for potassium-ion batteries with conventional carbonate electrolyte *J. Power Sources* **378** 66–72
- [104] Tai Z, Zhang Q, Liu Y, Liu H and Dou S 2017 Activated carbon from the graphite with increased rate capability for the potassium ion battery *Carbon* **123** 54–61
- [105] Liu Q, Rao A M, Han X and Lu B 2021 Artificial SEI for superhigh-performance K-graphite anode *Adv. Sci.* **8** 1–8
- [106] Xie J, Zhu Y, Zhuang N, Lei H, Zhu W, Fu Y, Javed M S, Li J and Mai W 2018 Rational design of metal organic framework-derived FeS_2 hollow nanocages@reduced graphene oxide for K-ion storage *Nanoscale* **10** 17092–8
- [107] Ge J, Wang B, Wang J, Zhang Q and Lu B 2019 Nature of $FeSe_2/N-C$ anode for high performance potassium ion hybrid capacitor *Adv. Energy Mater.* **10** 1903277
- [108] Fan L, Chen S, Ma R, Wang J, Wang L, Zhang Q, Zhang E, Liu Z and Lu B 2018 Ultrastable potassium storage performance realized by highly effective solid electrolyte interphase layer *Small* **14** 1801806
- [109] Wang J, Fan L, Liu Z, Chen S, Zhang Q, Wang L, Yang H, Yu X and Lu B 2019 *In situ* alloying strategy for exceptional potassium ion batteries *ACS Nano* **13** 3703–13
- [110] Yao Q, Zhang J, Li J, Huang W, Hou K, Zhao Y and Guan L 2019 Yolk-shell $NiS_x@C$ nanosheets as K-ion battery anodes with high rate capability and ultralong cycle life *J. Mater. Chem. A* **7** 18932–9
- [111] Zhao Y, Zhu J, Ong S J H, Yao Q, Shi X, Hou K, Xu Z J and Guan L 2018 High-rate and ultralong cycle-life potassium ion batteries enabled by *in situ* engineering of yolk-shell $FeS_2@C$ structure on graphene matrix *Adv. Energy Mater.* **8** 1802565
- [112] Chang C H, Chen K T, Hsieh Y Y, Chang C B and Tuan H Y 2022 Crystal facet and architecture engineering of metal oxide nanonetwork anodes for high-performance potassium ion batteries and hybrid capacitors *ACS Nano* **16** 1486–501
- [113] Fan L, Hu Y Y, Rao A M, Zhou J, Hou Z H, Wang C X and Lu B A 2021 Prospects of electrode materials and electrolytes for practical potassium-based batteries *Small Methods* **5** 2101131
- [114] Li D, Dai L, Ren X, Ji F, Sun Q, Zhang Y and Ci L 2021 Foldable potassium-ion batteries enabled by free-standing and flexible $SnS_2@C$ nanofibers *Energy Environ. Sci.* **14** 424–36
- [115] Xie J, Li X, Lai H, Zhao Z, Li J, Zhang W, Xie W, Liu Y and Mai W 2019 A robust solid electrolyte interphase layer augments the ion storage capacity of bimetallic-sulfide-containing potassium-ion batteries *Angew. Chem., Int. Ed.* **58** 14740–7
- [116] Shan H, Qin J, Ding Y, Sari H M K, Song X, Liu W and Li X 2021 Controllable heterojunctions with a semicoherent phase boundary boosting the potassium storage of $CoSe_2/FeSe_2$ *Adv. Mater.* **33** e2102471
- [117] Huang M, Xi B, Mi L, Zhang Z, Chen W, Feng J and Xiong S 2022 Rationally designed three-layered $TiO_2@amorphous MoS_3@carbon$ hierarchical microspheres for efficient potassium storage *Small* **18** e2107819
- [118] Wu Z, Liang G, Pang W K, Zhou T, Cheng Z, Zhang W, Liu Y, Johannessen B and Guo Z 2020 Coupling topological insulator $SnSb_2 Te_4$ nanodots with highly doped graphene for high-rate energy storage *Adv. Mater.* **32** e1905632

- [119] Wang S, Xiong P, Guo X, Zhang J, Gao X, Zhang F, Tang X, Notten P H L and Wang G 2020 A stable conversion and alloying anode for potassium-ion batteries: a combined strategy of encapsulation and confinement *Adv. Funct. Mater.* **30** 2001588
- [120] Wang T, Shen D, Liu H, Chen H, Liu Q and Lu B 2020 A Sb₂S₃ nanoflower/MXene composite as an anode for potassium-ion batteries *ACS Appl. Mater. Interfaces* **12** 57907–15
- [121] Wu J, Liu S, Rehman Y, Huang T, Zhao J, Gu Q, Mao J and Guo Z 2021 Phase engineering of nickel sulfides to boost sodium- and potassium-ion storage performance *Adv. Funct. Mater.* **31** 2010832
- [122] Ge J, Fan L, Wang J, Zhang Q, Liu Z, Zhang E, Liu Q, Yu X and Lu B 2018 MoSe₂/N-doped carbon as anodes for potassium-ion batteries *Adv. Energy Mater.* **8** 1801477
- [123] Wang J, Liu Z, Zhou J, Han K and Lu B 2021 Insights into metal/metalloid-based alloying anodes for potassium ion batteries *ACS Mater. Lett.* **3** 1572–98
- [124] Kim H, Kim J C, Bianchini M, Seo D-H, Rodriguez-Garcia J and Ceder G 2018 Recent progress and perspective in electrode materials for K-ion batteries *Adv. Energy Mater.* **8** 1702384
- [125] Zhang W, Liu Y and Guo Z 2019 Approaching high-performance potassium-ion batteries via advanced design strategies and engineering *Sci. Adv.* **5** eaav7412
- [126] Song K, Liu C, Mi L, Chou S, Chen W and Shen C 2019 Recent progress on the alloy-based anode for sodium-ion batteries and potassium-ion batteries *Small* **15** 1903194
- [127] Wu Y, Hu S, Xu R, Wang J, Peng Z, Zhang Q and Yu Y 2019 Boosting potassium-ion battery performance by encapsulating red phosphorus in free-standing nitrogen-doped porous hollow carbon nanofibers *Nano Lett.* **19** 1351–8
- [128] Sultana I, Rahman M M, Chen Y and Glushenkov A M 2018 Potassium-ion battery anode materials operating through the alloying-dealloying reaction mechanism *Adv. Funct. Mater.* **28** 1703857
- [129] Loaiza L C, Monconduit L and Seznec V 2020 Si and Ge-based anode materials for Li-, Na-, and K-ion batteries: a perspective from structure to electrochemical mechanism *Small* **16** e1905260
- [130] Lee S, Jung S C and Han Y-K 2019 First-principles molecular dynamics study on ultrafast potassium ion transport in silicon anode *J. Power Sources* **415** 119–25
- [131] Wang Q, Zhao X, Ni C, Tian H, Li J, Zhang Z, Mao S X, Wang J and Xu Y 2017 Reaction and capacity-fading mechanisms of tin nanoparticles in potassium-ion batteries *J. Phys. Chem. C* **121** 12652–7
- [132] Gabaudan V, Berthelot R, Stievano L and Monconduit L 2018 Inside the alloy mechanism of Sb and Bi electrodes for K-ion batteries *J. Phys. Chem. C* **122** 18266–73
- [133] Huang X, Sui X, Ji W, Wang Y, Qu D and Chen J 2020 From phosphorus nanorods/C to yolk-shell P@hollow C for potassium-ion batteries: high capacity with stable cycling performance *J. Mater. Chem. A* **8** 7641–6
- [134] Wang A, Hong W, Yang L, Tian Y, Qiu X, Zou G, Hou H and Ji X 2020 Bi-based electrode materials for alkali metal-ion batteries *Small* **16** 2004022
- [135] Wu J et al 2020 Synergy of binders and electrolytes in enabling micro-sized alloy anodes for high performance potassium-ion batteries *Nano Energy* **77** 105118
- [136] Zhang R, Bao J, Wang Y and Sun C F 2018 Concentrated electrolytes stabilize bismuth-potassium batteries *Chem. Sci.* **9** 6193–8
- [137] Ge X, Liu S, Qiao M, Du Y, Li Y, Bao J and Zhou X 2019 Enabling superior electrochemical properties for highly efficient potassium storage by impregnating ultrafine Sb nanocrystals within nanochannel-containing carbon nanofibers *Angew. Chem., Int. Ed. Engl.* **58** 14578–83
- [138] He X-D, Liu Z-H, Liao J-Y, Ding X, Hu Q, Xiao L-N, Wang S and Chen C-H 2019 A three-dimensional macroporous antimony@carbon composite as a high-performance anode material for potassium-ion batteries *J. Mater. Chem. A* **7** 9629–37
- [139] Zheng J, Wu Y, Sun Y, Rong J, Li H and Niu L 2020 Advanced anode materials of potassium ion batteries: from zero dimension to three dimensions *Nano-Micro Lett.* **13** 12
- [140] Kennedy T, Brandon M and Ryan K M 2016 Advances in the application of silicon and germanium nanowires for high-performance lithium-ion batteries *Adv. Mater.* **28** 5696–704
- [141] Imtiaz S, Amiin I S, Storan D, Kapuria N, Geaney H, Kennedy T and Ryan K M 2021 Dense silicon nanowire networks grown on a stainless steel fiber cloth: a flexible and robust anode for lithium-ion batteries *Adv. Mater.* **33** e2105917
- [142] Liu N, Lu Z, Zhao J, McDowell M T, Lee H W, Zhao W and Cui Y 2014 A pomegranate-inspired nanoscale design for large-volume-change lithium battery anodes *Nat. Nanotechnol.* **9** 187–92
- [143] Hwang T H, Lee Y M, Kong B S, Seo J S and Choi J W 2012 Electrospun core-shell fibers for robust silicon nanoparticle-based lithium ion battery anodes *Nano Lett.* **12** 802–7
- [144] Xie J, Zhu Y, Zhuang N, Li X, Yuan X, Li J, Hong G and Mai W 2019 High-concentration ether-based electrolyte boosts the electrochemical performance of SnS₂-reduced graphene oxide for K-ion batteries *J. Mater. Chem. A* **7** 19332–41
- [145] Cho E, Mun J, Chae O B, Kwon O M, Kim H-T, Ryu J H, Kim Y G and Oh S M 2012 Corrosion/passivation of aluminum current collector in bis(fluorosulfonyl)imide-based ionic liquid for lithium-ion batteries *Electrochem. Commun.* **22** 1–3
- [146] Wu X, Zhao W, Wang H, Qi X, Xing Z, Zhuang Q and Ju Z 2018 Enhanced capacity of chemically bonded phosphorus/carbon composite as an anode material for potassium-ion batteries *J. Power Sources* **378** 460–7
- [147] Naguib M, Kurtoglu M, Presser V, Lu J, Niu J, Heon M, Hultman L, Gogotsi Y and Barsoum M W 2011 Two-dimensional nanocrystals produced by exfoliation of Ti₃AlC₂ *Adv. Mater.* **23** 4248–53
- [148] Zou J et al 2022 Additive-mediated intercalation and surface modification of MXenes *Chem. Soc. Rev.* **51** 2972–90
- [149] VahidMohammadi A, Rosen J and Gogotsi Y 2021 The world of two-dimensional carbides and nitrides (MXenes) *Science* **372** eabf1581
- [150] Anasori B, Lukatskaya M R and Gogotsi Y 2017 2D metal carbides and nitrides (MXenes) for energy storage *Nat. Rev. Mater.* **2** 16098
- [151] Okubo M, Sugahara A, Kajiyama S and Yamada A 2018 MXene as a charge storage host *Acc. Chem. Res.* **51** 591–9
- [152] Zhang D, Shah D, Boltasseva A and Gogotsi Y 2022 MXenes for photonics *ACS Photonics* **9** 1108–16
- [153] Han M et al 2020 Tailoring electronic and optical properties of MXenes through forming solid solutions *J. Am. Chem. Soc.* **142** 19110–8
- [154] Ming F, Liang H, Huang G, Bayhan Z and Alshareef H N 2021 MXenes for rechargeable batteries beyond the lithium-ion *Adv. Mater.* **33** 2004039
- [155] Xie Y, Dall'Agnese Y, Naguib M, Gogotsi Y, Barsoum M W, Zhuang H L and Kent P R C 2014 Prediction and characterization of MXene nanosheet anodes for non-lithium-ion batteries *ACS Nano* **8** 9606–15

- [156] Er J L, Naguib M, Gogotsi Y and Shenoy V B 2014 Ti_3C_2 MXene as a high capacity electrode material for metal (Li, Na, K, Ca) ion batteries *ACS App. Mater. Interfaces* **6** 11173–9
- [157] Naguib M, Adams R A, Zhao Y, Zemlyanov D, Varma A, Nanda J and Pol V G 2017 Electrochemical performance of MXenes as K-ion battery anodes *Chem. Commun.* **53** 6883–6
- [158] Ming F, Liang H, Zhang W, Ming J, Lei Y, Emwas A-H and Alshareef H N 2019 Porous MXenes enable high performance potassium ion capacitors *Nano Energy* **62** 853–60
- [159] Liu C, Zhou J, Li X, Fang Z, Sun R, Yang G and Hou W 2022 Surface modification and *in situ* carbon intercalation of two-dimensional niobium carbide as promising electrode materials for potassium-ion batteries *Chem. Eng. J.* **431** 133838
- [160] Dillon A D, Ghidui M J, Krick A L, Griggs J, May S J, Gogotsi Y, Barsoum M W and Fafarman A T 2016 Highly conductive optical quality solution-processed films of 2D titanium carbide *Adv. Funct. Mater.* **26** 4162–8
- [161] Paton K R et al 2014 Scalable production of large quantities of defect-free few-layer graphene by shear exfoliation in liquids *Nat. Mater.* **13** 624–30
- [162] Li X, Huang Z, Shuck C E, Liang G, Gogotsi Y and Zhi C 2022 MXene chemistry, electrochemistry and energy storage applications *Nat. Rev. Chem.* **6** 389–404
- [163] Borysiuk V N, Mochalin V N and Gogotsi Y 2015 Molecular dynamic study of the mechanical properties of two-dimensional titanium carbides $\text{Ti}_{n+1}\text{C}_n$ (MXenes) *Nanotechnology* **26** 265705
- [164] Bertolazzi S, Brivio J and Kis A 2011 Stretching and breaking of ultrathin MoS_2 *ACS Nano* **5** 9703–9
- [165] Huang H, Cui J, Liu G, Bi R and Zhang L 2019 Carbon-coated MoSe_2 /MXene hybrid nanosheets for superior potassium storage *ACS Nano* **13** 3448–56
- [166] Cao J, Wang L, Li D, Yuan Z, Xu H, Li J, Chen R, Shulga V, Shen G and Han W 2021 $\text{Ti}_3\text{C}_2\text{T}_x$ MXene conductive layers supported bio-derived $\text{Fe}_{x-1}\text{Se}_x$ /MXene/carbonaceous nanoribbons for high-performance half/full sodium-ion and potassium-ion batteries *Adv. Mater.* **33** 2101535
- [167] Xia Z, Chen X, Ci H, Fan Z, Yi Y, Yin W, Wei N, Cai J, Zhang Y and Sun J 2021 Designing N-doped graphene/ ReSe_2 / Ti_3C_2 MXene heterostructure frameworks as promising anodes for high-rate potassium-ion batteries *J. Energy Chem.* **53** 155–62
- [168] Cao J, Li J, Li D, Yuan Z, Zhang Y, Shulga V, Sun Z and Han W 2021 Strongly coupled 2D transition metal chalcogenide-MXene-carbonaceous nanoribbon heterostructures with ultrafast ion transport for boosting sodium/potassium ions storage *Nano-Micro Lett.* **13** 113
- [169] Naguib M, Mashtalir O, Lukatskaya M R, Dyatkin B, Zhang C, Presser V, Gogotsi Y and Barsoum M W 2014 One-step synthesis of nanocrystalline transition metal oxides on thin sheets of disordered graphitic carbon by oxidation of MXenes *Chem. Commun.* **50** 7420–3
- [170] Tang H, Zhuang S, Bao Z, Lao C and Mei Y 2016 Two-step oxidation of MXene in the synthesis of layer-stacked anatase titania with enhanced lithium-storage performance *ChemElectroChem* **3** 871–6
- [171] Zeng C, Xie F, Yang X, Jaroniec M, Zhang L and Qiao S-Z 2018 Ultrathin titanate nanosheets/graphene films derived from confined transformation for excellent Na/K ion storage *Angew. Chem., Int. Ed.* **57** 8540–4
- [172] Fang Y, Hu R, Liu B, Zhang Y, Zhu K, Yan J, Ye K, Cheng K, Wang G and Cao D 2019 MXene-derived TiO_2 /reduced graphene oxide composite with an enhanced capacitive capacity for Li-ion and K-ion batteries *J. Mater. Chem. A* **7** 5363–72
- [173] Tao M, Du G, Zhang Y, Gao W, Liu D, Luo Y, Jiang J, Bao S and Xu M 2019 TiO_xN_y nanoparticles/C composites derived from MXene as anode material for potassium-ion batteries *Chem. Eng. J.* **369** 828–33
- [174] Tang J, Huang X, Lin T, Qiu T, Huang H, Zhu X, Gu Q, Luo B and Wang L 2020 MXene derived TiS_2 nanosheets for high-rate and long-life sodium-ion capacitors *Energy Storage Mater.* **26** 550–9
- [175] Dong Y, Wu Z-S, Zheng S, Wang X, Qin J, Wang S, Shi X and Bao X 2017 Ti_3C_2 MXene-derived sodium/potassium titanate nanoribbons for high-performance sodium/potassium ion batteries with enhanced capacities *ACS Nano* **11** 4792–800
- [176] Hwang J-Y, Myung S-T and Sun Y-K 2018 Recent progress in rechargeable potassium batteries *Adv. Funct. Mater.* **28** 1802938
- [177] Liu S, Kang L, Henzie J, Zhang J, Ha J, Amin M A, Hossain M S A, Jun S C and Yamauchi Y 2021 Recent advances and perspectives of battery-type anode materials for potassium ion storage *ACS Nano* **15** 18931–73
- [178] Wang C, Tang W, Yao Z, Chen Y, Pei J and Fan C 2018 Using an organic acid as a universal anode for highly efficient Li-ion, Na-ion and K-ion batteries *Org. Electron.* **62** 536–41
- [179] Wang C, Tang W, Yao Z, Cao B and Fan C 2019 Potassium perylene-tetracarboxylate with two-electron redox behaviors as a highly stable organic anode for K-ion batteries *Chem. Commun.* **55** 1801–4
- [180] Zhu Y, Chen B, Zhou Y, Nie W and Xu Y 2019 New family of organic anode without aromatics for energy storage *Electrochim. Acta* **318** 262–71
- [181] Liang Y, Luo C, Wang F, Hou S, Liou S-C, Qing T, Li Q, Zheng J, Cui C and Wang C 2019 An organic anode for high temperature potassium-ion batteries *Adv. Energy Mater.* **9** 1802986
- [182] Chen X D, Zhang H, Ci C G, Sun W W and Wang Y 2019 Few-layered boronic ester based covalent organic frameworks/carbon nanotube composites for high-performance K-organic batteries *ACS Nano* **13** 3600–7
- [183] Zhang H, Sun W, Chen X and Wang Y 2019 Few-layered fluorinated triazine-based covalent organic nanosheets for high-performance alkali organic batteries *ACS Nano* **13** 14252–61
- [184] Tang M, Wu Y, Chen Y, Jiang C, Zhu S, Zhuo S and Wang C 2019 An organic cathode with high capacities for fast-charge potassium-ion batteries *J. Mater. Chem. A* **7** 486–92
- [185] Zou J, Fan K, Chen Y, Hu W and Wang C 2022 Perspectives of ionic covalent organic frameworks for rechargeable batteries *Coord. Chem. Rev.* **458** 214431
- [186] Chen Y, Zhuo S, Li Z and Wang C 2020 Redox polymers for rechargeable metal-ion batteries *EnergyChem* **2** 100030
- [187] Fan C, Zhao M, Li C, Wang C, Cao B, Chen X, Li Y and Li J 2017 Investigating the electrochemical behavior of cobalt(II) terephthalate ($\text{CoC}_8\text{H}_4\text{O}_4$) as the organic anode in K-ion battery *Electrochim. Acta* **253** 333–8
- [188] Fan K, Zhang C, Chen Y, Wu Y and Wang C 2021 The chemical states of conjugated coordination polymers *Chemistry* **7** 1224–43
- [189] Chen Y et al 2019 A one-dimensional π -d conjugated coordination polymer for sodium storage with catalytic activity in Negishi coupling *Angew. Chem., Int. Ed.* **58** 14731–9
- [190] Booth S G et al 2021 Perspectives for next generation lithium-ion battery cathode materials *APL Mater.* **9** 109201
- [191] Tapia-Ruiz N et al 2021 2021 roadmap for sodium-ion batteries *J. Phys. Energy* **3** 031503
- [192] Kim H, Ji H, Wang J and Ceder G 2019 Next-generation cathode materials for non-aqueous potassium-ion batteries *Trends Chem.* **1** 682–92
- [193] Hurlbutt K, Wheeler S, Capone I and Pasta M 2018 Prussian blue analogs as battery materials *Joule* **2** 1950–60

- [194] Yang Y, Zhou J, Wang L, Jiao Z, Xiao M, Huang Q, Liu M, Shao Q, Sun X and Zhang J 2022 Prussian blue and its analogues as cathode materials for Na-, K-, Mg-, Ca- Zn- and Al-ion batteries *Nano Energy* **99** 107424
- [195] Yu S, Kim S-O, Kim H-S and Choi W 2019 Computational screening of anode materials for potassium-ion batteries *Int. J. Energy Res.* **43** 7646–54
- [196] Zhu B and Scanlon D O 2022 Predicting lithium iron oxysulfides for battery cathodes *ACS Appl. Energy Mater.* **5** 575–84
- [197] Zhu B, Lu Z, Pickard C J and Scanlon D O 2021 Accelerating cathode material discovery through *ab initio* random structure searching *APL Mater.* **9** 121111
- [198] Lu Z, Zhu B, Shires B W B, Scanlon D O and Pickard C J 2021 *Ab initio* random structure searching for battery cathode materials *J. Chem. Phys.* **154** 174111
- [199] Harper A F, Evans M L, Darby J P, Karasulu B, Koçer C P, Nelson J R and Morris A J 2020 *Ab initio* structure prediction methods for battery materials: a review of recent computational efforts to predict the atomic level structure and bonding in materials for rechargeable batteries *Johns. Matthey Technol. Rev.* **64** 103–18
- [200] Ells A W, Evans M L, Groh M F, Morris A J and Marbella L E 2022 Phase transformations and phase segregation during potassiation of SnxPy anodes *Chem. Mater.* **34** 7460–7
- [201] Neilson W D and Murphy S T 2022 DefAP: a Python code for the analysis of point defects in crystalline solids *Comput. Mater. Sci.* **210** 111434
- [202] Broberg D, Medasani B, Zimmermann N E R, Yu G, Canning A, Haranczyk M, Asta M and Hautier G 2018 PyCDT: a Python toolkit for modeling point defects in semiconductors and insulators *Comput. Phys. Commun.* **226** 165–79
- [203] Goyal A, Gorai P, Peng H, Lany S and Stevanović V 2017 A computational framework for automation of point defect calculations *Comput. Mater. Sci.* **130** 1–9
- [204] Eckhoff M, Schönwald F, Risch M, Volkert C A, Blöchl P E and Behler J 2020 Closing the gap between theory and experiment for lithium manganese oxide spinels using a high-dimensional neural network potential *Phys. Rev. B* **102** 174102
- [205] Eckhoff M, Lausch K N, Blöchl P E and Behler J 2020 Predicting oxidation and spin states by high-dimensional neural networks: applications to lithium manganese oxide spinels *J. Chem. Phys.* **153** 164107
- [206] Ko T W, Finkler J A, Goedecker S and Behler J 2021 A fourth-generation high-dimensional neural network potential with accurate electrostatics including non-local charge transfer *Nat. Commun.* **12** 398
- [207] Eckhoff M and Behler J 2021 Insights into lithium manganese oxide–water interfaces using machine learning potentials *J. Chem. Phys.* **155** 244703
- [208] Pickard C J 2022 Ephemeral data derived potentials for random structure search *Phys. Rev. B* **106** 014102
- [209] Pickard C J and Needs R J 2011 *Ab initio* random structure searching *J. Phys.: Condens. Matter* **23** 053201
- [210] Collins C, Dyer M S, Pitcher M J, Whitehead G F S, Zanella M, Mandal P, Claridge J B, Darling G R and Rosseinsky M J 2017 Accelerated discovery of two crystal structure types in a complex inorganic phase field *Nature* **546** 280–4
- [211] Pétuya R, Durdy S, Antypov D, Gaultois M W, Berry N G, Darling G R, Katsoulidis A P, Dyer M S and Rosseinsky M J 2022 Machine-learning prediction of metal-organic framework guest accessibility from linker and metal chemistry *Angew. Chem., Int. Ed.* **61** e202114573
- [212] Zhou M, Bai P, Ji X, Yang J, Wang C and Xu Y 2021 Electrolytes and interphases in potassium ion batteries *Adv. Mater.* **33** 2003741
- [213] Han Y, Saroja V K P, Tinker H R and Xu Y 2022 Interphases in the electrodes of potassium ion batteries *J. Phys. Mater.* **5** 022001
- [214] Sankarasubramanian S, Kahky J and Ramani V 2019 Tuning anion solvation energetics enhances potassium–oxygen battery performance *Proc. Natl Acad. Sci. USA* **116** 14899–904
- [215] Hosaka T, Kubota K, Kojima H and Komaba S 2018 Highly concentrated electrolyte solutions for 4 V class potassium–ion batteries *Chem. Commun.* **54** 8387–90
- [216] Han J G, Kim K, Lee Y and Choi N S 2019 Scavenging materials to stabilize LiPF₆-containing carbonate-based electrolytes for Li-ion batteries *Adv. Mater.* **31** 1804822
- [217] Ignat'ev N V, Barthen P, Kucheryna A, Willner H and Sartori P 2012 A convenient synthesis of triflate anion ionic liquids and their properties *Molecules* **17** 5319–38
- [218] Qin L, Zhang S, Zheng J, Lei Y, Zhai D and Wu Y 2020 Pursuing graphite-based K–ion O₂ batteries: a lesson from Li-ion batteries *Energy Environ. Sci.* **13** 3656–62
- [219] Qin L, Xiao N, Zheng J, Lei Y, Zhai D and Wu Y 2019 Localized high-concentration electrolytes boost potassium storage in high-loading graphite *Adv. Energy Mater.* **9** 1902618
- [220] Zhang Q, Mao J, Pang W K, Zheng T, Sencadas V, Chen Y, Liu Y and Guo Z 2018 Boosting the potassium storage performance of alloy-based anode materials via electrolyte salt chemistry *Adv. Energy Mater.* **8** 1703288
- [221] Qin L, Schkeryantz L, Zheng J, Xiao N and Wu Y 2020 Superoxide-based K–O₂ batteries: highly reversible oxygen redox solves challenges in air electrodes *J. Am. Chem. Soc.* **142** 11629–40
- [222] Liu S, Mao J, Zhang Q, Wang Z, Pang W K, Zhang L, Du A, Sencadas V, Zhang W and Guo Z 2020 An intrinsically non-flammable electrolyte for high-performance potassium batteries *Angew. Chem., Int. Ed.* **59** 3638–44
- [223] Yang H, Chen C Y, Hwang J, Kubota K, Matsumoto K and Hagiwara R 2020 Potassium difluorophosphate as an electrolyte additive for potassium-ion batteries *ACS Appl. Mater. Interfaces* **12** 36168–76
- [224] Wang H, Dong J, Guo Q, Xu W, Zhang H, Lau K C, Wei Y, Hu J, Zhai D and Kang F 2021 Highly stable potassium metal batteries enabled by regulating surface chemistry in ether electrolyte *Energy Storage Mater.* **42** 526–32
- [225] Yao Y X, Chen X, Yan C, Zhang X Q, Cai W L, Huang J Q and Zhang Q 2021 Regulating interfacial chemistry in lithium-ion batteries by a weakly solvating electrolyte *Angew. Chem., Int. Ed.* **60** 4090–7
- [226] Nan B et al 2022 Enhancing Li⁺ transport in NMC811/graphite lithium-ion batteries at low temperatures by using low-polarity-solvent electrolytes *Angew. Chem., Int. Ed.* **61** e202205967
- [227] Schkeryantz L, Zheng J, McCulloch W D, Qin L, Zhang S, Moore C E and Wu Y 2020 Designing potassium battery salts through a solvent-in-anion concept for concentrated electrolytes and mimicking solvation structures *Chem. Mater.* **32** 10423–34
- [228] Schkeryantz L, Nguyen P, McCulloch W D, Moore C E, Lau K C and Wu Y 2021 Unusual melting trend in an alkali asymmetric sulfonamide salt series: single-crystal analysis and modeling *Inorg. Chem.* **60** 14679–86
- [229] Zhang S, Li S and Lu Y 2021 Designing safer lithium-based batteries with nonflammable electrolytes: a review *eScience* **1** 163–77
- [230] Lei Y, Qin L, Liu R, Lau K C, Wu Y, Zhai D, Li B and Kang F 2018 Exploring stability of nonaqueous electrolytes for potassium-ion batteries *ACS Appl. Energy Mater.* **1** 1828–33
- [231] Naylor A J, Carboni M, Valvo M and Younesi R 2019 Interfacial reaction mechanisms on graphite anodes for K-ion batteries *ACS Appl. Mater. Interfaces* **11** 45636–45

- [232] Yuan F, Hu J, Lei Y, Zhao R, Gao C, Wang H, Li B, Kang F and Zhai D 2022 Key factor determining the cyclic stability of the graphite anode in potassium-ion batteries *ACS Nano* **16** 12511–9
- [233] Lei K, Li F, Mu C, Wang J, Zhao Q, Chen C and Chen J 2017 High K-storage performance based on the synergy of dipotassium terephthalate and ether-based electrolytes *Energy Environ. Sci.* **10** 552–7
- [234] Zhao J, Zou X, Zhu Y, Xu Y and Wang C 2016 Electrochemical intercalation of potassium into graphite *Adv. Funct. Mater.* **26** 8103–10
- [235] Deng L et al 2020 A nonflammable electrolyte enabled high performance $K_{0.5}MnO_2$ cathode for low-cost potassium-ion batteries *ACS Energy Lett.* **5** 1916–22
- [236] Xu K 2014 Electrolytes and Interphases in Li-ion batteries and beyond *Chem. Rev.* **114** 11503–618
- [237] Ren X et al 2019 High-concentration ether electrolytes for stable high-voltage lithium metal batteries *ACS Energy Lett.* **4** 896–902
- [238] Xu Y, Ding T, Sun D, Ji X and Zhou X 2022 Recent advances in electrolytes for potassium-ion batteries *Adv. Funct. Mater.* **33** 2211290
- [239] Yoon S U, Kim H, Jin H-J and Yun Y S 2021 Effects of fluoroethylene carbonate-induced solid-electrolyte-interface layers on carbon-based anode materials for potassium ion batteries *Appl. Surf. Sci.* **547** 149193
- [240] Ells A W, May R and Marbella L E 2021 Potassium fluoride and carbonate lead to cell failure in potassium-ion batteries *ACS Appl. Mater. Interfaces* **13** 53841–9
- [241] Liu G, Cao Z, Zhou L, Zhang J, Sun Q, Hwang J-Y, Cavallo L, Wang L, Sun Y-K and Ming J 2020 Additives engineered nonflammable electrolyte for safer potassium ion batteries *Adv. Funct. Mater.* **30** 2001934
- [242] Sun H et al 2020 A high-performance potassium metal battery using safe ionic liquid electrolyte *Proc. Natl Acad. Sci. USA* **117** 27847–53
- [243] Yoshii K, Masese T, Kato M, Kubota K, Senoh H and Shikano M 2019 Sulfonamide-based ionic liquids for high-voltage potassium-ion batteries with honeycomb layered cathode oxides *ChemElectroChem* **6** 3901–10
- [244] Onuma H et al 2020 Application of ionic liquid as K-ion electrolyte is of graphite/ $K_2Mn[Fe(CN)_6]$ cell *ACS Energy Lett.* **5** 2849–57
- [245] Arnaiz M, Bothe A, Dsoke S, Balducci A and Ajuria J 2019 Aprotic and protic ionic liquids combined with olive pits derived hard carbon for potassium-ion batteries *J. Electrochem. Soc.* **166** A3504–10
- [246] Beltrop K, Beuker S, Heckmann A, Winter M and Placke T 2017 Alternative electrochemical energy storage: potassium-based dual-graphite batteries *Energy Environ. Sci.* **10** 2090–4
- [247] Golding J J, MacFarlane D R, Spiccia L, Golding J J, Forsyth M, Skelton B W and White A H 1998 Weak intermolecular interactions in sulfonamide salts: structure of 1-ethyl-2-methyl-3-benzyl imidazolium bis[(trifluoromethyl)sulfonyl]amide *Chem. Commun.* 1593–4
- [248] MacFarlane D R, Meakin P, Sun J, Amini N and Forsyth M 1999 Pyrrolidinium imides: a new family of molten salts and conductive plastic crystal phases *J. Phys. Chem. B* **103** 4164–70
- [249] Shkrob I A, Marin T W, Zhu Y and Abraham D P 2014 Why Bis(fluorosulfonyl)imide is a “magic anion” for electrochemistry *J. Phys. Chem. C* **118** 19661–71
- [250] MacFarlane D R, Sun J, Golding J, Meakin P and Forsyth M 2000 High conductivity molten salts based on the imide ion *Electrochim. Acta* **45** 1271–8
- [251] Brutti S 2020 Pyr1,xTFSI ionic liquids (x = 1–8): a computational chemistry study *Sci. Rep.* **10** 8552
- [252] Morozova P A, Luchinin N D, Rupasov D P, Katorova N S, Fedotov S S, Nikitina V A, Stevenson K J and Abakumov A M 2020 Electrochemical instability of bis(trifluoromethylsulfonyl)imide based ionic liquids as solvents in high voltage electrolytes for potassium ion batteries *Mendeleev Commun.* **30** 679–82
- [253] Barthen P, Frank W and Ignatiev N 2015 Development of low viscous ionic liquids: the dependence of the viscosity on the mass of the ions *Ionics* **21** 149–59
- [254] Tsuzuki S, Shinoda W, Saito H, Mikami M, Tokuda H and Watanabe M 2009 Molecular dynamics simulations of ionic liquids: cation and anion dependence of self-diffusion coefficients of ions *J. Phys. Chem. B* **113** 10641–9
- [255] Siqueira L J A and Ribeiro M C C 2009 Alkoxy chain effect on the viscosity of a quaternary ammonium ionic liquid: molecular dynamics simulations *J. Phys. Chem. B* **113** 1074–9
- [256] Chen Z J, Xue T and Lee J-M 2012 What causes the low viscosity of ether-functionalized ionic liquids? Its dependence on the increase of free volume *RSC Adv.* **2** 10564–74
- [257] Fang Y, Ma P, Cheng H, Tan G, Wu J, Zheng J, Zhou X, Fang S, Dai Y and Lin Y 2019 Synthesis of low-viscosity ionic liquids for application in dye-sensitized solar cells *Chem. Asian J.* **14** 4201–6
- [258] Gerhard D, Alpaslan S C, Gores H J, Uerdingen M and Wasserscheid P 2005 Trialkylsulfonium dicyanamides—a new family of ionic liquids with very low viscosities *Chem. Commun.* 5080–2
- [259] Yuan W-L, Yang X, He L, Xue Y, Qin S and Tao G-H 2018 Viscosity, conductivity, and electrochemical property of dicyanamide ionic liquids *Front. Chem.* **6**
- [260] MacFarlane D R, Golding J, Forsyth S, Forsyth M and Deacon G B 2001 Low viscosity ionic liquids based on organic salts of the dicyanamide anion *Chem. Commun.* 1430–1
- [261] Benayad A, Morales-Ugarte J E, Santini C C and Bouchet R 2021 Operando XPS: a novel approach for probing the lithium/electrolyte interphase dynamic evolution *J. Phys. Chem. A* **125** 1069–81
- [262] Yue Z, Dunya H, Mei X, McGarry C and Mandal B K 2019 Synthesis and physical properties of new low-viscosity sulfonium ionic liquids *Ionics* **25** 5979–89
- [263] Peled E 1979 The electrochemical behavior of alkali and alkaline earth metals in nonaqueous battery systems—the solid electrolyte interphase model *J. Electrochem. Soc.* **126** 2047
- [264] Liu P and Mitlin D 2020 Emerging potassium metal anodes: perspectives on control of the electrochemical interfaces *Acc. Chem. Res.* **53** 1161–75
- [265] Liu P, Wang Y, Hao H, Basu S, Feng X, Xu Y, Boscoboinik J A, Nanda J, Watt J and Mitlin D 2020 Stable potassium metal anodes with an all-aluminum current collector through improved electrolyte wetting *Adv. Mater.* **32** e2002908
- [266] Liu P et al 2022 Multifunctional separator allows stable cycling of potassium metal anodes and of potassium metal batteries *Adv. Mater.* **34** e2105855
- [267] Liu P, Wang Y, Gu Q, Nanda J, Watt J and Mitlin D 2020 Dendrite-free potassium metal anodes in a carbonate electrolyte *Adv. Mater.* **32** e1906735
- [268] Dey A N 1971 Electrochemical alloying of lithium in organic electrolytes *J. Electrochem. Soc.* **118** 1547–9
- [269] Goodenough J B and Kim Y 2010 Challenges for rechargeable Li batteries *Chem. Mater.* **22** 587–603

- [270] Chen B, Meinertzhagen I A and Shaw S R 1999 Circadian rhythms in light-evoked responses of the fly's compound eye, and the effects of neuromodulators 5-HT and the peptide PDF *J. Comp. Physiol. A* **185** 393–404
- [271] Peled E 1997 Advanced model for solid electrolyte interphase electrodes in liquid and polymer electrolytes *J. Electrochem. Soc.* **144** L208–10
- [272] Peled E and Menkin S 2017 Review—SEI: past, present and future *J. Electrochem. Soc.* **164** A1703–19
- [273] Aurbach D, Markovsky B, Shechter A, Ein-Eli Y and Cohen H 1996 A comparative study of synthetic graphite and Li electrodes in electrolyte solutions based on ethylene carbonate–dimethyl carbonate mixtures *J. Electrochem. Soc.* **143** 3809–20
- [274] Yu X and Manthiram A 2018 Electrode–electrolyte interfaces in lithium-based batteries *Energy Environ. Sci.* **11** 527–43
- [275] Hosaka T, Muratsubaki S, Kubota K, Onuma H and Komaba S 2019 Potassium metal as reliable reference electrodes of nonaqueous potassium cells *J. Phys. Chem. Lett.* **10** 3296–300
- [276] Monroe C and Newman J 2003 Dendrite growth in lithium/polymer systems *J. Electrochem. Soc.* **150** A1377
- [277] Chazalviel J 1990 Electrochemical aspects of the generation of ramified metallic electrodeposits *Phys. Rev. A* **42** 7355–67
- [278] Lee B, Paek E, Mitlin D and Lee S W 2019 Sodium metal anodes: emerging solutions to dendrite growth *Chem. Rev.* **119** 5416–60
- [279] Gao Y, Hou Z, Zhou R, Wang D, Guo X, Zhu Y and Zhang B 2022 Critical roles of mechanical properties of solid electrolyte interphase for potassium metal anodes *Adv. Funct. Mater.* **32** 2112399
- [280] Nanda J, Yang G, Hou T, Voylov D N, Li X, Ruther R E, Naguib M, Persson K, Veith G M and Sokolov A P 2019 Unraveling the nanoscale heterogeneity of solid electrolyte interphase using tip-enhanced Raman spectroscopy *Joule* **3** 2001–19
- [281] Li Y et al 2017 Atomic structure of sensitive battery materials and interfaces revealed by cryo-electron microscopy *Science* **358** 506–10
- [282] Zhou Y et al 2020 Real-time mass spectrometric characterization of the solid–electrolyte interphase of a lithium-ion battery *Nat. Nanotechnol.* **15** 224–30
- [283] Fang C et al 2019 Quantifying inactive lithium in lithium metal batteries *Nature* **572** 511–5
- [284] Tripathi A M, Su W N and Hwang B J 2018 *In situ* analytical techniques for battery interface analysis *Chem. Soc. Rev.* **47** 736–51
- [285] Lin F et al 2017 Synchrotron x-ray analytical techniques for studying materials electrochemistry in rechargeable batteries *Chem. Rev.* **117** 13123–86
- [286] Shearing P, Wu Y, Harris S J and Brandon N 2011 *In situ* x-ray spectroscopy and imaging of battery materials *Electrochem. Soc. Interface* **20** 43–47
- [287] Lytle F W 1999 The EXAFS family tree: a personal history of the development of extended x-ray absorption fine structure *J. Synchrotron. Radiat.* **6** 123–34
- [288] Mcbreen J, O'grady W E and Pandya K I 1988 EXAFS: a new tool for the study of battery and fuel cell materials *J. Power Sources* **22** 323–40
- [289] Wu Z, Kong Pang W, Chen L, Johannessen B and Guo Z 2021 *In situ* synchrotron x-ray absorption spectroscopy studies of anode materials for rechargeable batteries *Batter. Supercaps* **4** 1547–66
- [290] Min X et al 2021 Potassium-ion batteries: outlook on present and future technologies *Energy Environ. Sci.* **14** 2186–243
- [291] Borkiewicz O J, Wiaderek K M, Chupas P J and Chapman K W 2015 Best practices for operando battery experiments: influences of x-ray experiment design on observed electrochemical reactivity *J. Phys. Chem. Lett.* **6** 2081–5
- [292] Fehse M, Iadecola A, Simonelli L, Longo A and Stevano L 2021 The rise of x-ray spectroscopies for unveiling the functional mechanisms in batteries *Phys. Chem. Chem. Phys.* **23** 23445–65
- [293] Choi J U, Kim J, Hwang J-Y, Jo J H, Sun Y-K and Myung S-T 2019 $K_{0.54}[Co_{0.5}Mn_{0.5}]O_2$: new cathode with high power capability for potassium-ion batteries *Nano Energy* **61** 284–94
- [294] Ji B, Yao W, Zheng Y, Kidkhunthod P, Zhou X, Tunmee S, Sattayaporn S, Cheng H-M, He H and Tang Y 2020 A fluoroxalate cathode material for potassium-ion batteries with ultra-long cyclability *Nat. Commun.* **11** 1225
- [295] Xie F, Zhang L, Chen B, Chao D, Gu Q, Johannessen B, Jaroniec M and Qiao S-Z 2019 Revealing the origin of improved reversible capacity of dual-shell bismuth boxes anode for potassium-ion batteries *Matter* **1** 1681–93
- [296] Wu Z, Liang G, Wu J, Pang W K, Yang F, Chen L, Johannessen B and Guo Z 2021 Synchrotron x-ray absorption spectroscopy and electrochemical study of Bi_2O_2Se electrode for lithium-/potassium-ion storage *Adv. Energy Mater.* **11** 2100185
- [297] Zhang S, Fan Q, Liu Y, Xi S, Liu X, Wu Z, Hao J, Pang W K, Zhou T and Guo Z 2020 Dehydration-triggered ionic channel engineering in potassium niobate for Li/K-ion storage *Adv. Mater.* **32** 2000380
- [298] He H et al 2019 Anion vacancies regulating endows MoS_2 with fast and stable potassium ion storage *ACS Nano* **13** 11843–52
- [299] Wei J-S et al 2021 Self-assembled ZnO-carbon dots anode materials for high performance nickel-zinc alkaline batteries *Chem. Eng. J.* **425** 130660
- [300] Billinge S J L 2019 The rise of the x-ray atomic pair distribution function method: a series of fortunate events *Phil. Trans. R. Soc. A* **377** 20180413
- [301] Billinge S J L 2004 The atomic pair distribution function: past and present *Z. Kristallogr.* **219** 117–21
- [302] Borkiewicz O J, Shyam B, Wiaderek K M, Kurtz C, Chupas P J and Chapman K W 2012 The AMPIX electrochemical cell: a versatile apparatus for *in situ* x-ray scattering and spectroscopic measurements *J. Appl. Crystallogr.* **45** 1261–9
- [303] Diaz-Lopez M, Cutts G L, Allan P K, Keeble D S, Ross A, Pralong V, Spiekermann G and Chater P A 2020 Fast operando x-ray pair distribution function using the DRIX electrochemical cell *J. Synchrotron. Radiat.* **27** 1190–9
- [304] Farrow C L, Juhas P, Liu J W, Bryndin D, Božin E S, Bloch J, Proffen T and Billinge S J L 2007 PDFfit2 and PDFgui: computer programs for studying nanostructure in crystals *J. Phys.: Condens. Matter* **19** 335219
- [305] Glazer M P B, Okasinski J S, Almer J D and Ren Y 2016 High-energy x-ray scattering studies of battery materials *MRS Bull.* **41** 460–5
- [306] Xu J, Fan C, Ou M, Sun S, Xu Y, Liu Y, Wang X, Li Q, Fang C and Han J 2022 Correlation between potassium-ion storage mechanism and local structural evolution in hard carbon materials *Chem. Mater.* **34** 4202–11
- [307] Hartmann F, Etter M, Cibin G, Gross H, Kienle L and Bensch W 2022 Understanding sodium storage properties of ultra-small Fe_3S_4 nanoparticles—a combined XRD, PDF, XAS and electrokinetic study *Nanoscale* **14** 2696–710
- [308] Stratford J M, Kleppe A K, Keeble D S, Chater P A, Meysami S S, Wright C J, Barker J, Titirici M-M, Allan P K and Grey C P 2021 Correlating local structure and sodium storage in hard carbon anodes: insights from pair distribution function analysis and solid-state NMR *J. Am. Chem. Soc.* **143** 14274–86
- [309] Mathiesen J K, Väli R, Härmas M, Lust E, Fold von Bülow J, Jensen K M Ø and Norby P 2019 Following the in-plane disorder of sodiated hard carbon through operando total scattering *J. Mater. Chem. A* **7** 11709–17

- [310] Daemi S R *et al* 2020 Exploring cycling induced crystallographic change in NMC with x-ray diffraction computed tomography *Phys. Chem. Chem. Phys.* **22** 17814–23
- [311] Sottmann J, Di Michiel M, Fjellvåg H, Malavasi L, Margadonna S, Vajeeston P, Vaughan G B M and Wragg D S 2017 Chemical structures of specific sodium ion battery components determined by operando pair distribution function and x-ray diffraction computed tomography *Angew. Chem., Int. Ed.* **56** 11385–9
- [312] van Beek W, Emerich H, Chernyshov D, Dyadkin V, Wiker G and Dmitriev V 2019 SNBL'S BM31 at ESRF beyond 2020-Combined XRD-PDF-XAS *Acta Crystallogr. A* **75** E677
- [313] Pramudita J C, Sehrawat D, Goonetilleke D and Sharma N 2017 An initial review of the status of electrode materials for potassium-ion batteries *Adv. Energy Mater.* **7** 1602911
- [314] Chen J, Chua D H and Lee P S 2020 The advances of metal sulfides and *in situ* characterization methods beyond Li ion batteries: sodium, potassium, and aluminum ion batteries *Small Methods* **4** 1900648
- [315] Liu X, Tong Y, Wu Y, Zheng J, Sun Y and Li H 2021 In-depth mechanism understanding for potassium-ion batteries by electroanalytical methods and advanced *in situ* characterization techniques *Small Methods* **5** 2101130
- [316] Chen J and Lee P S 2021 Electrochemical supercapacitors: from mechanism understanding to multifunctional applications *Adv. Energy Mater.* **11** 2003311
- [317] Liu Y, Lu Y-X, Xu Y-S, Meng Q-S, Gao J-C, Sun Y-G, Hu Y-S, Chang -B-B, Liu C-T and Cao A-M 2020 Pitch-derived soft carbon as stable anode material for potassium ion batteries *Adv. Mater.* **32** 2000505
- [318] Deng H *et al* 2021 Radial pores in nitrogen/oxygen dual-doped carbon nanospheres anode boost high-power and ultrastable potassium-ion batteries *Adv. Funct. Mater.* **31** 2107246
- [319] Zhang C, Xu Y, He K, Dong Y, Zhao H, Medenbach L, Wu Y, Balducci A, Hannappel T and Lei Y 2020 Polyimide@ketjenblack composite: a porous organic cathode for fast rechargeable potassium-ion batteries *Small* **16** 2002953
- [320] Feng W, Wang H, Jiang Y, Zhang H, Luo W, Chen W, Shen C, Wang C, Wu J and Mai L 2022 A strain-relaxation red phosphorus freestanding anode for non-aqueous potassium ion batteries *Adv. Energy Mater.* **12** 2103343
- [321] Huang M, Wang X, Meng J, Liu X, Yao X, Liu Z and Mai L 2020 Ultra-fast and high-stable near-pseudocapacitance intercalation cathode for aqueous potassium-ion storage *Nano Energy* **77** 105069
- [322] Liu Y, Feo T, Harvey T A and Prum R O 2018 Boosting potassium-ion batteries by few-layered composite anodes prepared via solution-triggered one-step shear exfoliation *Nat. Commun.* **9** 1–10
- [323] Gao A, Li M, Guo N, Qiu D, Li Y, Wang S, Lu X, Wang F and Yang R 2019 K-birnessite electrode obtained by ion exchange for potassium-ion batteries: insight into the concerted ionic diffusion and K storage mechanism *Adv. Energy Mater.* **9** 1802739
- [324] Lee J, Kim S, Park J-H, Jo C, Chun J, Sung Y-E, Lim E and Lee J 2020 A small-strain niobium nitride anode with ordered mesopores for ultra-stable potassium-ion batteries *J. Mater. Chem. A* **8** 3119–27
- [325] Huang J, Lin X, Tan H and Zhang B 2018 Bismuth microparticles as advanced anodes for potassium-ion battery *Adv. Energy Mater.* **8** 1703496
- [326] Ozdogru B, Cha Y, Gwalani B, Murugesan V, Song M-K and M. O. Z. R. Çapraz O 2021 *In situ* probing potassium-ion intercalation-induced amorphization in crystalline iron phosphate cathode materials *Nano Lett.* **21** 7579–86
- [327] Li X, Xiao K, Huang C, Wang J, Gao M, Hu A, Tang Q, Fan B, Xu Y and Chen X 2021 *In situ* monitoring the potassium-ion storage enhancement in iron selenide with ether-based electrolyte *Nano-Micro Lett.* **13** 1–14
- [328] Share K, Cohn A P, Carter R E and Pint C L 2016 Mechanism of potassium ion intercalation staging in few layered graphene from *in situ* Raman spectroscopy *Nanoscale* **8** 16435–9
- [329] Wang H, Yu D, Kuang C, Cheng L, Li W, Feng X, Zhang Z, Zhang X and Zhang Y 2019 Alkali metal anodes for rechargeable batteries *Chemistry* **5** 313–38
- [330] Komaba S, Hasegawa T, Dahbi M and Kubota K 2015 Potassium intercalation into graphite to realize high-voltage/high-power potassium-ion batteries and potassium-ion capacitors *Electrochem. Commun.* **60** 172–5
- [331] Okoshi M, Yamada Y, Komaba S, Yamada A and Nakai H 2016 Theoretical analysis of interactions between potassium ions and organic electrolyte solvents: a comparison with lithium, sodium, and magnesium ions *J. Electrochem. Soc.* **164** A54
- [332] Yan Z and Obrovac M N 2020 Quantifying the cost effectiveness of non-aqueous potassium-ion batteries *J. Power Sources* **464** 228228
- [333] 2022 Mineral commodity summaries 2022 p 206
- [334] Vaalma C, Buchholz D and Passerini S 2018 Non-aqueous potassium-ion batteries: a review *Curr. Opin. Electrochem.* **9** 41–48
- [335] Vaalma C, Buchholz D, Weil M and Passerini S 2018 A cost and resource analysis of sodium-ion batteries *Nat. Rev. Mater.* **3** 1–11
- [336] Peters J F, Peña Cruz A and Weil M 2019 Exploring the economic potential of sodium-ion batteries *Batteries* **5** 10
- [337] Mauler L, Duffner F G, Zeier W and Leker J 2021 Battery cost forecasting: a review of methods and results with an outlook to 2050 *Energy Environ. Sci.* **14** 4712–39
- [338] n.d. Potash prices have more than trebled and keep climbing (MercoPress) (available at: <https://en.mercopress.com/2022/03/25/potash-prices-have-more-than-trebled-and-keep-climbing>) (Accessed 25 April 2022)
- [339] BloombergCom 2022 Fertilizer just got even more expensive as potash prices jump (available at: www.bloomberg.com/news/articles/2022-02-15/fertilizer-just-got-even-more-expensive-as-potash-prices-jump?leadSource=verify%20wall)
- [340] Duc Pham H, Padwal C, Fernando J F S, Wang T, Kim T, Golberg D and Dubal D P 2022 Back-integration of recovered graphite from waste-batteries as ultra-high capacity and stable anode for potassium-ion battery *Batter. Supercaps* **5** e202100335
- [341] Abdollahifar M, Doose S, Cavers H and Kwade A 2022 Graphite recycling from end-of-life lithium-ion batteries: processes and applications *Adv. Mater. Technol.* **8** 2200368
- [342] Zhang W, Lu J and Guo Z 2021 Challenges and future perspectives on sodium and potassium ion batteries for grid-scale energy storage *Mater. Today* **50** 400–17
- [343] Min X, Xiao J, Fang M, Wang W, Zhao Y, Liu Y, Abdelkader A M, Xi K, Kumarb R V and Huang Z 2021 Potassium-ion batteries: outlook on present and future technologies *Energy Environ. Sci.* **14** 2186–243
- [344] Kubota K, Dahbi M, Hosaka T, Kumakura S and Komaba S 2018 Towards K-ion and Na-ion batteries as “beyond Li-ion” *Chem. Rec.* **18** 459–79